Studies on synthesis, densification and oxidation of zirconium diboride based materials

By

Jitendra Kumar Sonber
Registration No. –ENGG01200904041

BHABHA ATOMIC RESEARCH CENTRE

A thesis submitted to the
Board of Studies in Engineering Sciences Discipline

In partial fulfillment of requirements

For the Degree of

DOCTOR OF PHILOSOPHY

of

HOMI BHABHA NATIONAL INSTITUTE

April, 2015

Homi Bhabha National Institute

Recommendation of the Viva Voce Board

As members of the Viva Voce Board, we certify that we have read the dissertation prepared by Shri. Jitendra Kumar Sonber entitled "Studies on synthesis, densification and oxidation of zirconium diboride based materials" and recommended that it may be accepted as fulfilling the dissertation requirement for the Degree of Doctor of Philosophy,

Date: 9th April, 2015

Chairman- Prof. (Smt.) S.B. Roy

Date: 9th April, 2015

Guide- Prof. R.C.Hubli

Parag Bhargava

Date: 9th April, 2015

External Examiner- Prof. Parag Bhargava

N. Krishnamurthy

Date: 9th April, 2015

Co-Guide- Prof. N.Krishnamurthy

Date: 9th April, 2015

Member-1: Prof. Dinesh Srivastava

Date: 9th April, 2015

Member-2: Prof. (Smt.) Sulekha Mukhopadhyay

Rajeev Kapoor

Date: 9th April, 2015

Member-3: Prof. Rajeev Kapoor

Final approval and acceptance of this dissertation is contingent up on the candidate's submission of the final copies of the dissertation to HBNI.

I hereby certify that I have read this dissertation prepared under my direction and recommend that it may be accepted as fulfilling the dissertation requirement.

Date: 9.4.2015

Place: Mumbai

Guide:

Co-Guide: N. Krishnamurthy

STATEMENT BY AUTHOR

This dissertation has been submitted in partial fulfillment of requirements for an advanced degree at Homi Bhabha National Institute (HBNI) and is deposited in the library to be made available to borrowers under rules of the HBNI.

Brief quotations from this dissertation are allowable without special permission, provided that accurate acknowledgement of source is made. Requests for permission for extended quotation from or reproduction of this manuscript in whole or in part may be granted by the Competent Authority of HBNI when in his or her judgment the proposed use of the material is in the interests of scholarship. In all other instances, however, permission must be obtained from the author.

(Jitendra Kumar Sonber)

DECLARATION

I, hereby declare that the investigations presented in the thesis have been carried out by me. The work is original and has not been submitted earlier as a whole or in part for a degree / diploma at this or any other Institution / University.

(Jitendra Kumar Sonber)

List of Publications arising from the thesis

Journals

1. "Synthesis and densification of ZrB_2: Review", J.K.Sonber and A.K. Suri, Advances in Applied Ceramics, **2011**, 110 [6], 321-334.
2. "Investigations on synthesis of ZrB_2 and development of new composites with HfB_2 and $TiSi_2$", J.K.Sonber, T.S.R.Ch.Murthy, C. Subramanian, Sunil Kumar, R.K. Fotedar and A. K. Suri, International journal of refractory metals and hard materials, **2011**, 29, 21-30.
3. "Effect of $CrSi_2$ and HfB_2 addition on densification and properties of ZrB_2.", J.K. Sonber, T.S.R.Ch. Murthy, C. Subramanian, N. Krishnamurthy, R.C. Hubli, A.K. Suri, International Journal of refractory metals and hard materials, **2012**, 31,125-131.
4. "Effect of EuB_6 addition on densification and properties of ZrB_2.", J.K. Sonber, T.S.R.Ch. Murthy, C. Subramanian , R.C. Hubli and A.K. Suri, International Journal of refractory metals and hard materials **2012**, 35, 96-101.
5. "Synthesis, densification and characterization of EuB_6 ", J.K. Sonber, T.S.R.Ch. Murthy, C. Subramanian , R.C. Hubli and A.K. Suri. International Journal of refractory metals and hard materials **2013,** 38, 67-72.

Conferences:

1. "High temperature solid-solid reaction for synthesis of ZrB_2", J.K. Sonber and T. S. R. Ch. Murthy, Proceedings of the 17th National Symposium on thermal analysis (2010)
2. "Processing and properties of ZrB_2 based material", J. K. Sonber, T.S.R.Ch. Murthy, Sairam K., R.D. Bedse, R.C. Hubli & A.K. Suri, Presented in International Conference on New Vistas in Particulate Materials Technology PM-12, at The Residence Hotel, Saki Vihar Road, Powai, Mumbai 400 087 (2012)

Jitendra Kumar Sonber

Dedicated to my Family

ACKNOWLEDGEMENTS

It is a great pleasure in presenting my thesis on completion of my project and in expressing my deepest regards and deep sense of gratitude and sincere thanks to my research guide Prof. (Dr.) R. C. Hubli, Head, Materials Processing Division, Prof. (Dr.) A. K. Suri, Former director, Materials Group, BARC and co-guide Prof. (Dr.) N. Krishnamruthy, Head, Fusion Reactor Materials Section for their valuable guidance in hours of need, constant encouragement, keen interest, good wishes and valuable suggestions throughout my entire research tenure. I am also grateful to them for critically reviewing this thesis.

It gives me immense pleasure to acknowledge Prof. (Dr.) P.K.Tewari, Head, Desalination Division (DD) BARC, for his constant support and for critically evaluating my research activities time to time.

It is also my great pleasure to thank Shri. R.K.Fotedar and Sri. C.Subramanian, for their support in carrying out the research work.

I wish to express my sincere thanks to my colleague Dr. T.S.R.Ch. Murthy for his diversified help, fruitful scientific discussions and moral support offered to me from time to time throughout the course of the PhD work. My special thanks goes to my colleague and my dear friends, Dr. Sanjay Singh, Shri R D Bedse, Shri K Sairam and Shri Palash Mollick for their moral support and diversified help. I would like to thank Shri. Bhaskar Paul, Shri Sunil Kumar, , Dr. S.Roy choudhary, Dr A.K.Sahu, Dr. Abhijit Ghosh, Dr. Tarashankar Mahta, Dr. Abhishek Mukherjee and Shri A. Nagraj for helping me in characterization of samples. I would like to thank my colleagues Shri. P.S.Yadav, Shri. S.B.Chavan, Shri. K.M.Prasad, Shri Sumantha Behra and Smt. Arati Sonawane for their co-opration and help during the experiments. It gives me immense pleasure to thank the members of the doctoral committee Prof. S.B.Roy (Chairman), Prof. Dinesh Srivastava (Member), Dr.

(Smt.) Sulekha Mukhopadhyay and Dr. Rajeev Kapoor for their critical review and suggestions during the progress review and pre-synopsis viva-voce. I also gratefully acknowledge the help rendered by all the members of Materials Processing Division, Materials Science Division and Fusion Reactor Materials Section for their co-operation and help during my PhD work. I wish to express my sincere gratitude and indebtedness to my parents, parents-in-laws for their blessings, for their love and support to me. I am extremely thankful to my spouse Smt. Varsha Sonber and my son Vaibhav for their patience and understanding. At the last, I am thankful to all the reviewer of my published paper whose comments on my manuscript always upgraded my scientific thought and open a new way of thinking.

(Jitendra Kumar Sonber)

Contents

Synopsis

Title: Studies on the synthesis, densification and oxidation of zirconium diboride based materials

1. Introduction

Zirconium diboride (ZrB_2) is considered a leading material in the category of ultra high temperature ceramics (UHTC) due to very high melting point (3245^oC), high thermal conductivity (57.9 $Wm^{-1`}K^{-1}$), good thermal shock resistance, low coefficient of thermal expansion ($5.9x10^{-6}$ $^oC^{-1}$), retention of strength at elevated temperatures and stability in extreme environments [1-3]. ZrB_2 is considered a candidate material for hypersonic flight, atmospheric re-entry and rocket propulsion [1, 4, 5]. It gets wetted but not attacked by molten metals and hence used for holding molten metal and as thermo-well tubes in metal processing [6]. Good electrical conductivity makes it suitable for electrode application in Hall -Heroult cell and electric discharge machining [7-9].

Zirconium diboride has two major limitations, (1) poor sinterability and (2) low fracture toughness. Densification of monolithic ZrB_2 is very difficult due to strong covalent bonding and low self-diffusion [1, 10]. In this study, efforts were made to overcome these limitations by using suitable sinter additives. Zirconium diboride can be densified by liquid phase sintering or by solid phase sintering. Titanium disilicide ($TiSi_2$) and Chromium disilicide ($CrSi_2$) have been selected as sinter additives for liquid phase sintering process. These silicides have low melting point and thus can be useful in liquid phase sintering.

For solid state sintering, Europium hexaboride (EuB_6) was selected as sinter additive. EuB_6 is a boron rich boride and thus can introduce structural defects (interstitial point defects) in ZrB_2 lattice on formation of solid solution. Presence of point defects would result in enhanced diffusion and thus may be helpful in densification.

Additives are also expected to improve fracture toughness by crack deflection which could be due to presence of second phase. $TiSi_2$ and $CrSi_2$ are expected to increase the oxidation resistance of ZrB_2 by formation of silica based protective layer. Effect of EuB_6 on oxidation behavior of ZrB_2 is not reported till date. In this study, investigations were carried out in this direction.

Objective:

The first objective of present study is to carry out detailed investigation on synthesis of ZrB_2 by boron carbide reduction of ZrO_2 in presence of carbon according to reaction (1).

$$ZrO_2 + 1/2B_4C + 3/2C \rightarrow ZrB_2 + 2CO \ldots\ldots\ldots\ldots\ldots\ldots (1)$$

Though this synthesis route has been used by some researchers [11, 12], detailed results are not available in the open literature. Detailed investigations were therefore planned to study the influence of process parameters on the product quality.

The second objective is to carry out investigation on densification of ZrB_2. Effect of sinter additives ($TiSi_2$, $CrSi_2$, EuB_6) on densification of ZrB_2 was studied.

The third objective of this study is to carry out oxidation study of ZrB_2 based composites. ZrB_2 is candidate for high temperature applications and thus oxidation resistance is of vital importance.

2. Experimental Procedure

Raw materials used for synthesis of ZrB_2 were ZrO_2 (99% purity; 8.34 μm median diameter), boron carbide powder (78.5% B, 19.5%C, <1% O, 0.02% Fe, 0.02% Si, 5.34 μm median diameter; supplied by M/S Boron Carbide India) and petroleum coke (C-99.4%, 13.9 μm median dia., supplied by M/S Assam Carbon, India). All the raw materials were dried in an oven at 100°C to remove moisture content before use.

For synthesis of ZrB_2 powders, weighed quantities of ZrO_2, boron carbide and petroleum coke in various ratios were mixed thoroughly, pelletized and heated in an induction furnace at fixed temperature between 1200 and 1875 ^{o}C. Major phases of powders were identified by XRD and impurities were analyzed by chemical methods. Similar procedure was used for synthesis of EuB_6 and HfB_2 powder.

For densification, weighed quantities of fine zirconium diboride and sinter additives ($TiSi_2$/$CrSi_2$/EuB_6/HfB_2) were mixed thoroughly, filled into a graphite die and hot pressed at temperatures of 1650 ^{o}C to 1850°C under a pressure of 20 to 35 MPa for 60 minutes in a high vacuum (1×10^{-5} mbar) chamber. Hardness was measured on the polished surface at a load of 100 g and dwell time of 10 sec. The indentation fracture toughness (K_{IC}) data were evaluated by crack length measurement of the crack pattern formed around Vickers indents. Fractured surface of dense pellets was analyzed by scanning electron microscope.

Oxidation tests were conducted in a resistance heated furnace. The samples were oxidized for different time intervals (0.5, 1, 2, 4, 8, 16, 32, and 64 h) at 900 ◦C. The samples were weighed before and after exposure, to determine the weight change during the oxidation process. The oxidation products were identified using XRD. The morphology and nature of oxide layer was elucidated by observing the surface in a scanning electron microscope (SEM).

3. Results and discussion

This chapter summarizes the results obtained during the various experiments giving details of starting powder preparations till microstructural and mechanical characterization. This chapter is divided into three major sections representative for the three phases in the research: section-3.1 on synthesis of boride powders, section-3.2 on densification, mechanical properties and microstructure and section- 3.3 on oxidation study of prepared composites.

3.1 Synthesis

Experiments were carried out to study the effect of process parameters on synthesis of boride powders. ZrB_2, EuB_6, and HfB_2 powders were synthesized by boron carbide reduction of respective oxides.

3.1.1 ZrB_2 synthesis

Studies were carried out to prepare pure ZrB_2 containing oxygen less than 1.0 wt%. Oxygen is an impurity in boride powders, which reduces its sinterability.

A stoichiometric charge mixture (according to reaction 1) was heated at various temperatures from 1200°C to 1800°C and weight loss during the experiment is recorded.

$$ZrO_2 + 1/2B_4C + 3/2C \rightarrow ZrB_2 + 2CO \quad \ldots\ldots(1)$$

Weight loss in the reaction is due to formation of carbon mono-oxide. The theoretical weight loss after completion of reaction is 33 wt % of charge. The observed weight loss gives indication for completion of reaction.

The obtained product was analyzed by XRD and chemical analysis. Results on synthesis of ZrB_2 is summarized in Table-1

Table 1 Effect of temperature and charge composition on ZrB_2 synthesis

S.No.	Molar ratio ZrO_2: B_4C: C	Temperature (^oC)	Weight loss (wt.%)	Phases present in XRD pattern	Carbon (wt.%)	Oxygen (wt.%)
1.	2: 1: 3	1200	18.47	ZrB_2, ZrO_2	9.7	5.2
2.	2: 1: 3	1400	27.15	ZrB_2, ZrO_2	8.2	2.4
3.	2: 1: 3	1650	30.28	ZrB_2, ZrB, ZrO_2 ,C	7.3	2.4
4.	2: 1: 3	1700	31.66	ZrB_2, ZrB, C	3.5	2.0
5.	2: 1: 3	1800	33.04	ZrB_2, ZrB, C	3.2	0.5
6.	2: 1.1: 2.7	1800	32.67	ZrB_2	1.3	1.5
7.	2: 1.1: 2.7	1875	33.01	ZrB_2	0.06	0.5

It was found that weight loss is close to theoretical loss (33 wt.%) at 1800 ^oC but the product is composed of ZrB_2, ZrB and carbon phases. The presence of boron deficient phase (ZrB) even after the treatment at 1800 ^oC indicates the loss of boron from the charge, which could occur by following reaction.

$$ZrO_2 + 3/4B_4C = ZrB_2 + 1/2B_2O_3 + 1/2CO + 1/4C \quad \ldots\ldots\ldots\ldots\ldots\ldots\ldots\ldots(2)$$

Single phase ZrB_2 was obtained by modifying the charge composition by increasing the B_4C content and reducing the carbon content in the charge. To further reduce the carbon and oxygen content in the product, the synthesis temperature was increased to 1875 ^oC.

3.1.2 EuB_6 synthesis

In this study, EuB_6 was used as sinter additive to ZrB_2. It was synthesized by reduction of Eu_2O_3 by B_4C according to reaction (3).

$$Eu_2O_3 + 3B_4C \rightarrow 2EuB_6 + 3CO \quad \ldots\ldots(3)$$

Stochiometric mixture as per reaction (3) was heated between 1200 to 1400^oC in vacuum for 2 hours and then the product was analyzed by XRD and chemical analysis. At 1200^oC, weight loss is only 2.65% and product is composed of both EuB_6 and Eu_2O_3 phases. At 1300 ^oC, loss in weight is 19.56 %, which is higher than the theoretical loss of 16.23%. Though the product contains only EuB_6, its carbon and oxygen content is high at 3.8 and 2.1% respectively. On increasing synthesis temperature to 1400 ^oC, oxygen content of the product was decreased to 0.4% and relatively pure EuB_6 has been formed. Product obtained at 1400 ^oC contains 2.6% carbon. The higher carbon content and higher weight loss could be due to the formation of volatile boron oxide during reaction. To reduce carbon in the product, the charge was modified by adding elemental boron and lowering B_4C addition. Carbon content was reduced to 0.7 % by using modified charge.

3.1.3 HfB_2 synthesis

In this study, HfB_2 was used as sinter additive to ZrB_2. It was synthesized by reduction of HfO_2 by B_4C in presence of carbon according to reaction (4).

$$HfO_2 + 1/2B_4C + 3/2C \rightarrow HfB_2 + 2CO \quad \ldots\ldots(4)$$

The synthesis was carried out at 1875 ^oC in vacuum. The product obtained was found to be pure HfB_2 containing 0.5% Oxygen and 0.4 % Carbon.

3.2 Densification, mechanical properties and microstructure

This section describes the results on densification, mechanical properties and microstructural characterization of prepared composites. Densification studies were carried out on monolithic ZrB_2 by pressureless sintering and hot pressing. Effect of sinter additives on densification, mechanical properties and microstructure were investigated.

3.2.1 Monolithic ZrB_2

Pressureless sintering experiments were carried out in vacuum induction furnace in the temperature range of 1800-2000^oC. Pressureless sintering has resulted in maximum density of 78% only. In Hot pressing ZrB_2 was densified to near theoretical density at 1850^oC and 35 MPa pressure. Hardness and fracture toughness values were measured as 23.95 GPa and 3.31 MPa.m$^{1/2}$ respectively. Fractured surface of the dense bodies revealed that intergranular fracture is predominant mechanism. Regular faceted grains of 4-6 micron are visible.

3.2.2 Effect of $TiSi_2$ addition

Effect of $TiSi_2$ on densification of ZrB_2 was investigated. Addition of 10% $TiSi_2$ lowered the hot pressing temperature to 1650^oC from 1850^oC, which was required for monolithic ZrB_2. The enhanced sintering is attributed to liquid phase sintering resulted by formation of $ZrSi_2$ which forms during hot pressing. Formation of $ZrSi_2$ phase was observed by XRD analysis and SEM –EDS analysis of hot pressed sample. $ZrSi_2$ has low melting point (1620 ^oC) and hence results in liquid phase sintering. XRD pattern of the dense pellets indicated the presence of crystalline ZrB_2 and $ZrSi_2$. Zirconium disilicide is formed during sintering by the following reaction.

$$ZrB_2 + TiSi_2 \rightarrow ZrSi_2 + TiB_2 \quad \ldots\ldots(6)$$

The reaction is thermodynamically feasible at temperatures higher than 1100 K. TiB_2 was not observed as separate phase as it formed solid solution with ZrB_2. The formation of solid solution was confirmed by elemental analysis of different phases observed in microstructure.

Hardness of ZrB_2 + 10%$TiSi_2$ sample is measured as 19.5 GPa which is lower than that of monolithic ZrB_2 (23.91 GPa). The lower hardness is due to the presence of relatively soft phase $ZrSi_2$ which was formed during hot pressing. To compensate the hardness reduction, HfB_2 was added and two more samples of composition (a) ZrB_2+10%$TiSi_2$+10%HfB_2 and (b) ZrB_2+10%$TiSi_2$+20%HfB_2 were also prepared. Near theoretical density was obtained in both the samples at 1650 ^oC and 20 MPa. Hardness of ZrB_2+10%$TiSi_2$+10%HfB_2 was measured as 23.08 GPa, which is comparable to that of monolithic ZrB_2.

Fracture toughness of ZrB_2 + 10%$TiSi_2$ was measured as 6.36 MPa.$m^{1/2}$ which is higher than that of the monolithic ZrB_2. The increased fracture toughness is due to crack deflection. Thermal expansion mismatch between the matrix and second phase results in residual stresses which causes crack deflection. Crack deflections were found in the microstructure.

3.2.3 Effect of $CrSi_2$ addition

Effect of $CrSi_2$ addition on densification and properties of ZrB_2 was studied. It was observed that $CrSi_2$ has similar effects as $TiSi_2$ on densification and properties of ZrB_2. Addition of $CrSi_2$ lowered the densification temperature, lowered the hardness and increased the fracture toughness.

3.2.4 Effect of EuB_6 addition

Effect of EuB_6 addition on densification and properties of ZrB_2 was investigated. EuB_6 is a boron rich additive, which is expected to create structural defects (interstitial point defects) in ZrB_2 lattice on formation of solid solution and thus can enhance the densification. Addition of 2.5 weight% EuB_6 resulted in densification of 98.3% ρ_{th} at a temperature of 1750 ^oC and a pressure of 35 MPa. Composites with 5% EuB_6 was also hot pressed up to 98.1% density at similar processing conditions. A density of 96.0% was achieved in ZrB_2+10%EuB_6 composite. In case of monolithic ZrB_2, a near full density (99.8% TD) was obtained at a higher temperature and pressure of 1850 ^oC and 35 MPa respectively. In this case, the hot pressing temperature was lower by 100^oC. Addition of EuB_6 to ZrB_2 results in the formation of solid solution of ZrB_2 and EuB_6. On the formation of ZrB_2-EuB_6 solid solution, Eu will go to Zr site and Boron will go to boron site. Due to large number of boron atoms from EuB_6, there will be formation of point defects in ZrB_2. The point defects are known to enhance the diffusional mass transfer and thus assist in densification at slightly lower temperature. Formation of solid solution was confirmed by elemental analysis (EDS) of phases present in microstructure and change in lattice parameter measured by XRD.BSE image of ZrB_2 + 10%EuB_6 sample (Fig.1) has shown the presence of light gray matrix in which dark gray phase is dispersed. In EDS spectra, dark gray phase was analyzed to contain only Zr and B indicating that it is ZrB_2. The light gray matrix was analyzed to contain Zr, Eu and B indicating the formation of ZrB_2-EuB_6 solid solution. XRD pattern of the dense pellet of ZrB_2+10%EuB_6 indicates the presence of crystalline ZrB_2, EuB_6 and carbon. Presence of EuB_6 in XRD pattern indicates that the ZrB_2 and EuB_6 does not form complete solid solution and so EuB_6 is also present as second phase in the composite.

Hardness of monolithic sample was measured as 23.91 GPa, which increased to 24.8 GPa with the addition of 2.5wt% EuB_6. The increase in hardness is due to the formation of solid solution.

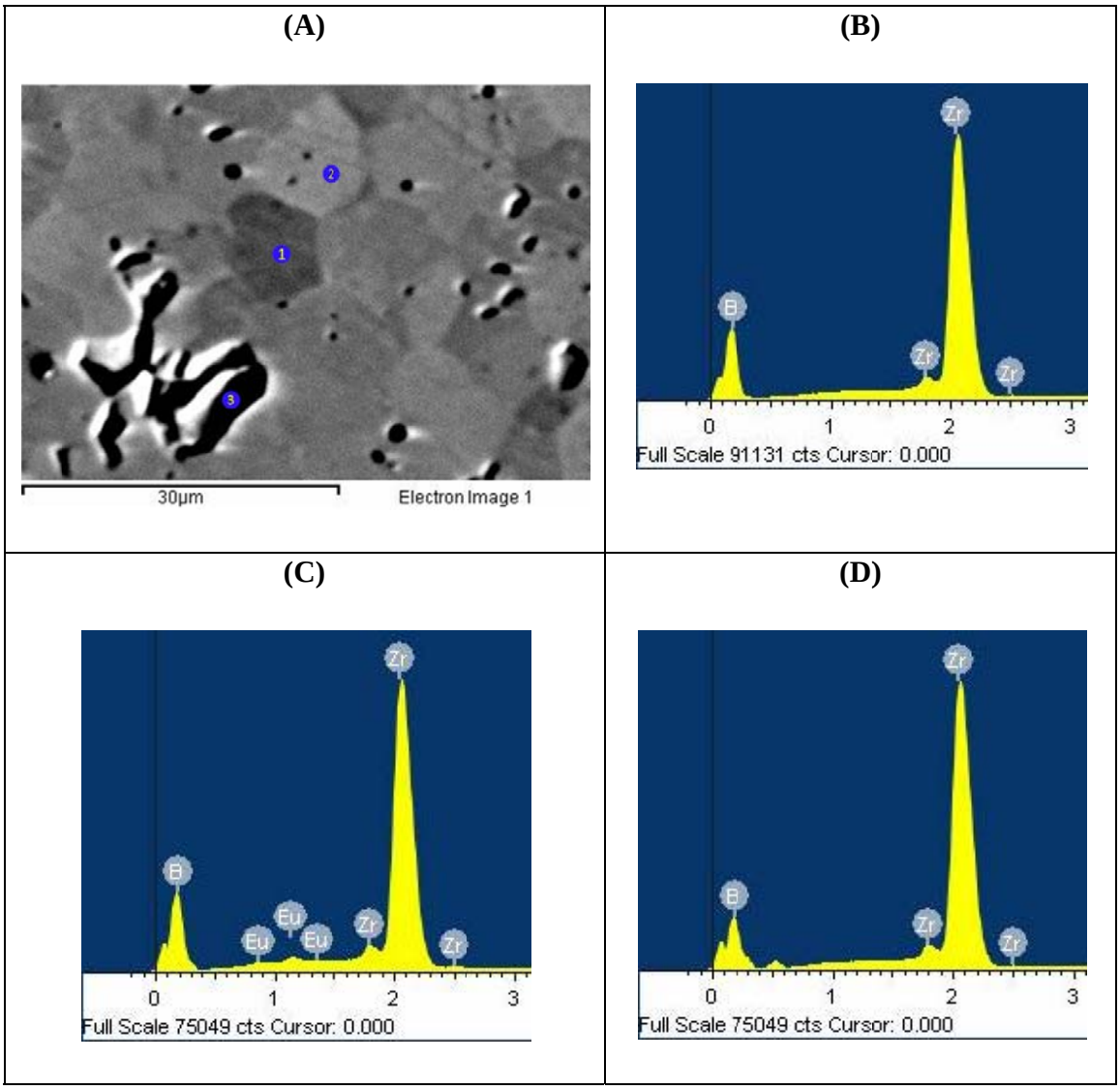

Fig.1 (A) BSE image of ZrB_2+ 5%EuB_6 (B) EDS spectra of phase marked as 1 in (A), (C) EDS spectra of phase marked as 2 in (A), and (D) EDS spectra of phase marked as 3 in (A),

3.3 Oxidation study

Non oxide ceramics are susceptible to oxidation at high temperatures. For any high temperature application in air, the material must be resistant to oxidation. In this study, oxidation test were carried out at 900 ^{o}C in air for different time interval. Following sub-sections will describe the results obtained by oxidation test of different composites.

3.3.1 Monolithic ZrB_2

The weight gain data obtained during oxidation at 900 ^{o}C as a function of time for monolithic ZrB_2 is presented in Fig 2. It shows that weight gain is linear indicating non-protective nature of oxide. The test was stopped after 32 hours as the oxide layer was broken and spalled off from the sample.

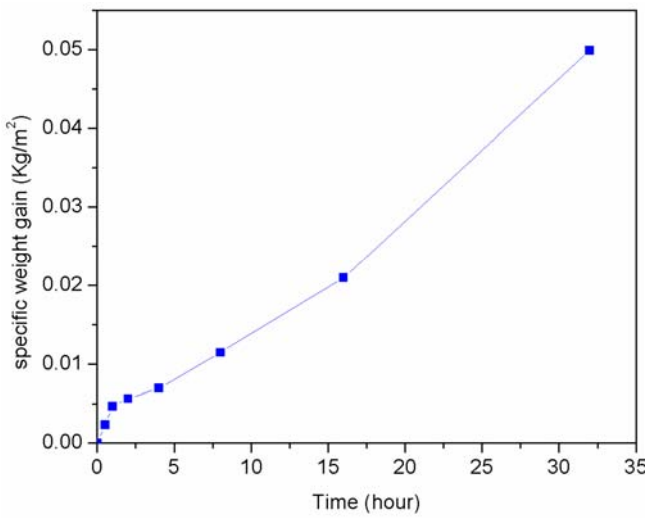

Fig. 2 Specific weight gain vs. time plot for monolithic ZrB_2 at 900 ^{o}C in air

3.3.2 Effect of $TiSi_2$ and HfB_2 addition

The weight gain data obtained during oxidation at 900 ^{o}C as a function of time for ZrB_2 composites containing $TiSi_2$ and HfB_2 are presented in Fig.3. Continuous weight gain with time is observed in all the samples. In case of composites, the rate of oxidation was found to decrease with

increase in time which indicates the formation of protective layer. In monolithic ZrB_2, oxidation rate was found to be constant. Samples containing HfB_2 has shown highest oxidation resistance.

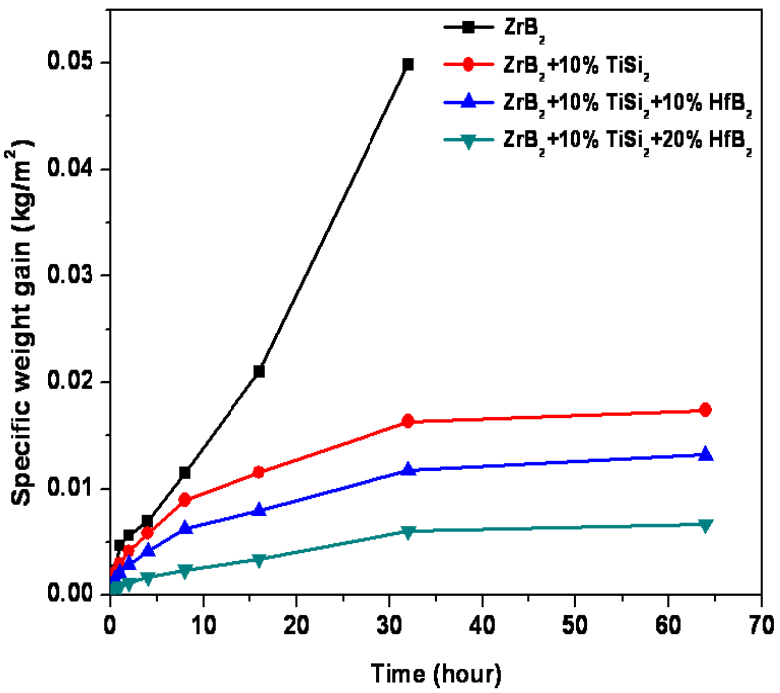

Fig. 3 Specific weight gain vs time plot for ZrB_2 based composites.

Better oxidation resistance of the composite samples is attributed to the formation of silica based glassy layer. SEM microstructures of oxidized surfaces evidently showed the formation of protective glassy phase. The glassy phase was analysed by EDS to contain mainly silicon (~ 46 at%) and oxygen (~52 at%). Zirconium (~ 0.8 at%) and titanium (~0.2 at%) are also present in very small quantity.

3.3.3 Effect of $CrSi_2$ and HfB_2 addition

Oxidation study of ZrB_2 +10%$CrSi_2$ and ZrB_2+10%$CrSi_2$+10%HfB_2 samples were carried out at 900 ^oC for 64 hour. Both the samples have shown continuous weight gain with time. However, the rate of oxidation is found to decrease with increase in time which indicates the formation of protective layer. The final weight gain in ZrB_2+10%$CrSi_2$ sample is 0.0397 kg/m^2 after 64 hours whereas in ZrB_2+10%$CrSi_2$+10%HfB_2 sample is 0.0171 kg/m^2 which is lower. The lower weight gain in the HfB_2 containing sample could be attributed to lower diffusivity of oxygen ion through HfO_2 [13,14].

3.3.5 Effect of EuB_6 addition

Oxidation study of ZrB_2 +2.5%EuB_6, ZrB_2 +5%EuB_6 and ZrB_2 +10%EuB_6 samples were carried out at 900 ^oC for 64 hour. All the three samples have shown continuous weight gain with time (Fig.4). In the initial 8 hours, the weight gain is very small which increases during the exposure at 8-16 hour and then the rate of oxidation gets decreased. The decrease in rate of oxidation after 16 hour is due to the formation of a protective layer. The oxidized layer was analyzed by EDS to contain mainly zirconium (~21.67 at%) Europium (6.49 at %) and oxygen (~71.84 at%).

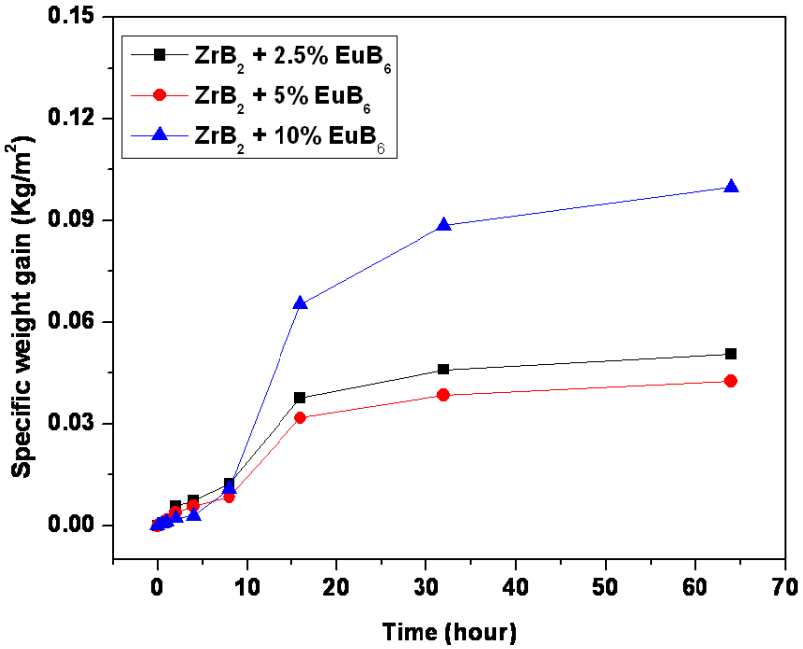

Fig. 4 Specific weight gain vs time in ZrB_2 based composite samples oxidized at 900^oC

4. Conclusion

The major findings of the present thesis have been summarized below.

- Heating of stoichiometric charge for synthesis of ZrB_2 by boron carbide reduction of zirconia in presence of carbon results in formation of ZrB phase along with ZrB_2. This boron deficient phase is formed due to loss of boron in the form of its volatile oxides.
- The boron deficient phase ZrB can be avoided and single phase ZrB_2 can be obtained by adjusting the molar ratio of charge by increasing B_4C and reducing carbon.

- Synthesis of pure ZrB_2 by this method requires a temperature of 1875 ^oC. The High temperature is required due to low diffusivity of all the elements through boride phase which is predominantly covalently bonded.
- Synthesis of single phase EuB_6 is possible by using the stoichiometric charge but the product contains around 2% carbon which can be reduced by addition of elemental boron in the charge mixture.
- Synthesis of pure EuB_6 is possible at temperature of 1400 ^oC, which is relatively lower than that required for ZrB_2.
- Pressureless sintering of Monolithic ZrB_2 results in maximum density of 78% at 2000 ^oC. Near theoretical density of Monolithic ZrB_2 can be obtained by hot pressing at 1850 ^oC and 35 MPa pressure for 2 hour
- Addition of $TiSi_2$ or $CrSi_2$ lowers the hot pressing temperature by 200 ^oC. This decrease is attributed to liquid phase sintering caused by reaction product $ZrSi_2$ which forms during hot pressing.
- Addition of EuB_6 lowers the hot pressing temperature by 100 ^oC. This is due to the formation of solid solution of ZrB_2 and EuB_6 which in turn results in the formation of point defects and diffusion is enhanced.
- $TiSi_2$ and $CrSi_2$ addition results in formation of $ZrSi_2$ which is responsible of liquid phase sintering.
- EuB_6 is only partially soluble in ZrB_2 and also exist as a distinct phase in the material.
- $TiSi_2$ and $CrSi_2$ addition has resulted in lower hardness whereas EuB_6 addition has increased the hardness.
- Fracture toughness values of all composite samples are higher than the monolithic sample. This is due to crack deflection caused by the presence of second phase in microstructure.
- Monolithic ZrB_2 does not have good oxidation resistance at 900 ^oC. Linear oxidation kinetics was observed in case of monolithic ZrB_2.
- $TiSi_2$, $CrSi_2$ addition as well as EuB_6 addition has improved the oxidation resistance of ZrB_2 at the temperature of 900 ^oC. The good oxidation resistance is due to the formation of protective oxide layer.

5. References:

1. Fahrenholtz WG and. Hilmas GE. Refractory diborides of zirconium and hafnium. J Am Ceram Soc 2007; 90(5):1347-64.
2. Bauccio ML. ASM Engineered Materials Reference book. United States of America: ASM International;1994.
3. Upadhyay K, Yang JM and Hoffman WP. Materials for ultrahigh temperature structural application. Am Ceram Soc Bull 1997;76: 51-6.
4. Opeka MM,. Talmy IG and Zaykoski JA. Oxidation-based materials selection for 2000°C + hypersonic aerosurfaces: Theoretical considerations and historical experience. J Mater Sci 2004;39: 5887-904.
5. Levine SR, Opila EJ, Halbig MC, Kiser JD, Singh M and Salem JA. Evaluation of ultra-high temperature ceramics for aeropropulsion use. J Euro Ceram Soc 2002;22: 2757-67
6. Mroz C. Annual Mineral review: zirconium diboride. Am Ceram Soc Bull 1995; 74:164-5
7. Mroz C. Annual Mineral review: zirconium diboride. Am Ceram Soc Bull 1994; 73:141-2.
8. Zaw HM, Fuh JYH, Nee AYC and Lu L.Formation of a new EDM electrode material using sintering techniques. J Mater Process Techno 1999;89-90:182-6.
9. Khanra AK, Sarkar BR, Bhattacharya B, Pathak LC and Godkhindi MM. Performance of ZrB_2-Cu composite as an EDM electrode. J Mater Process Techno 2007;83:122-6.
10. Matkovich VI. Boron and refractory borides. New York: Springler – Verlag;1977.
11. Zhao H, He Y and Jin Z. Preparation of zirconium boride powder. J Am Ceram Soc 1995;78(9):2534-36.
12. WM Guo and GJ Zhang: 'Reaction processes and characterization of zrb_2 powder prepared by boro/carbothermal reduction of ZrO_2 in vacuum', *J. Am. Ceram. Soc.,* 2009, 92, (1), 264–267.
13. Mallik M, Ray KK and Mitra R. Oxidation behavior of hot pressed ZrB_2–SiC and HfB_2–SiC composites. J Euro Ceram Soc 2011;31:199–215.
14. Parthasarathy TA, Rapp RA, Opeka M, Kerans RJ. Effects of phase change and oxygen permeability in oxide scales on oxidation kinetics of ZrB_2 and HfB_2. J Am Ceram Soc 2009;**92**(5):1079–86.

List of Tables and Figures

List of Tables: **Page No.**

List of Figures

Page No.

Acronyms

T	Temperature
K	Kelvin
^{o}C	Degree Celsius
Wt.%	Weight percent
at%	Atom percent
ΔG	Gibbs Free energy change
min	Minutes
Å	Angstrom
nm	nanometer
µm	Micrometer
mm	millimeter
D_{50}	median particle diameter
m	meter
gm	gram
kg	kilogram
h	hour
Sub	Substrate
H_V	Vickers's hardness
K_{IC}	Fracture Toughness
E	Young's Modulus
P	Applied load
c	half crack length
λ	wavelength
d	Inter planar spacing
GPa	Giga Pascal
MPa	Mega Pascal

w	whiskers
Re	Rare earth
WC	Tungsten carbide
atm	atmosphere
Pa	Pascal
mbar	mili bar
kV	Kilo Volt
kJ	Kilo Joule
cc	Cubic centimeter
ρ_{th}	Theoretical density
A	Surface area
Δw	Change in weight
K_m	General rate constant
K_p	parabolic rate constant
t	time
m	General rate equation exponent

Chapter –1

Introduction

Chapter-1

Introduction

Zirconium diboride (ZrB_2) is considered a leading material in the category of ultra high temperature ceramics (UHTC) due to very high melting point (3245^oC), high thermal conductivity (57.9 $Wm^{-1`}K^{-1}$), good thermal shock resistance, low coefficient of thermal expansion ($5.9x10^{-6}$ K^{-1}), retention of strength at elevated temperatures and stability in extreme environments [1-3]. ZrB_2 is considered a candidate material for hypersonic vehicle, atmospheric re-entry and rocket propulsion [1, 4, 5]. It gets wetted but not attacked by molten metals and hence used for holding molten metal and as thermo-well tubes in metal processing [6]. Good electrical conductivity makes it suitable for electrode application in Hall -Heroult cell and electric discharge machining [7-9].

ZrB_2 crystallizes into a hexagonal crystal structure of the AlB_2 type. This crystal structure consists of alternating layers of hexagonally closed packed metal atoms (M) and graphite-like boron (B). This structure results in strong covalent bonding between boron–boron and metal–boron atoms, while the close packed metal layers exhibit characteristics consistent with metallic bonding. The combination of covalent and metallic bonding gives ZrB_2 an unusual combination of properties. The strong covalent bonding leads to a
high melting temperature, high hardness and strength. The metallic bonding leads to high electrical and thermal conductivity.

ZrB_2 can be synthesized by (a) reaction between Zr and B [10] (b) borothermic reduction of ZrO_2 [11], (c) carbothermic reduction of ZrO_2 in presence of B_4C [12], (d) carbothermic reduction of ZrO_2 and B_2O_3 [1] (e) Metallothermic reduction of ZrO_2 and B_2O_3 [13-15] and (f) chemical vapour deposition [16-18]. Synthesis of ZrB_2 from its elements is uneconomical due to the high cost of both Zr and B powders. Borothermic reduction of ZrO_2 to obtain ZrB_2 also involves use of expensive boron powder. In carbothermic reduction of ZrO_2 and B_2O_3, loss of boron occurs due to evaporation of boron oxides during the reaction and the product is not pure ZrB_2 but a mixture of borides of different B/Zr atom ratio. In case of metallothermic reduction of ZrO_2 and B_2O_3 the product gets contaminated with the metal borides of reductant

metal. ZrB_2 powder can also be synthesized by SHS reaction between ZrO_2, B_2O_3 and Mg. Chemical vapor deposition techniques are suitable for coating and not for bulk production of powders.

Preparation of ZrB_2 by carbothermic reduction of ZrO_2 in presence of B_4C [12] according to reaction (1) seems to be an attractive route since it involves use of easily available raw materials and may results in pure boride with minimum boron loss.

$$ZrO_2 + 1/2B_4C + 3/2C \rightarrow ZrB_2 + 2CO\uparrow \ldots\ldots\ldots\ldots\ldots\ldots(1)$$

In this study, this route was used for synthesis of ZrB_2 powder. Detailed studies were carried out on synthesis process and the influence of process parameters on the yield and the product quality was investigated.

Zirconium diboride has two major limitations, (1) poor sinterability and (2) low fracture toughness. Densification of monolithic ZrB_2 is very difficult due to strong covalent bonding and low self-diffusion [1, 10]. In this study, efforts were made to overcome these limitations by using suitable sinter additives. Zirconium diboride can be densified by liquid phase sintering or by solid phase sintering. Titanium disilicide ($TiSi_2$) and Chromium disilicide ($CrSi_2$) have been selected as sinter additives for liquid phase sintering process. These silicides have low melting point and thus can be useful in liquid phase sintering. For solid state sintering, Europium hexaboride (EuB_6) was selected as sinter additive. EuB_6 is a boron rich boride and thus can introduce point defects in ZrB_2 lattice on formation of solid solution. Presence of point defects would result in enhanced diffusion and thus may be helpful in densification. Additives are also expected to improve fracture toughness by crack deflection which could be due to presence of second phase. $TiSi_2$ and $CrSi_2$ are expected to increase the oxidation resistance of ZrB_2 by formation of silica based protective layer. Effect of EuB_6 on oxidation behavior of ZrB_2 is not reported till date, which has been one of the objectives of the present investigation. In this study, investigations were carried out in this direction.

ZrB_2 is a non oxide ceramic material and hence is susceptible to oxidation in air at high temperature. For any application in air atmosphere at high temperature, material must have sufficient oxidation resistance. In this study, investigations were carried out on oxidation of ZrB_2 based materials in air at 900 ^oC.

Objectives and workplan of present study

The objectives of this study can be divided in three categories. (1) Studies on synthesis (2) studies on densification and (3) studies on oxidation behavior of ZrB_2 based material.

Studies on synthesis:

The objective is to carry out a detailed investigation on synthesis of ZrB_2 by carbothermic reduction of ZrO_2 in presence of boron carbide. It was planned to carry out different experiments by varying temperature and charge composition and analyze the product by XRD and chemical analysis. Based on XRD and chemical analysis results the process parameters were fixed to produce pure powder which is used in densification studies.

Studies on densification

The objectives of densification studies are listed below.

- Study on densification of ZrB_2 with and without additive by hot pressing
- Study the effect of silicide ($TiSi_2$, $CrSi_2$) addition on densification and properties of ZrB_2
- Study the effect of hexaboride (EuB_6) addition on densification and properties of ZrB_2

It was planned to carry out hot pressing experiments by varying the additive content and characterizing the densified pellets by measuring the density, hardness and fracture toughness. It was planned to analyze the sintering mechanism with the help of XRD analysis and microstructural characterization. It was also planned to analyze the effect of sinter additives on oxidation resistance of developed composites.

Studies on oxidation behavior

The objective is to carry out a study on oxidation of ZrB_2 based materials at high temperature in air atmosphere. It was planned to carry out isothermal oxidation study at certain temperature for different time interval. It was planned to analyze the oxidation mechanism by analyzing the specific weight gain in the sample with holding time and by characterizing the oxidized surface by X-Ray diffraction and scanning electron microscopy.

Chapter –2

Background Literature

Contents

Chapter –2

Background Literature

A detailed literature survey on the synthesis, densification and oxidation of ZrB_2 is presented. ZrB_2 can be synthesized by various routes. This chapter gives the details of different methods used for ZrB_2 synthesis. Merits and demerits of different process routes have been described. Issues related with densification of ZrB_2 were discussed in the chapter. Literature available on densification of ZrB_2 is discussed in details. Effect of sintering additives on densification and properties was discussed. Literature review on oxidation behaviour of ZrB_2 based materials is also presented.

2.1 Synthesis of Zirconium Diboride:

The powder characteristics such as purity, morphology, surface area, defects concentration strongly influence the sinterability of powder. All these properties are determined by the synthesis conditions. Thus selection of synthesis route and processing parameters are of vital importance in the actual application of the powder. In this section different routes of ZrB_2 synthesis will be discussed. ZrB_2 can be synthesized by (a) synthesis from elements [10] (b) borothermic reduction of zirconia [11], (c) carbothermic reduction of zirconia in presence of boron carbide [12], (d) carbothermic reduction of ZrO_2 and B_2O_3 [1](e) Metallothermic reduction of ZrO_2 and B_2O_3 [13-15] and (f) molten salt electrolysis [19] (g) solution based techniques [20] (h) synthesis from polymer precursors [21] (i) chemical vapor deposition [16-18].

2.1.1 Synthesis from elements:

Reaction between elemental boron and zirconium can have excellent control on the stoichiometry of the resultant zirconium diboride. This route gives pure ZrB_2 but cannot be considered for commercial production as it involves expensive charge materials. This route can

give dense bodies by hot pressing of mixed powder if the reaction with die is avoided. To avoid any reaction with the die, the graphite die is coated with boron nitride.

As the formation of ZrB_2 ceramic from elemental powders is thermodynamically favorable (ΔG^0_{2000K} = -279.6 kJ /mol), this route can also be used to produce ZrB_2 by self propagating high temperature synthesis. SHS is a technique that takes advantage of the high exothermic energy of chemical reactions to generate high-temperature and fast combustion reactions. Some of the advantages of SHS, with respect to many traditional solid state synthesis routes, are the high purity of the products, short process times (typically on the order of few second or less), and the low energy consumption (limited to the ignition step), as well as low cost of the experimental apparatus. ZrB_2 powders formed using SHS have exhibited increased sinterability, which has been attributed to the presence of lattice defects. These defects were attributed to the rapid heating and cooling rates (~200,000 K/min) associated with SHS. However, rapid heating rates can also result in incomplete reaction, the formation of non-equilibrium phases, the formation of stable oxides, or the retention of large amounts of porosity (>50%).

In the last decade, there has been a growing interest on the production of nanosized ceramic particles. Exceptional properties such as excellent sinterability of nano-powder and improved mechanical properties of the formed nano-grained materials are the motivation for this appeal. Camrulu *et al.*[22] have prepared nano size ZrB_2 powder via SHS by using Zr and B as starting material. Addition of 5-10% NaCl decreases adiabatic temperature of the reactions, reaction wave velocity, average crystallite size and particle size of the formed ZrB_2. Chamberlain *et al.* [23] reported the formation of ZrB_2 by reaction of attrition milled Zr and boron powder on heating at 600 ^oC for 6 hours. Nanoscale ZrB_2 particles were formed using elemental Zr and B. The Zr and B precursors, with average crystallite sizes of ~10 nm, were produced by attrition milling and then reacted to produce nanosized ZrB_2 crystallites. Because of the fine precursor particle size and the intimate mixing, the reaction of Zr and B to ZrB_2 went to completion at 600 ◦C. Tsuchida *et al.*[24] have prepared ZrB_2-ZrC composite by Mechanical activation assisted SHS using a mixture of Zr, B and C powder. Table 2.1 summarizes the work reported on synthesis of ZrB_2 from its elements [22-26].

Table 2.1 Synthesis of ZrB_2 by reaction between its elements

Reactant	Processing conditions	Product quality	Reference
Zr + B	SHS, 30%NaCl, Ar	<200 nm	22
Zr + B	600, 6 hours	Fine particles	23
Zr + B	SHS, Ar	Zr =80.7% B =19.1%	25
Zr + B	2000, 1 hour	72% dense pellet	26
Zr + B + C	SHS, Air	ZrB_2 + ZrC	24

2.1.2 Borothermic reduction of ZrO_2:

Borothermic reduction of ZrO_2 gives pure ZrB_2 at temperature higher than 1600°C. This method is not economical for commercial production as it involves the loss of expensive boron in the form of boron oxide. Excess boron is required to be added to get stoichiometric ZrB_2. Peshev *et al.*[11] have reported the preparation of ZrB_2 by borothermic reduction of ZrO_2 in vacuum at 1750°C for 1 hour. It is noticed that boron content in the product is less than theoretical value which could be due to the loss of boron in the form of oxide. Millet *et al.*[27] have prepared ZrB_2 by reaction of ZrO_2 and boron (milled for 70 hours) at 1100°C in vacuum. XRD results had shown the presence of ZrO_2 along with ZrB_2 product. The use of mechanical milling enhanced the reactivity of powder and thus the reaction temperature is brought down considerably. Such activation is due to two main effects: (i) intimate mixing at the chemical level as a result of particle size reduction and impacts, and (ii) introduction of lattice imperfections into ZrO_2 grains during milling [27].

Ran *et al.*[28] have studied the borothermic reduction process by using nanometric ZrO_2 powder. B_2O_3 was identified as a possible intermediate reaction product. ZrO_2 completely

converted to ZrB_2 when thermally treated at 1000^oC for 2 h in vacuum, but the removal of residual boron-related species required a temperature above 1500^oC. ZrB_2 powders obtained at 1000–1200 ^oC showed a faceted morphology, whereas those prepared above 1500 ^oC had a nearly spherical morphology. The particle size that was calculated from the measured surface area increased with the increasing synthesis temperature from 0.15 µm at 1000 ^oC to 0.66 µm at 1650 ^oC. The oxygen content of the ZrB_2 powders synthesized at 1650 ^oC was as low as 0.43 wt%.

2.1.3 Carbothermic reduction of ZrO_2 in presence of boron carbide

This is another interesting method for synthesis of ZrB_2, as it involves relatively less expensive charge material. ZrB_2 powder is prepared by reaction (2.1) at a temperature of higher than 1800^oC and holding time of more than 1 hour.

$$ZrO_2 + 1/2B_4C + 3/2C \rightarrow ZrB_2 + + 4CO \quad \text{.....(2.1)}$$

Guo *et al*.[29-30] have studied the boron carbide reduction of ZrO_2 for synthesis of ZrB_2. Another phase, ZrC was observed alongwith ZrB_2. The presence of the ZrC phase in the synthesized powder was mainly attributed to the vaporization and removal of the intermediate B_2O_3 product. With the increase of B_4C, ZrC phase gradually decreased. When B_4C was in a 20-25 wt% excess, the ZrC phase disappeared and only ZrB_2 phase existed in powder. In the present work, investigation has been carried out on synthesis of ZrB_2 using this route.

2.1.4 Metallothermic reduction of ZrO_2 and B_2O_3

Metallothermic reduction of ZrO_2 and B_2O_3 involves cheap raw material and are self sustainable due to their exothermic nature. Mostly magnesium is used as reducing agent and ZrB_2 powder is prepared by using reaction (2.2).

$$ZrO_2 + B_2O_3 + 5Mg \rightarrow ZrB_2 + 5MgO \quad (2.2)$$

The use of magnesium as the reductant instead of aluminum allowed acid leaching of the unwanted oxide product leaving behind a pure boride phase. In any process for the formation of ZrB_2, it would be necessary to ensure that all of the ZrO_2 is consumed by reaction as ZrO_2 is difficult to remove by dissolution. This could be achieved by using a stoichiometric excess of both Mg and B_2O_3. Mechanical alloying technique can be exploited in this route to reduce the reaction temperature and time. The loss of B_2O_3 and the formation of non stoichiometric powder are some issues in this route. As the reactions are exothermic, this synthesis route can utilize SHS process. It is predicted that, due to high rate of heating and cooling the SHS process will introduce higher concentration of defect structures in the raw powder. These defects play an important role in various physical and chemical phenomena, particularly at high temperatures. For example, the high defect concentration in the SHS produced powders is expected to enhance the mass transfer processes during sintering, which may lower the sintering temperatures. As production of ZrB_2 powder through self-propagating high-temperature synthesis (SHS) from ZrO_2, Mg and H_3BO_3 mixture often leads to incomplete conversion, Khanra *et al.*[31] have developed a new technique, called DSHS (double SHS), wherein the reaction product of the first SHS is mixed with calculated amounts of Mg and H_3BO_3 powder and subjected to a second SHS.

The ZrB_2 powder produced by DSHS technique yields increased conversion. The NaCl is used as a diluent during SHS to control the particle size of the product. The average particle size of SHS ZrB_2 powder found to be 75–125nm in range, which decrease to 25–40 nm after DSHS.

Nishiyama *et al.*[14] have synthesized ZrB_2 by magnesiothermic reduction of ZrO_2 and B_2O_3 at 800 ^oC. Setoudeh *et al.*[13] have prepared pure ZrB_2 by mechanical alloying of ZrO_2,

B_2O_3 and Mg for 15 hours. After milling, separation of the ZrB_2 from the co-product MgO was easily achieved by a mild acid leaching leaving essentially pure ZrB_2 with a crystallite size of ~75 nm. Mishra *et al.*[15,32,33] have used SHS process to produce submicron ZrB_2 powder by magnesiothermic reduction. Aluminum was also reported to be used as reducing agent and ZrB_2-Al_2O_3 composite was made by this technique [34, 35]. Lee *et al.*[36] have prepared ZrB_2 by SHS using ZrO_2, B_2O_3 and Al as reactants. Fe_2O_3 and excess Al were added to produce molten product. The resulting ZrB_2 particles exhibited hexagonal or disk plate-like shapes on solidification.

Table 2.2 summarizes the work reported on metallothermic reduction route for ZrB_2 synthesis [13-15, 33-34].

Table 2.2 Synthesis of ZrB_2 by Metallothermic reduction of ZrO_2 and B_2O_3

Reactant	**Processing conditions**	**Product quality**	**Reference**
ZrO_2 + B_2O_3 + Mg	Mechanical alloying, 15 hour, Ar	Pure ZrB_2	13
ZrO_2 + B_2O_3 + Mg	800,1 hour, Ar	ZrO_2 peaks are also present with ZrB_2, D_{50} : 0.2µm	14
ZrO_2 + H_3BO_3 + Mg	SHS process	Submicron size	33
ZrO_2 + B_2O_3 + Mg	SHS process	200-1000 nm	15
ZrO_2 + B_2O_3 + Al	SHS process, Ar	ZrB_2+ Al_2O_3 composite	34

2.1.5 Carbothermic reduction of ZrO_2 and B_2O_3

Carbothermic reduction of ZrO_2 and B_2O_3 involves cheap raw material but results in the loss of B_2O_3 and the formation of non stoichiometric powder. The resultant powder also contains some residual carbon. Mishra *et al.*[15,33] have reported the synthesis of micron sized ZrB_2 powder by carbothermic reduction of ZrO_2 and B_2O_3 at 1800 ^oC in vacuum. Minor peaks of ZrO_2 were observed in the XRD pattern. Khanra *et al.*[37] have prepared ZrB_2 whiskers by reaction between zirconia, boric acid and carbon black. The synthesized product contains B_4C

and ZrC as minor phases along with ZrB_2. The whisker yield is low at lower pyrolysis temperature and maximum whisker yield is found at 1500–1700^oC. It was confirmed that, the whisker is grown by combined V–S and V–L–S mechanism. The different whisker morphologies are found with the use of different catalysts. The Ni addition seems more effective as a catalyst than Co or Fe. Shorter length whiskers are found in the case of Co catalyst, whereas use of Fe catalyst shows whisker with rod shape and a special bird's nest type whiskers. The electron microscope study of whisker reveals the presence of various defects.

2.1.6 Solution based methods

The solution based methods are effective for low-temperature synthesis of ultra-fine powders because of the formation of amorphous phases and the intimate contact of the reactants. However, very limited studies were conducted on the synthesis of metal borides using solution-phase reactions. Yan *et al.* [20] have synthesized ultra-fine zirconium diboride (ZrB_2) powders using inorganic–organic hybrid precursors of zirconium oxychloride ($ZrOCl_2 .8H_2O$), boric acid, and phenolic resin as sources of zirconia, boron oxide, and carbon, respectively. The reactions were substantially completed at a relatively low temperature (1500^oC). The synthesized powders had a smaller average crystallite size (~200 nm), a larger specific surface area (32 m^2/g), and a lower oxygen content (~1.0 wt%), which were superior to some commercially available ZrB_2 powders. Xie *et al.* [38] have studied the synthesis of zirconium diboride by solution-based processing. Zirconium n-propoxide was refluxed with 2,4-pentanedione to form zirconium diketonate. This compound hydrolyzed in a controllable fashion to form a zirconia precursor. B_2O_3 and carbon precursors were formed via solution additions of boric acid and phenol–formaldehyde, respectively. Solution was concentrated, dried, pyrolyzed (800–1100^oC, 2 h, flowing argon), and exposed to carbothermal reduction heat treatments (1150–1800^oC, 2 h, flowing argon). Spherical particles of 200–600 nm for pure ZrB_2 and ZrB_2–TaB_2 mixtures were formed.

2.1.7 Molten salt Electrolysis

From literature it is known that borides of various metals (Ti, Mg, Gd, Ta, Mo W) can be prepared by molten salt electrolysis. In case of ZrB_2, only two articles are cited. Frazer *et al.* [19] have deposited ZrB_2 from ZrO_2 and B_2O_3 dissolved in molten Na_3AlF_6 at 1020°C. Nickel was used as cathode. The graphite crucible was used as anode. A series of nickel boride diffusion compounds were also identified by electron microprobe analysis. The compounds Ni_3B, Ni_2B, Ni_4B_3 and NiB were formed quite readily at lower current densities. The ZrB_2 deposit was mainly scaly or dendritic and was usually non-adherent. Devyatkin [39] has also reported the electrosynthesis of ZrB_2 on nickel cathode from cryolite- alumina melts containing zirconium and boron oxide.

2.1.8 Synthesis by polymer precursor route:

A processable precursor to ZrB_2 can be obtained by dispersing a ZrO_2 in a boron carbide polymeric precursor. Heating the mixture then results in either the in situ generation of boron carbide and carbon followed by reaction to produce the boride or direct reaction of the polymer with the ZrO_2 to give the final boride product [21, 40]. The key requirements of the polymer component are that, it is stable, processable and contain both the boron needed to form the metal boride and carbon to aid in the removal of the oxygen. One series of polymers satisfying these criteria are the dinitrile polymers, which can be prepared in good yield from the condensation polymerization of deca-borane with dinitriles.

Su *et al*.[21,40] have obtained the polymer precursor by dispersing ZrO_2 into decaborane dicyanopentane polymer, $(-B_{10}H_{12}-NC-(CH_2)_5-CN-)_x$. Subsequent pyrolysis of the precursor at 1450°C resulted in the formation of crystalline ZrB_2.

2.1.9 Chemical vapor deposition

Chemical vapor deposition gives coating of ZrB_2 by vapor phase reaction of zirconium and boron containing gaseous precursors. $ZrCl_4$ and BCl_3 are the most commonly used

precursors and hydrogen is generally used as reducing agent. This is a low temperature route and gives good purity. This technique is more suitable for thin films and involves complex setup. In general researchers have used following reaction.

$$ZrCl_4 + 2BCl_3 + 5H_2 \rightarrow ZrB_2 + 10HCl \quad \text{.....(2.3)}$$

Temperature, pressure and flow rate of reactants are the major processing parameters, which influences the composition and structure of the product formed. Deposition rate generally increases with increase in temperature and hydrogen concentration. The deposition rate is more influenced by the hydrogen concentration in the gas mixture than by the temperature.

Motojima *et al.*[16] have obtained adherent ZrB_2 coating on Cu substrate at 700-900 ^oC using above reaction. Wang *et al.* [17] have prepared ZrB_2 coating on graphite substrate by low pressure CVD using above reaction at 1200^oC. Chen *et al.*[18] have prepared nanosized ZrB_2 powder (20 nm) by reacting $ZrCl_4$ and $NaBH_4$ in an autoclave at 700 ^oC under 1 bar pressure of Argon.

Plasma enhanced CVD has also been reported for the formation of ZrB_2. In PECVD chemical reaction takes place after the creation of plasma of reacting gases. The plasma is generally created by RF (AC) frequency or DC discharge between two electrodes, the space between which is filled with the reacting gases. The necessary energy for the chemical reaction is not introduced by heating the whole reaction chamber but just by heated gas or plasma. The deposition takes place at lower temperature as compared to traditional CVD. Since the formation of the reactive and energetic species in the gas phase occurs by collision in the gas phase, the substrate can be maintained at a low temperature. Hence, film formation can occur on substrates at a lower temperature than is possible in the conventional CVD process, which is a major advantage of PECVD. Piersion *et al.*[41] have used plasma enhanced CVD to obtain ZrB_2 coating on zircalloy-4 at 580^oC. The coating consists of ZrB_2 nanograins dispersed in amorphous solid solution of boron and zirconium oxides. Oxygen mainly comes by etching of the quartz discharge tube by Ar-BCl_3 plasma. Vapour phase reaction can also be used to form ceramic matrix composite by chemical vapor infiltration in three dimensional porous perform. Berthon *et al.*[42] have deposited ZrB_2 into carbon fiberous perform at 800 ^oC. Dilution of the reactants (BCl_3, $ZrCl_4$, H_2) by helium improves in infiltration quality.

Zirconium borohydride ($Zr(BH)_4$) is a useful single precursor for vapor phase synthesis of ZrB_2. Thermal decomposition of this compound results in ZrB_2 coating at very low temperature (100-270 ^oC). The ease of deposition of the films and their favorable mechanical and electronic properties suggest that $Zr(BH)_4$ is excellent precursor complex for ZrB_2 films useful in electronic applications. Wayda *et al.* [43] have prepared ZrB_2 coating on various substrate (quartz, sapphire and silicon) by thermal decomposition of $Zr(BH)_4$. The films were amorphous and conductive. Reich *et al.*[44] have prepared amorphous ZrB_2 coating by using $Zr(BH)_4$ as a single precursor at temperature of 150-400 ^oC.

Table 2.3 gives the comparative summary of studies reported on the synthesis of ZrB_2 by vapour phase reaction [38-41, 43-45].

Table 2.3 Synthesis of ZrB_2 by vapor phase reaction

Technique	Reactants	Process parameters	Product quality	Reference
Reaction in autoclave	$ZrCl_4$ + $NaBH_4$	T: 700 Argon: 1 bar	Nanosized powder ,20 nm	18
PECVD	$ZrCl_4$ + BCl_3 +H_2	T: 580 ^oC Substrate; zircalloy 4	Crystalline, nanograins	41
CVD	$ZrCl_4$ + BCl_3 +H_2	T: 700-900 Sub: Cu	Single phase ZrB_2, adherent	16
PECVD	$Zr(BH)_4$	T: 150-400, RF power: 80 W	amorphous	44
LPCVD	$ZrCl_4$ + BCl_3 +H_2	T: 1050-1200 Sub; graphite	Crystalline, pure H_V = 21.5-26 GPa	17
CVD	$ZrCl_4$ + BCl_3 +H_2	T: 952 Sub; graphite	Thickness: 15-30 µm	45
Thermal decomposition	$Zr(BH)_4$	T:100-270 ^oC, Sub: Si, quartz	Amorphous and conductive	43

T: Temperature

2.2. Densification of zirconium diboride:

Densification of monolithic ZrB_2 is extremely difficult due to high melting point, strong covalent bonding and low self-diffusion rates. ZrB_2 powder surface is always covered with B_2O_3 and ZrO_2 which leads to evaporation condensation mechanism that causes mass transfer without densification. At lower temperature surface diffusion and evaporation condensation mechanism are favored which results in mass transfer without densification. At higher temperature exaggerated grain growth takes place which results in poor mechanical properties. High temperature and external pressure are required to densify monolithic ZrB_2 [1, 10] Densification is achieved only above 1800^oC, when grain boundary diffusion and volume diffusion mechanisms become active. Basically there are three ways to achieve better densification in borides at low temperature and pressure.

(1) Use an additive which forms a liquid phase at sintering temperature
(2) Increase the surface energy of powder by removing the surface oxide layer
(3) Increase the defect concentration by mechanical activation

Several additives have been tried to improve the sinterability and properties of ZrB_2. Metallic additives assist in densification by liquid phase sintering but they deteriorate high temperature properties. Room temperature mechanical properties also degrade due to lower hardness of metals. Carbon and carbides (such as SiC) reacts with oxide layer on ZrB_2 and provide fresh surface of ZrB_2 which has higher surface energy. Mechanical activation results in increase in point defects which help in densification.

Sintering behavior and final properties of dense bodies are influenced by powder characteristics such as particle morphology, surface purity, particle size distribution and processing parameters such as temperature, external pressure, time, environment, heating rate etc. Unintentional impurities or processing additives, which affect both the sintering behavior and high temperature performance, are often incorporated during processing. Additives or

impurities can form low melting eutectics with UHTCs that have a deleterious effect on high temperature performance.

The consolidation processes are classified as; (i) pressureless sintering (ii) hot pressing (iii) spark plasma sintering (iv) microwave sintering and (v) laser sintering

2.2.1 Pressureless Sintering:

Pressureless sintering is a simple and economic process to produce dense compacts. This operation is carried out in two steps. In the first step green compacts with sufficient handling strength are prepared by uniaxial die compaction. These green pellets are then fired at chosen high temperatures in controlled atmosphere. Pressureless sintering is required to fabricate near-net-shape components, which will drastically reduce subsequent needs for diamond machining. The properties obtained are slightly lower than that for the hot-pressed sample and were attributed to their larger grain size. One of the crucial problems faced during sintering of borides is the exaggerated grain growth during sintering, which hinders the densification process. Following the initial stage of rapid shrinkage, excessive coarsening is induced by the partial predominance of evaporation–condensation mechanism at the densification temperatures and results in a rapid diminution of the driving force for sintering.

Despite the low-intrinsic sinterability, which is attributed to highly covalent bonds and low volume and grain boundary diffusion rates, significant advances in pressureless sintering of ZrB_2 have been made. Some applications for thermal protection systems may not require very high-mechanical strengths of fully dense materials. Lower cost processing techniques that can produce large parts in complex shapes with some porosity may find application for thermal protection, as long as the material meets some threshold strength criterion for the particular design. The material porosity may even provide some benefit by lowering the stiffness and the thermal conductivity of the part.

Full densification of monolithic ZrB_2 requires very high temperature and longer duration. Farehnholtz *et al.*[46] have reported only 78% densification of monolithic ZrB_2 by sintering at 2050°C for 2 hour. Chamberlain *et al.*[47] have obtained a density of ~98%ρ_{th} by pressure less sintering ZrB_2 at 2150°C for 9 hours. Khanra *et al.*[31] have obtained 97.5% density on sintering

at 1950°C using ZrB_2 powder prepared by SHS. The activation energy for sintering was estimated at 43 kJ for coarse and 37 kJ for fine SHS powder.

Various additives have been tried to improve the densification of ZrB_2. Metals, carbon, carbides and silicides were used to enhance the densification. Zhu *et al*.[48] have used 1.7% carbon and obtained 99% dense ZrB_2 at 1900°C for 2 hours. Farehnholtz *et al*.[46] have added 4% B_4C to get 94 % density at 2050°C for 2 hour. Zhang *et al*.[49] have added 4%WC and 2% B_4C and reported a density of 98% on pressureless sintering at 2050 for 3 hour. Zhang *et al*.[50] have used 3% carbon and 0.5%B_4C to ZrB_2+20% SiC and densified the composite to 99.3% density by pressureless sintering at 2100°C for 2 hr. Sciti *et al*.[51] have obtained 99% dense ZrB_2 at 1850°C with the help of 20% $MoSi_2$ addition. Mishra *et al*.[32, 33] has studied the effect of carbon and TiC addition on pressureless sintering of ZrB_2. Both the additive react with surface oxide layer and result in enhanced densification.The density was found to increase with the addition of C only upto 5 wt.%. Further increase in C content led to decrease in densification. The addition of TiC above 5 wt.% was found to be detrimental for the sintering of ZrB_2. The densification rates decreased due to increased volume fraction of second phase that acted as diffusion barrier. Wang *et al*.[52] have studied the effect of boron content as sintering aid for densification of ZrB_2. It was found that boron is an effective additive for the pressureless densification of ZrB_2– 20 vol.% SiC ceramics. Addition of 0.5 wt.% boron was not enough to effectively remove the surface oxide impurities and complete densification could not be achieved. However, due to the appearance of liquid phase, a boron content higher than 2 wt.% would lead to a densification deterioration and microstructure coarsening at temperature higher than 2100 ^{o}C. To obtain dense ZrB_2–SiC ceramics with a fine and stable microstructure, the content of the boron addition should be about 1 wt.%.

Mishra *et al*.[53] have studied the effect of Fe and Cr addition on sintering of ZrB_2. It was observed that Fe addition helps to enhance the density of ZrB_2 only up to 10 wt%. Further addition of Fe degrades the sintering by segregation of Fe-rich phases. The addition of Cr to a ZrB_2 matrix was found to result in swelling of the samples, leading to several cracks. Cheng *et al.* [54] have studied the effect of Mo and Cu addition on densification of ZrB_2. Addition of 22.1%Mo resulted in 88% of theoretical density on firing at 2100°C for 30 min. Yan *et al*.[55]

have reported that 4% Mo addition to ZrB2 + 20% SiC results in 97.7 % dense composite by pressureless sintering at 2250°C for 2 hr. Addition of Cu did not help in sintering as high vapour pressure of Cu resulted higher porosity in the samples during firing. Khanra *et al*.[56] have studied the effect of Ni addition on pressureless sintering of ZrB_2 over a temperature range of 1300-1600 ^{o}C. Sintered density was found to increase with sintering temperature and Ni content. This could be due to liquid phase sintering and the densification rate increase with sintering temperature. A maximum density of around 88% was achieved for the 50 wt-%Ni sample at 1600 ^{o}C. The XRD pattern showed formation of Ni_3Zr phase during pressureless sintering. The coefficient of thermal expansion increased with Ni addition.

Reported work on pressureless sintering of ZrB_2 based materials are summarized in Table 2.4. [32-33, 46-60]

2.2.1.1 Reactive sintering

Pressureless reactive processing offers the possibility of reduced processing time and temperature and is therefore an attractive alternative to conventional pressureless sintering of ZrB_2 powders. Reactive processing possesses advantages, such as lower processing temperatures and time, improvement in the cleanness of the grain boundaries etc. Among the controllable parameters, the initial density of the compact plays an important role. Independent of the sintering schedule, use of a green body with a porosity as low as possible maximizes the chance of obtaining the highest final density. Shock consolidation process generates defects and other features that can enhance the solid-solid diffusivity, such as dislocations, shorter diffusion distances, subgrain size structures, and clean/fresh interfaces, which could improve the densification behavior [61].

Brochu et al [61] have shock compacted Zr and B mixture to a density of 95% and then reacted the powder at 1600-2000 ^{o}C. Preparation of bulk ZrB_2 ceramic has been reported [26] by pressureless reactive sintering of elemental powder mixtures. After reaction, the samples had relative densities ranging between 58 and 79%. Results showed that reaction by itself does not provide sufficient driving force to produce fully dense ZrB_2 from the elemental powders.

Table 2.4 : Pressure less sintering of ZrB_2 based materials

Additive	Temp. (^oC)	Time(min)	Density (%)	Hardness (GPa)	Fracture Toughness ($MPa.m^{1/2}$)	Reference
monolithic	2150	540	98%	-	-	47
20%$MoSi_2$	1850	30	99.1	16	2.3	51
20% $MoSi_2$	1830	30	99.5	-	-	57
20%SiC+5%VC	2000-2100	120	100	15.4	4.9	58
monolithic	1800	30	87	-	-	32,33
5%C	1800	30	96.1	-	-	
5%TiC	1800	30	94.2	-	-	
20%$ZrSi_2$	1650	60	99.5	-	-	59
monolithic	2100	120	70	-	-	48
1.7%C	1900	120	99	15.5	2.8	
Monolithic	2050	120	78	-	-	46
4%B_4C	2050	120	94	17.9	3.3	
1%C	2100	120	96	-	-	
2%B_4C + 1%C	1900	120	100	19	3.5	
8% WC +4%B_4C	1850	60	100	18	3.1	
polycarbosilane	1900	120	95	-	-	60
20%SiC +3%C+0.5%B_4C	2100	120	99.3	14.7	4	50
4%WC + 2%B_4C	2050	180	98%	-	-	49
20%SiC + 4%Mo	2250	120	97.7	14.8	5.4	55
10% Fe	1800	120	93.5	-	-	53
22.1%Mo	2100	30	88	-	-	54
50% Ni	1600	60	88	11.5	-	56
20%SiC + 1% B	2100	120	99	16	-	52

2.2.2 Hot Pressing:

As pressure less sintering of ZrB_2 without additive is extremely difficult, hot pressing is the most popular method for obtaining densified compacts. Pressure assisted sintering involves heating a powder compact, with the simultaneous application of pressure. The powder compacts are typically heated externally using graphite heating elements and the pressure is applied hydraulically. Particle size influences the density and microstructure of the hot pressed compacts. Before hot pressing, ZrB_2 powder is milled by ball milling or attrition milling to obtain a powder of < 2μm size. The milled powder is filled in the graphite die and then heated to required temperature in vacuum or argon atmosphere. When the die temperature is reached at required temperature, uniaxial pressure of around 30-40 MPa is applied. Hot pressing temperature, pressure, heating rate, atmosphere and holding time affect the density and microstructure of the densified pellets. Hot pressing method is limited to simple shapes and complex geometry cannot be fabricated using this technique.

In general a temperature around 1800-2000°C and pressure of 30 MPa is reported for achieving greater than 99% density in ZrB_2 based materials. For monolithic ZrB_2, hot pressing temperature of 1900°C and pressure of 32 MPa is reported by chamberlain *et al.*[62]. Monteverde [63] has obtained 98% density at 1850 ^{o}C and 30 MPa by the addition of 5% Ni. Sciti *et al.*[64] have added 15% $TaSi_2$ and obtained 99% density at 1850°C. The most important microstructural features were the partial decomposition of $TaSi_2$ and the formation of solid solutions $(Zr,Ta)B_2$. Guo *et al.*[65] have densified ZrB_2+ 20%$MoSi_2$+ 5% SiC to 100% of theoretical density at 1800°C and 30 MPa. Monteverde *et al.*[66] have added 5% Si_3N_4 and obtained 98% density at 1700°C and 30 MPa. Han *et al.*[67] have studied the effect of AlN as sinter additive and 97.7 % dense ceramic was obtained by 5% AlN addition. Aluminum nitride improves the sinterability of ZrB_2 powder by eliminating the oxide layer according to following reaction[67].

$$AlN + B_2O_3 \rightarrow BN + Al_2O_3 \ldots\ldots\ldots\ldots\ldots\ldots\ldots\ldots\ldots\ldots (1)$$

Effect of SiC addition on processing and properties of ZrB_2 has been studied by many researchers. SiC reacts with surface oxides according to following reaction and thus enhances densification by removing B_2O_3 from particle surfaces. Furthermore, the addition of SiC also

limits the grain growth during densification. Monteverde *et al.*[68] have added 10% SiC and obtained 100% density by hot pressing at 1900 and 50 MPa. Onset of densification takes place at 1260 ^{o}C but a marked increase in densification rate was observed only at temperature above 1500 ^{o}C. Guo *et al.*[69] have studied the effect of nanosize SiC addition to ZrB_2. The strength of ZrB_2 with nano-sized SiC particles is higher than that with micron-sized SiC particles. This is attributed to a more uniform dispersion of nano-sized SiC particles at grain boundaries and within the grains, whereas the micron-sized SiC particles are located at multiple grain pockets. Zhou *et al.*[70] have added 5% carbon black to ZrB_2 + 20% SiC and obtained near theoretical density by hot pressing at 1900°C. Tian *et al.*[71] have added 2% carbon nanotube into ZrB_2-SiC composite and obtained near theoretical density by hot pressing at 1900 ^{o}C and 30 MPa for 1 hr. Yang *et al.*[72] have obtained near theoretical density of ZrB_2 +20%SiC +20%C_{fiber} by hot pressing at 2000°C and 30MPa. Carbon fiber reinforcement resulted in remarkable increase in fracture toughness

Zhu *et al.*[73] have studied the effect of Al_2O_3 plus Y_2O_3 addition on hot pressing of ZrB_2–SiCw composites at 1800 ^{o}C. Analysis revealed that additives may react with impurities (i.e. surface oxygen impurities and residual metallic impurities) to form a transient liquid phase, thus promote the sintering and densification of ZrB_2–SiC_w composites. The content of additives was found to have a significant influence on the sinterability, microstructure and mechanical properties of ZrB_2–SiC_w composites. ZrB_2–SiC_w composite prepared with a small amount of additives (3 vol.%) provided the optimal combination of microstructure (relative density of 98.3%) and excellent properties, including flexural strength of 783MPa and fracture toughness of 6.7 MPa $m^{1/2}$. With further addition of additives, SiC whiskers were inclined to gather together and be enveloped by excessive liquids to form core-rim-like structures, which lead to little decrease in mechanical properties. Li *et al.*[74] have densified ZrB_2–ZrO_2 ceramics, with ZrO_2 content ranged from 15 to 30 vol.%, by hot pressing at 1850 ^{o}C under a pressure of 30MPa. Higher content of ZrO_2 was beneficial to decrease the grain size, which was also advantageous for the strength. Zhang *et al.*[75] have hot pressed ZrB_2 +10%SiC + (10-30%) ZrO_2 composite to 98% density at 1850 ^{o}C and 30MPa. Addition of ZrO_2 was found to increase the fracture toughness to 6.0 MPa $m^{1/2}$. Addition of rare earth oxides such as Y_2O_3, Yb_2O_3, La_2O_3, and Nd_2O_3 lowers the densification temperature. Zhang *et al.*[76] have also reported that small

addition (3 vol%) of Y_2O_3 reacts with surface oxides and help in densification. Near theoretical density was obtained at 1900°C.

Guo *et al.*[77] have observed that addition of rare earth oxide decreases hot pressing temperature by 50°C (from 1950 to 1900 ^{o}C). The addition of Re_2O_3 (Re =Y and Yb) resulted in the formation of $Re_2Zr_2O_7$ according to the following reaction:

$2ZrO_2 + Re_2O_3 \rightarrow Re_2Zr_2O_7$……(2.4)

Available literature on hot pressing of ZrB_2 based material is summarized in Table 2.5. [51, 62-70, 72-89].

2.2.2.1 Reactive hot pressing:

Reactive hot pressing (RHP) is another method that relies on thermodynamically favorable reactions to form intermetallics, non-oxide ceramics, and metals. Unlike SHS, RHP relies on a controlled (i.e., non-self-propagating) reaction in which the products are formed relatively slowly by a solid-state diffusion-controlled process. The use of controlled reactions ensures that the reactants are completely converted to the products. In addition, the combination of controlled reaction and the simultaneous application of pressure may produce dense bodies in a combined *in situ* synthesis and densification process, thereby eliminating the need for further powder processing after the reaction is complete.

ZrB_2 ceramics can be densified at temperatures that are 200–300 $^\circ$C lower than conventional processing. This reduction in processing temperature may be related to the minimization of oxide impurities (B_2O_3 and ZrO_2) that are thought to promote coarsening and inhibit densification of the boride ceramics. The use of high energy milling to reduce the size of the metallic precursors may also result in the development of large defect concentrations in the precursors, which, in turn, may enhance densification of the resulting ceramics. In reactive hot pressing the graphite die must be coated with boron nitride to avoid any reaction with die.

Chamberlain *et al.*[23] have obtained 99% dense ZrB_2 by reactive hot pressing at 2100°C. Dense ZrB_2 produced by the reactive hot pressing process had mechanical properties that were comparable to ceramics produced by conventional processes. The four-point flexure strength of ZrB_2 produced in this study was 434MPa.

Table 2.5 Hot Pressing of ZrB_2 based materials

Additive	Temp. (^oC)	Pressure (MPa)	Time (min)	Density (%)	Hardness (GPa)	Fracture Toughness ($MPa.m^{1/2}$)	Reference
20vol%SiC	2000	30	60	100	-	4.2	72
20vol%SiC+20%C_{fiber}	2000	30	60	98.4	-	6.3	
15% $MoSi_2$	1750	30	20	97.7	14.9	-	51
20%$MoSi_2$	1800	30	5	98.1	15	-	
20%$MoSi_2$+ 2.3%C	1780	30	12	99.2	17	-	
10-40% $MoSi_2$	1800	30	30	99.8	13-15	2.8-3.7	65
20%$MoSi_2$ +5%SiC	1800	30	30	100	16.1	3.4	
15% $TaSi_2$	1850	30	10	99	17.8	3.8	64
20%SiC	1900	30	60	97.5	18.0	3.6	77
20%SiC +3%Nd_2O_3	1900	30	60	99.9	19.1	3.7	
20%SiC +3%La_2O_3	1900	30	60	99.9	19.4	3.4	
20%SiC +3%Y_2O_3	1900	30	60	99.1	19.8	4.7	
20%SiC +3%Yb_2O_3	1900	30	60	99.7	20.1	4.9	
5%Ni	1850	30	30	98	14.4	2.8	63
13%B4C+ 4%Ni	1870	30	10	99.6	19.2	4.5	
Monolithic	1900	30	30	87	8.7	2.3	78
5% Si_3N_4	1700	30	30	98	13.4	3.7	
20% SiC +4% Si_3N_4	1870	30	30	98	14.6	-	
18.5%SiC + 3.7% Si_3N_4 + 1%Al_2O_3 +0.5%Y_2O_3	1760	30	30	98	14.2	4.5	
Monolithic	1900	30	30	86.5	8.7	3.5	79
4%Ni	1850	30	30	98	14.4	2.8	
Monolithic	1870	30	30	90	-	-	66
2.5%Si_3N_4	1700	30	15	98	-	-	
10%ZrO_2+10%SiC	1950	30	60	99.6	20.5	4.5	80

20%SiC +10% LaB_6	2000	30	60	99.2	-	-	81
25% Nb	1800	30	60	97.2	16.3	6.7	82
20%SiC_W + 3%(Al2O3 + Y2O3)	1800	30	60	98.3	-	6.7	73
10%Mo	1950	30	60	98.9	-	6.7	83
Monolithic	2000	30	60	90.4	-	-	69
20%SiC	2000	30	60	98.2	-	-	
Monolithic	1900	32	45	99.8	23	3.5	62
20%SiC	1900	32	45	99.7	24	4.4	
10 % SiC	1900	50	20	100		4.8	68
20%SiC + 10% LaB_6	2000	30	60	99	17.1	5.7	89
25% SiC + 35% BN	1800	23	60	92.6	5.2	4.1	84
30% ZrO_2	1850	30	60	98.9	22	7.9	74
10%SiC + 10%ZrO_2	1850	30	60	98.2	19.3	6.0	75
20%$MoSi_2$ + 20%ZrO_2	1850	30	60	98.5	19.9	6.5	85
30% SiC	1850	32	45	99.5	22	3.9	86
30% SiC	1900	32	45	100%	24	5	87
20% SiC+ 5%C	1900	30	60	100	12.3	6.6	70
20%SiC + 5% AlN	1850	30	60	100	-	5.3	67
20% SiC + 3% Y_2O_3	1900	30	60	99.3	17.6	5.6	76
20% SiC + 20% Graphite	1950	30	60	90	-	-	88

2.2.3 Spark plasma sintering:

Spark plasma sintering (SPS) makes it possible to densify ZrB_2 based materials at a lower temperature and in a shorter time compared with conventional techniques. In the SPS technique, a pulsed direct current passes through graphite punch rods and dies simultaneously with a uniaxial pressure. Thus, the grain growth can be suppressed by rapid heating and the densification is accelerated at high temperature. Furthermore, the microstructure can be controlled by a fast heating rate and shorter processing times. Higher densities, refined microstructures, clean grain boundaries, elimination of surface impurities as well as an overall improvement in the materials performance have been reported in the literature for several ceramic materials densified by spark plasma sintering. In SPS, the actual temperature inside the specimens is significantly higher than that recorded on the surface of the die. The temperature mismatch depends on many factors such as the size of the die, the quality of vacuum, the level of insulation of the die, thermal and electrical conductivity of the die, etc.

It is well known that oxygen contamination, in the form of B_2O_3 and ZrO_2 is present on the surface of the ZrB_2 starting powders, and this limits the densification. During SPS, the use of a pulsed current may generate an electrical discharge and the local spark discharge cleans the surface oxides of the powder, and possibly enhances grain-boundary diffusion and migration, which is assumed to promote transfer of material and also enhance densification. The high heating rate increases the current, enhances spark discharge and further promotes grain-boundary diffusion for rapid densification. Due to the high densification rate, some gaseous B_2O_3 has no time to escape and is encapsulated into the ceramics. Of the surface oxides (B_2O_3, ZrO_2) present on the raw materials, B_2O_3 is considered the most important factor in promoting coarsening of boride-based ceramics through evaporation–condensation kinetics. The rapid heating through the range 1500–1900 ^{o}C minimizes the time over which coarsening could occur by evaporation and condensation of B_2O_3. Therefore fine microstructure is obtained by SPS. In other words, the fast heating rate is effective in reducing the adverse effect of B_2O_3 for grain coarsening. Under electric field grain boundary migration is enhanced which in turn reduces the closed porosity [90]. Despite the numerous published works on field assisted sintering techniques, it is still very

difficult to identify which are the critical factors that determine the eventual changes and improvements in the materials densified by spark plasma sintering. In other words, it is difficult to assess if these improvements are related to the more favourable sintering parameters (higher heating rates, lower holding times) or to intrinsic effects related to electric field.

Venktesh *et al.*[91] have studied the spark plasma sintering of ZrB_2 + 6 wt% Cu and obtained a density of 95% at 1500 ^oC and 15 minute. Akin *et al.* [92] and Carney *et al.*[93] have obtained 99% dense bodies of ZrB_2 -20% SiC by SPS at 2000^oC in 5 minutes only. Song *et al.*[94] have densified ZrB_2 + 10% YAG composite to 99% density at 1700^oC, and 20 MPa and 4 min. Guo *et al.*[90] have reported the optimum condition of SPS to obtain 100% ZrB_2 as 1900^oC temperature, 3 min holding time and heating rate of 200-300 ^oC/min. A temperature higher than 1900^oC results in rapid grain growth. Most of the densification in the green compacts occurred during heating and within very short holding time (within 3 min) accompanying neck formation between the powders. Balbo *et al.*[95] have prepared ZrB_2 +15%$MoSi_2$ by both SPS and hot pressing using same sintering conditions. No differences were observed in terms of microstructural features and mechanical properties when the composite was densified either by spark plasma sintering or by hot pressing using the same sintering parameters. The spark plasma sintering technique is effective mainly due to the high heating rate and high efficiency of the heating process. Sciti *et al.*[51] have densified ZrB_2 +15%$MoSi_2$ composite by SPS at 1700 ^oC in 7 minutes. Sciti *et al.*[96] have also studied the spark plasma sintering of ZrB_2 with decreasing amount of $MoSi_2$ as sintering aid. After decreasing the amount of sintering aid, increased sintering temperatures were necessary to obtain the same level of density. For 9% and 3% doping, 98% dense samples were obtained at 1700 and 1750 °C, respectively, whilst for 1% doping, the temperature had to be raised to 1850 °C. Hu *et al.*[97] have fabricated ZrB_2–SiC composites by spark plasma sintering (SPS) using $TaSi_2$ as sintering additive. The composites could be densified at1600 ◦C and the core–shell structure with the core being ZrB_2 and the shell containing both Ta and Zr as (Zr, Ta)B_2 appeared in the samples. When the sintering temperature was increased up to1800 ◦C, only (Zr,Ta)B_2 and SiC phases could be detected in the samples and the core–shell structure disappeared. Generally, the composites with core–shell structure and fine- grained microstructure showed the high electrical conductivity and Vickers hardness.

Zhao *et al.*[98] have prepared ZrB_2-SiC composite by spark plasma sintering reactive synthesis method. Zr, Si and B_4C powder was taken as starting material and the composite was made at 1400 ^oC and 9 min. It was discovered that density increases with holding time but hardness decreases slightly due to grain growth.

SPS is suitable technique for the preparation of nanocomposites as no grain growth takes place in this process. Nanocomposite ceramics have superior mechanical properties and good application prospects. Cao *et al.*[99] have used nanosized SiC as additive and prepared nanocomposite using spark plasma sintering. Available literature on SPS of ZrB_2 is summarized in Table 2.6 [51, 90-93, 95-96, 98, 100-103].

Table 2.6 Spark plasma sintering of ZrB_2 based materials

Additive	Temp. (^oC)	Pressure (MPa)	Time (minute)	Density (%)	Hardness (GPa)	Fracture Toughness ($MPa.m^{1/2}$)	reference
15% $MoSi_2$	1750	30	7	98.1	16.2	2.6	51
15% $MoSi_2$	1750	30	8	98	16.2	3.5	95
15% $MoSi_2$	1750	30	7	97.7	16.2	4.4	100
30%ZrC +10%SiC	1750	30	20	99	18.8	3.5	
Zr+Si+B_4C	1400	30	9	98.3	18.1	4.3	98
20 to 60% SiC	2000-2100	20	3	99	26.8	2.5-4.1	92
20% SiC	2000	32	5	>99	-	-	93
monolithic	1900-1950	50	3	>97	-	-	90
monolithic	2300	75	3	98	15.6	< 2	96
9% $MoSi_2$	1700	100	5	100	18.2	3.3	
6% Cu	1500	40	15	94.8	19.1	7.4	91
20% SiC + 5% Yb_2O_3	1900	30	4	-	-	-	101
0.1% SiC	1900	40	30	99.4			102
25% SiC	1800	20	30	99.6	16.7	5.0	103

2.2.4 Microwave sintering:

Microwave sintering is another alternative to hot pressing and conventional sintering. Microwave sintering has the advantages of uniform and rapid heating since the energy is directly coupled into the specimen rather than being conducted into the specimen from an external heat source. Generally, enhanced densification and finer microstructures have been reported for microwave sintered materials. However, only one literature was cited on microwave sintering of ZrB_2, probably because ZrB_2 is electrically conductive and has limited coupling with microwave energy.

Zhu *et al.*[104] have studied the microwave sintering of ZrB_2 – 4%B_4C particulate composites. B_4C particles contributed to the densification of ZrB_2 by reacting with surface oxides and acting as a microwave absorber for heating of the ZrB_2 matrix. Compared to conventional sintering, microwave sintering promoted the densification of the composite at lower temperatures without significant grain growth. Relative densities of >98% were achieved at microwave sintering temperature as low as 1720 ^{o}C. The ZrB_2 matrix grain size increased from 2 to 15.9 μm when the microwave sintering temperature increased from 1630 to 1920°C. The composite fabricated by microwave sintering at 1820 ^{o}C had a Vickers' hardness of 17.5 GPa and a fracture toughness of 2.8 MPa.m$^{1/2}$, which were comparable to specimens with the same composition produced by conventional sintering.

2.2.5 Laser sintering

Laser sintering is a rapid prototyping technique that builds objects layer by layer from powders. It offers a promising direction to fabricate cladding layers as well as free standing 3-dimensional structures for UHTC. When the laser beam irradiates the powder surface, it absorbs light energy and the temperature rises, giving rise to necking, grain growth, partial, or full melting in some cases, and eventually densification. Moreover, it is a non-contact process, so contamination is minimized. However, due to the small beam size, this technique is limited to manufacturing of small to medium scale objects. Recent research has shown that laser sintering holds great promise in processing high temperature, high performance materials into functional

components. Laser power, beam spot size and scan speed are major processing parameters in laser sintering. Sun *et al.*[105] have obtained ZrB_2 sintered layer with uniform surface morphology. In addition, the rapid cooling rate of laser sintering enabled the formation of needle-like nanostructures at the sintered surface. They have also prepared 3-D structures of ZrB_2-Zr composite by a combination of laser sintering and induction heating technique [106]. Sintered objects have densities >95% of theoretical values and have microhardness values up to 16.0 GPa. This technique seems capable to create complex structures or repair UHTC objects and thus would be especially beneficial in saving time and reducing overall cost.

In literature survey it was found that studies on synthesis of ZrB_2 by boron carbide reduction method is very limited and hence it was planned to carry out detailed investigation on synthesis of ZrB_2 by this route. In literature it was found that several additives have been used for enhancement of densification and properties of ZrB_2. As per my knowledge there is no report on the use of $TiSi_2$, $CrSi_2$ as sinter additive. These additives have potential for improving the densification as well as properties of ZrB_2 and hence study was carried out on the effect of these sinter additives on densification and properties of ZrB_2. In literature, it was seen that there is no effort on improving densification of ZrB_2 by solid solution formation. Effect of rare earth borides on densification and properties were also not studied. In this study, effect of rare earth boride (EuB_6) on densification and properties of ZrB_2 were studied.

2.3 Oxidation behavior of ZrB_2 based materials

ZrB_2 is a candidate material for many applications which involve oxidizing conditions. So its oxidation behaviour at different temperatures and different partial pressure of oxygen is of vital interest. Several researchers have carried out studies on oxidation behaviour of ZrB_2 based materials. Pure ZrB_2 oxidises in air at elevated temperatures and gives ZrO_2 and B_2O_3 according to following reaction (reaction (1)). The reaction is thermodynamically feasible at all temperatures with ΔG^0 =-1977 + 0.361T (kJ). [1]

$$ZrB_2 + 5/2\ O_2 \rightarrow ZrO_2 + B_2O_3 \quad (1)$$

Below 700 ^{o}C, the mass gain is negligible. At temperatures below1100 ^{o}C, ZrO_2 and B_2O_3 form a continuous layer that provides passive oxidation protection.[1,114]. The rate limiting step for oxidation is the transport of oxygen through B_2O_3, which results in parabolic (diffusion-limited growth) kinetics for mass gain. Between 1100 and 1400 ^{o}C, the weight change reflects a combination of mass loss due to B_2O_3 evaporation and mass gain due to the formation of condensed oxide (ZrO_2). Specimens continue to gain mass as the mass of oxide (ZrO_2) formed is greater than the mass of diboride reacted plus the mass of B_2O_3 lost. As B_2O_3 evaporates, a porous ZrO_2, layer remains, although a small amount of B_2O_3 may be retained. Above 1400 ^{o}C, the oxide layer is not protective and rapid linear mass gain takes place. .[1,107]

Additives which change the composition of the oxide scale improve the oxidation resistance of ZrB_2. The most common additive used is SiC, which reduces the oxidation rate of ZrB_2 by forming a silica-rich scale.[1,108]. Below 1100 ^{o}C, the addition of SiC does not alter the oxidation behavior of the diborides. In this temperature regime, the oxidation rate of SiC is several orders of magnitude slower than that of the diborides. Consequently, the oxide scale on ZrB_2– SiC below 1100 ^{o}C consists of ZrO_2 and B_2O_3, as it was for pure ZrB_2. Above 1100 ^{o}C, two factors affect oxidation. First, the rate of SiC oxidation increases and the SiC particles are converted to SiO_2 and CO. Second, the rate of B_2O_3 evaporation becomes significant. Oxidation of ZrB_2–SiC results in a mass loss between 1200 and 1300 ^{o}C due to B_2O_3 evaporation. The silica-rich layer provides protective behavior, which results in mass gain with parabolic kinetics from room temperature to 1600°C [1, 4]. Above 1600°C, active oxidation of SiC takes place and results in formation of SiO which is not protective [109]. Besides SiC, additives such as $MoSi_2$ [110], $TaSi_2$, [111], AlB_2 [112], improve the oxidation resistance of diborides. Results of some of the studies on oxidation of ZrB_2 based material is discussed below.

Voitovich et al. [113] have reported that at 600-800 ^{o}C, ZrB_2 is virtually immune against oxidtation. At 900-1000° C, barely perceptible oxidation begins and at 1100°C-1200°C, the rate of the oxidation grows a little. At 1400 ^{o}C, a marked increase is observed in the intensity of oxidation in the initial stage of oxidation. However in the later stage the scale layer undergoes sintering and protects the base material. At lower temperature (upto 1000 ^{o}C) oxidation product was ZrO_2 and B_2O_3. At 1200 and 1300 ^{o}C, zirconium borate was observed and at higher temperatures (1400 ^{o}C) only ZrO_2 was found.

Opeka et al. [114] have reported that ZrB_2 ceramics did not oxidize significantly even after 2 h heating at 1200 ^oC. The ceramic was protected by liquid boria. Above 1200 ^oC, pure ZrB_2 oxidized very actively due to the intensive evaporation of B_2O_3. It was also reported that thickness of the oxide layer increases with temperature which indicates that boria alone does not prevent oxidation. ZrB_2 ceramic containing SiC was reported to have good oxidation resistance due to formation of borosilicate glassy layer which has higher viscosity, higher melting point, lower oxygen diffusivity and lower vapour pressure. Monteverde et al [107] have reported that oxidation of monolithic ZrB_2 takes place rapidly due to the weak ability of B_2O_3 to hinder intensive oxidation. ZrO_2 has a semi-protective action at elevated temperatures due to its anion-deficit structure permitting inward transport of oxygen via lattice vacancies. The introduction of SiC particles markedly improved the oxidation resistance of the ZrB_2-SiC -based composites in comparison to the monolithic ZrB_2. An adherent and protective borosilicate glassy layer coats the sample surface, greatly limiting the inward diffusion of oxygen into the unreacted bulk. Opila et al . [111] have studied the oxidation behaviour of ZrB_2+20%SiC and ZrB_2+20%SiC+20% $TaSi_2$ at 1627 ^oC and at 1927 ^oC. Both the sample have shown parabolic kinetics at 1627 ^oC due to formation of protective layer. Addition of 20% $TaSi_2$ was found to improve the oxidation resistance of ZrB_2 at 1627 ^oC. Sample containing 20%$TaSi_2$ has shown poor oxidation resistance at 1927 ^oC due to melting of Ta_2O_5. Han et al.[115] have studied the oxidation behaviour of ZrB_2 containing 20% and 30% SiC at 1800 ^oC in different partial pressure of oxygen. ZrB_2 containing 30 vol.% SiC particulates exhibited higher oxidation resistance at 1800 ^oC under an oxygen partial pressure of 0.2 atm compared with ZrB_2 + 20 vol.% SiC. High SiC content is beneficial for oxidation resistance at 1800 ^oC in air due to a large amount of silica glass formation. However, this trend is reversed at a reduced oxygen partial pressure (2×10^{-4} atm) due to rapid active oxidation of SiC resulting in little formation of silica glass. Han et al [116] have carried out oxidation test of ZrB_2+20%SiC composite at 2200 ^oC for 10 minutes. The composites exhibited excellent oxidation resistance at 2200 ^oC.. No macro-cracks or spallation were detected after oxidation. SiC was no longer responsible for the improvement in oxidation resistance of the composites in this case. ZrO_2 recrystallized into a dense coherent subscale, which protected the underlying ceramic from catastrophic oxidation. Rezaie et al. [108] have studied the isothermal oxidation behavior of ZrB_2 +20%SiC in air at temperature range from

800 ^{o}C to 1500 ^{o}C for a holding time of 30 minutes. Below 1200 ^{o}C, a protective B_2O_3 rich scale was observed on the surface. At 1200 ^{o}C and above, the B_2O_3 evaporated and the SiO_2-rich scale that formed was stable up to at least 1500 ◦C. Thermogravimetric study revealed that oxidation starts at 800 ^{o}C. . Hwang et al. [117] have studied the effect of particle size of SiC on oxidation of ZrB_2-SiC composite at 1500 ^{o}C. It was found that SiC size reduction results in a dramatic reduction in the thicknesses of the oxide layers. The largest improvement in oxidation resistance occurs by going from a SiC grain size of 1.8 μm –0.8 μm. With further decrease in the SiC grain size, the decrease in the oxide layer thicknesses is marginal. Seong et al. [144] have carried out TEM study of oxidation of ZrB_2-SiC material at 1500 ^{o}C at different partial pressure of oxygen (10^4 and 10^{-4} Pa). Based on TEM results, the three layers (surface SiO_2 layer, ZrO_2 layer, and unreacted layers) were observed at high partial pressure and the two layers (ZrO_2 layer, and unreacted layer) were observed at low partial pressure. No surface SiO_2 layer was observed at low partial pressure due to active oxidation.

Sciti et al. [110] have carried out oxidation study of ZrB_2 + 20%$MoSi_2$ material in the temperature range of 700 to 1400 ^{o}C for exposure time of 30 hour. At 700°C, the extent of oxidation at is very limited. The sample surface after oxidation at 700 appears covered with small crystals belonging to zirconia, but the oxide layer is porous. At 800 and 1000 °C also the surface oxide is porous and traversed by big cracks. A subsurface oxidation was noticed during the treatment at 1000 °C. Samples oxidized at temperature range 1200-1400 ^{o}C was found to be covered by a continuous silica-rich glassy layer, in which small zirconia and/or zircon grains are embedded. Sciti et al [57] have also studied the long term oxidation behaviour of ZrB_2 + 20%$MoSi_2$ material. Oxidation tests carried out between 700 and 1400 ^{o}C for 100 h showed that this material was heavily oxidized at temperatures >1200 ^{o}C. Peng et al. [118] have studied the oxidation behaviour of ZrB_2 ceramic containing B_4C, SiC,TaB_2 and $TaSi_2$ by scanning thermogravimetry in the temperature range of 1150 to 1550 ^{o}C. SiC additions improved oxidation resistance over a broadening range of temperatures. Tantalum additions to ZrB_2–B_4C–SiC in the form of TaB_2 and/or $TaSi_2$ increased oxidation resistance over the entire evaluated spectrum of temperatures. $TaSi_2$ proved to be a more effective additive than TaB_2. Silicon-containing compositions formed a glassy surface layer, covering an interior oxide layer. Dehdashti et al. [119] have studied the effect of tungsten addition on oxidation of ZrB_2. For pure

ZrB_2, the protective liquid/glassy layer covering the surface as a result of oxidation was evaporated above 1500°C. For $(Zr,W)B_2$ specimens, the liquid/glassy layer was present after exposure up to 1600°C. The higher stability of the liquid/glassy phase in the W-containing compositions was attributed to the presence of tungsten in the liquid/glassy phase, resulting in improved oxidation resistance for ZrB_2 samples containing tungsten. Zhao et al [112] studied the effect of AlB_2 addition on oxidation of ZrB_2 at 1500 ^{o}C. The oxidation tests revealed that the AlB_2 phase improved the oxidation resistance for the ZrB_2 based ceramics, owing to the Al–B–O liquid phase formed on the surface of the oxidized specimen, which slows down the oxygen transportation velocity.

Effects of $TiSi_2$, $CrSi_2$ and EuB_6 on oxidation behavior of ZrB_2 have not been reported so far. In this study, effects of these additives were investigated at 900 ^{o}C for long duration of 64 hour in air atmosphere.

Chapter –3

Experimental Procedure

Contents

Chapter –3

Experimental Procedure

This chapter gives the detail of experimental procedure employed in this study. It consists of three parts (1) Synthesis (2) Densification and characterization (3) Mechanical properties and (4) oxidation study.

3.1. Synthesis

Raw materials used for synthesis of ZrB_2 were ZrO_2 (99% purity; 8.34 μm median diameter), boron carbide powder (78.5% B, 19.5%C, <1% O, 0.02% Fe, 0.02% Si, 5.34 μm median diameter; supplied by M/S Boron Carbide India) and petroleum coke (C-99.4%, 13.9 μm median dia., supplied by M/S Assam carbon, India). All the raw materials were dried in an oven at 100°C to remove moisture content before use. XRD pattern of the raw materials are presented in Fig.3.1. It shows that all the raw materials (ZrO_2, B_4C and carbon) are pure. No peaks of impurity phases are detected. For synthesis of ZrB_2, weighed quantities of zirconium dioxide, boron carbide and petroleum coke in various ratios were mixed thoroughly in motorized mortar and pestle. The powder mixture was then pelletized under pressure of about 280 MPa to obtain pellets of 20 mm dia. Mortar pestle and die sets used for powder processing was made of tungsten carbide to avoid contaminations. The pellets were then charged in a graphite crucible and heated in an induction furnace under a dynamic vacuum of 2×10^{-5} mbar and at fixed temperature between 1200 and 1875 ^{o}C for 2 h. Temperature of the charge was measured using a two-color pyrometer with an accuracy of ±22 ^{o}C. After completion of reaction, the furnace was cooled to room temperature in vacuum and the reacted pellets taken out, crushed and ground to fine size using high-energy cup grinding mill with tungsten carbide lining. Major phases of powders were identified by XRD (Cu Kα, λ = 1.5404 Å) radiation in an Inel make, X-ray diffractometer). Oxygen was measured by inert gas fusion method. Carbon was measured by combustion and IR detection method. The median particle diameter and particle size distribution were measured using laser particle size analyzer (CILAS PSA 1064L). Scanning Electron Microscope (20 kV, Cam Scan

MV2300CT/100) was used to analyze the morphology of the powders. Similar procedure was used for synthesis of EuB_6 and HfB_2 powder.

3.2 Densification and characterization

Raw materials used for densification were ZrB_2, HfB_2 and EuB_6 powder which were synthesized in Lab. Silicides of Ti and Cr were used as sinter additives. Aldrich make silicides ($TiSi_2$ and $CrSi_2$) were procured from market and used in present study. For densification, weighed quantities of fine zirconium diboride and sinter additives ($TiSi_2$/$CrSi_2$/EuB_6/HfB_2) were mixed thoroughly using a motorized mortar and pestle in dry condition for 1 h to obtain powder mixture of different composition.

Titanium disilicide ($TiSi_2$) and Chromium disilicide ($CrSi_2$) have been selected as sinter additives for liquid phase sintering process. These silicides have low melting point and thus can be useful in liquid phase sintering. For solid state sintering, Europium hexaboride (EuB_6) was selected as sinter additive. EuB_6 is a boron rich boride and thus can introduce point defects in ZrB_2 lattice on formation of solid solution. Presence of point defects would result in enhanced diffusion and thus may be helpful in densification. Additives are also expected to improve fracture toughness by crack deflection which could be due to presence of second phase. $TiSi_2$ and $CrSi_2$ are expected to increase the oxidation resistance of ZrB_2 by formation of silica based protective layer. Effect of EuB_6 on oxidation behavior of ZrB_2 is not reported till date, which has been one of the objectives of the present investigation. In this study, investigations were carried out in this direction.

Compositions of samples prepared for densification is listed in Table 3.1.

Table 3.1: Sample composition of powders used for densifications

$TiSi_2$ addition	ZrB_2 +10%$TiSi_2$ ZrB_2 +10%HfB_2 +10%$TiSi_2$ ZrB_2 +20%HfB_2 +10%$TiSi_2$
$CrSi_2$ addition	ZrB_2 +10%$CrSi_2$ ZrB_2 +10%HfB_2 +10%$CrSi_2$
EuB_6 addition	ZrB_2 +2.5%EuB_6 ZrB_2 +5%EuB_6 ZrB_2 +10%EuB_6

The mixed powders were loaded in a high density graphite die (12 mm diameter hole) and hot pressed at temperatures of 1650 ^oC to 1850^oC under a pressure of 20 to 35 MPa for 60 minutes in a high vacuum (1×10^{-5} mbar) chamber. The pellets were ejected from the die after cooling and the density was measured by Archimedes' principle. Densified samples were polished to mirror finish using diamond powder of various grades from 15 to 0.25 μm in an auto polisher (Laboforce-3, Struers). The phases present in the densified samples were examined by XRD. Scanning electron microscope with energy dispersive spectroscopy was used to analyze the composition and distribution of different phases.

3.3 Mechanical properties and fractography:

Microhardness was measured on the polished surface at a load of 100 g and dwell time of 10 sec. The indentation fracture toughness (K_{IC}) data were evaluated by crack length measurement of the crack pattern formed around Vickers indents (using 10 kg load), adopting the model formulation proposed by Anstis et al.[120]

$K_{IC} = 0.016(E/H)^{1/2}P/c^{3/2}$, where

E = Young's modulus,

H = Vickers's hardness,

P = applied indentation load, and

c = the half crack length.

The reported value of hardness and fracture toughness are the average of five measured values. Fractured surfaces of dense pellets were analyzed by scanning electron microscope.

3.4 Oxidation study

Hot pressed pellet of diameter 12 mm was cut into thin slice of 3 mm thickness by high speed diamond cutter. All the surfaces of the cut samples were polished with emery papers (1/0, 2/0, 3/0, 4/0) and finally with diamond paste up to 1µm finish. Oxidation tests were conducted in a resistance heated furnace. In order to avoid oxidation during heating, the sample was directly inserted into the furnace after the furnace temperature reached 900°C. Samples were placed in an alumina crucible kept into the furnace. The samples were oxidized for different time intervals (0.5, 1, 2, 4, 8, 16, 32, and 64 h) at 900◦C. The samples were carefully weighed before and after exposure to high temperature in order to determine the weight change during the oxidation process. The oxidation products were identified using XRD. The morphology and nature of oxide layer was investigated by observing the surface in a scanning electron microscope (SEM).

Chapter –4

Results and discussion

Contents

Chapter -4

Results and discussion

This chapter summarizes the results obtained during the various experiments giving a detailed overview from starting powder preparations till microstructural and mechanical characterization. This chapter is divided into three major sections representative for the three phases in the research: phase 1 on synthesis of boride powders, phase 2 on densification, mechanical properties and microstructure and phase 3 on oxidation study of prepared composites.

4.1 Synthesis of borides

Experiments were carried out to study the effect of process parameters on synthesis of boride powders. ZrB_2, EuB_6, and HfB_2 powder was synthesized by boron carbide reduction of respective oxides.

4.1.1 ZrB_2 synthesis

ZrB_2 was used as a base material for preparation of advanced composites. Studies were carried out on synthesis of ZrB_2 by carbothermic reduction of ZrO_2 in presence of boron carbide (reaction -4.1).

$$ZrO_2 + 1/2B_4C + 3/2C \rightarrow ZrB_2 + 2CO\uparrow \quad \ldots\ldots(4.1)$$

Raw materials used for synthesis of ZrB_2 were ZrO_2 (99% purity; 8.34 μm median diameter), boron carbide powder (78.5% B, 19.5%C, <1% O, 0.02% Fe, 0.02% Si, 5.34 μm median diameter; supplied by M/S Boron Carbide India) and petroleum coke (C-99.4%, 13.9 μm median dia., supplied by M/S Assam carbon, India). All the raw materials were dried in an oven at 100°C to remove moisture content before use. XRD pattern of the raw materials are presented

in Fig.4.1. It shows that all the raw materials (ZrO_2, B_4C and carbon) are pure. No peaks of impurity phases are detected

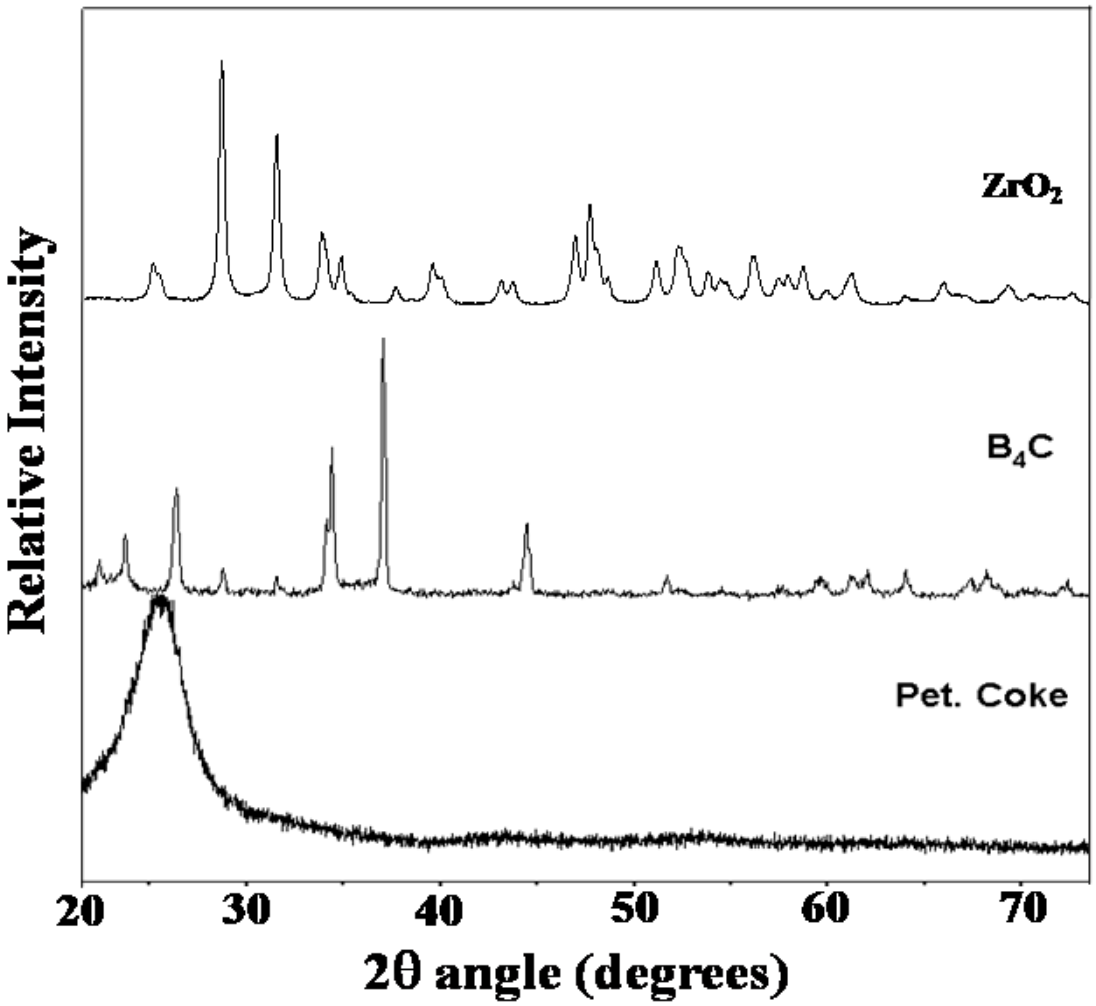

Fig.4.1 XRD pattern of raw materials

Thermogravimetric analysis was carried out to analyze the progress of reaction. Fig.4.2 presents the weight loss vs. time curve obtained by thermogravimetric experiment of stoichiometric charge mixture as per reaction 4.1. The reaction starts at 1200°C and results in a total weight loss of ~ 27.5 %. The weight loss observed is lower than the theoretical weight loss of 33.0 %. The XRD pattern revealed the presence of ZrB_2, ZrB and graphite phases (Fig.4.3).

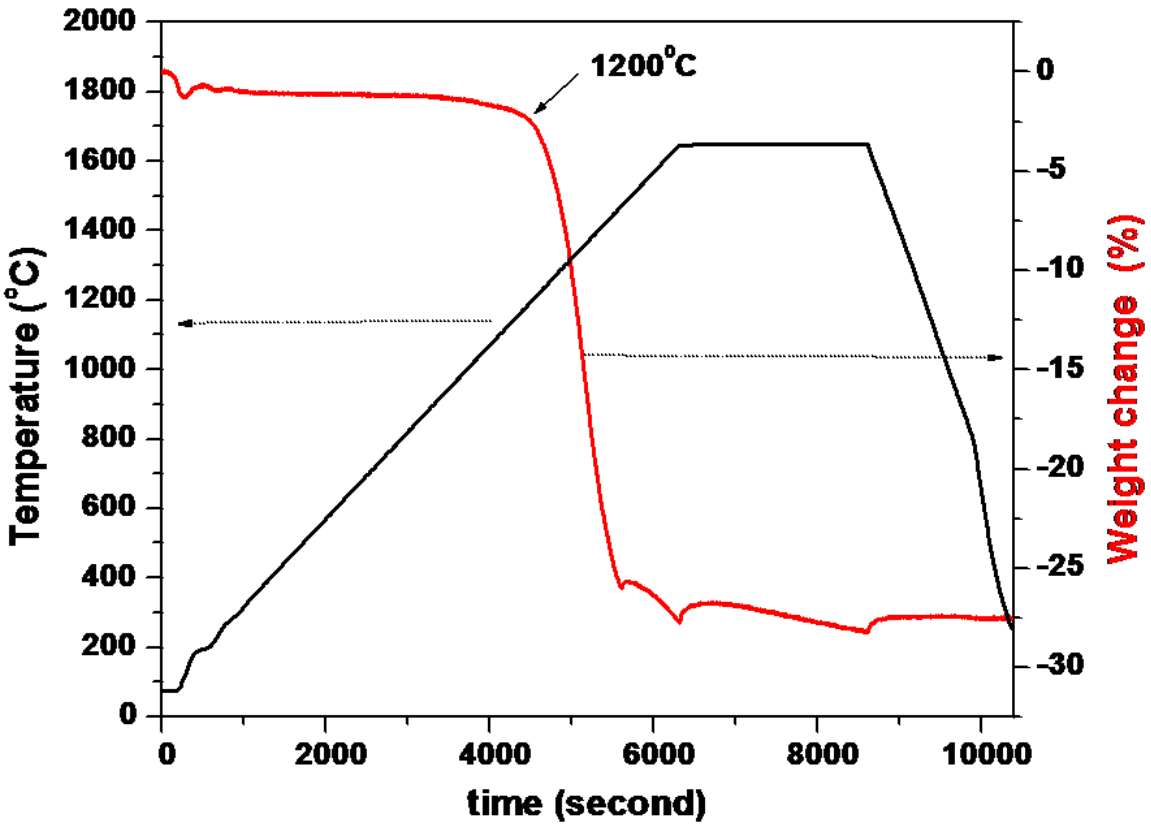

Fig. 4.2. Weight loss vs. time plot for ZrB_2 synthesis

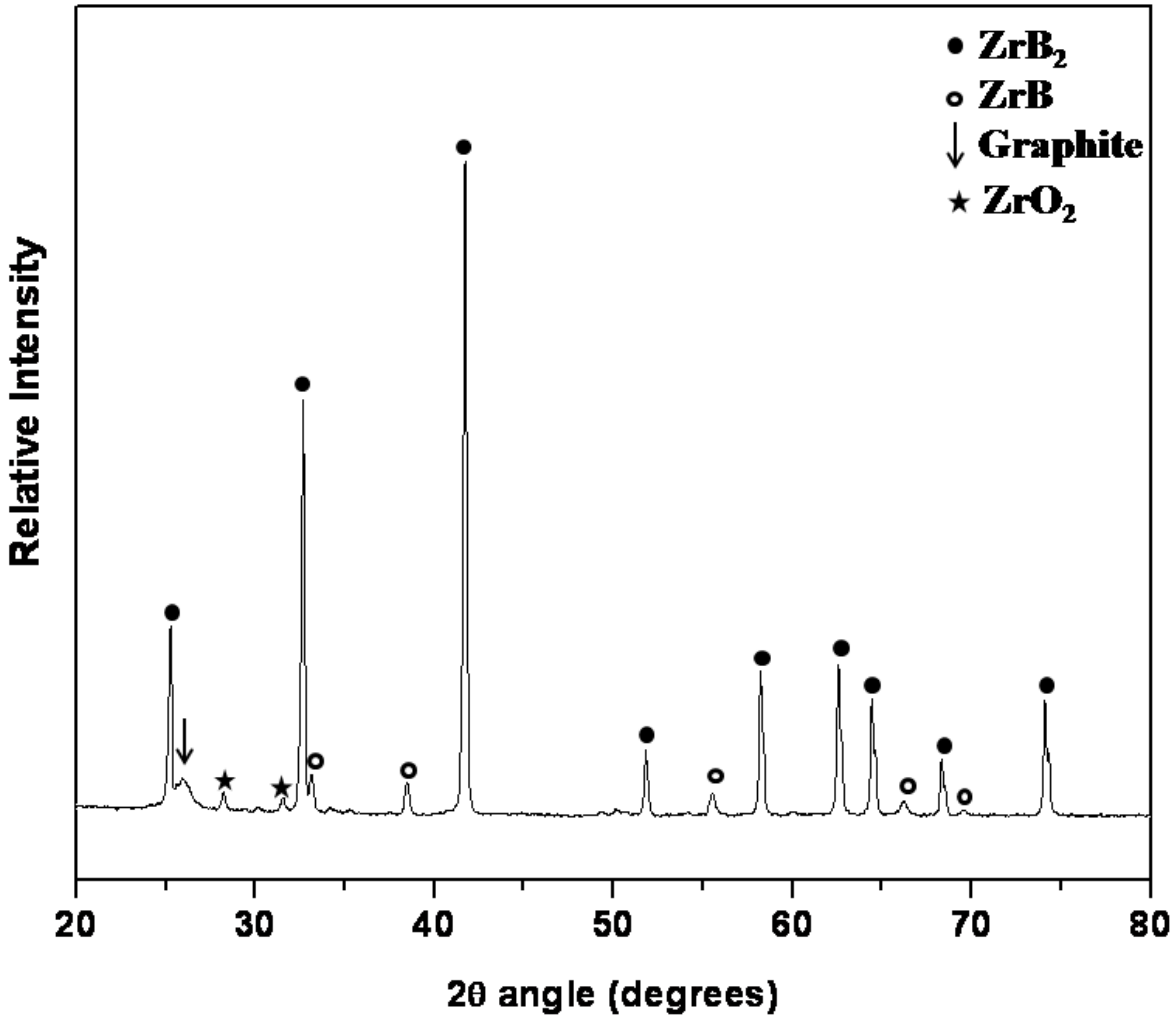

Fig.4.3 XRD Pattern of ZrB_2 powder obtained in thermogravimetry experiment

Results of synthesis experiments carried out in vacuum induction furnace is summarized in Table 4.1.

Table 4.1 Effect of temperature and charge composition on ZrB_2 synthesis

S.No.	Molar ratio ZrO_2: B_4C: C	Temperature (^oC)	Weight loss (%)	Phases present	Carbon (%)	Oxygen (%)
1.	2: 1: 3	1200	18.47	ZrB_2, ZrO_2	9.7	5.22
2.	2: 1: 3	1400	27.15	ZrB_2, ZrO_2	8.2	2.4
3.	2: 1: 3	1650	30.28	ZrB_2, ZrB, ZrO_2 ,C	7.3	2.4
4.	2: 1: 3	1700	31.66	ZrB_2, ZrB, C	3.5	2
5.	2: 1: 3	1800	33.04	ZrB_2, ZrB, C	3.2	0.57
6.	2: 1.1: 2.7	1800	32.67	ZrB_2	1.3	1.5
7.	2: 1.1: 2.7	1875	33.01	ZrB_2	0.06	0.5

It is seen that synthesis at 1200 ^oC results in the weight loss of only 18.47% and the product was impure, containing ZrB_2 and ZrO_2 phases. The carbon and oxygen content were 9.7 and 5.22 % respectively. At 1400 ^oC, the weight loss increased to 27.15 % and carbon and oxygen contents decreased to 8.2 and 2.9 % respectively. At 1600^oC, weight loss increases to 30.28 % but the product contained ZrB_2, ZrB, ZrO_2 and C. At temperatures of 1700 ^oC and above, ZrO_2 was absent in the product but ZrB was seen. At 1800^oC the weight loss was close to theoretical value of 33.0%, however the product was composed of ZrB_2, ZrB, and Carbon. The presence of boron deficient phase (ZrB) even after the treatment at 1800 ^oC indicates the loss of boron from the charge, which could occur in the form of boron oxides. The following reactions may result in loss of boron during ZrB_2 synthesis.

$$ZrO_2 + 3/4B_4C + 1/4C \rightarrow ZrB_2 + CO + BO \quad (5.1)$$

$$ZrO_2 + 3/4B_4C \rightarrow ZrB_2 + 1/2B_2O_3 + 1/2CO + 1/4C \quad (5.2)$$

$$ZrO_2 + B_4C \rightarrow ZrB_2 + B_2O + CO \quad (5.3)$$

$$ZrO_2 + 3/4B_4C \rightarrow ZrB_2 + 3/4C + BO_2 \quad (5.4)$$

Gibb's free energy change with temperature for all the above reaction in vacuum atmosphere ($1x10^{-5}$ mbar) is calculated and presented in Fig.4.4. It shows that all the above reactions are thermodynamically feasible at high temperatures and thus results in formation of boron oxides. Boron oxides are in gaseous state at high temperature and thus get removed from the reaction zone by vacuum pump and hence result in loss of boron in the final product. Due to loss of boron, the product contains ZrB as additional phase. Free energy of ZrB formation could not be calculated as data for ZrB is not available.

To carry out study on ZrB_2, it is necessary to form a single phase of ZrB_2. In order to achieve that, the charge composition was modified by adding excess B_4C. Addition of B_4C is supposed to compensate the loss of boron but at the same time it increases the carbon content so carbon in the charge was decreased and modified charge containing excess B_4C and less carbon was used to obtain single phase ZrB_2. Guo et al.[29] have also reported the loss of boron in the form of B_2O_3 and used excess boron in the charge to obtain pure ZrB_2. Zhao et al. [12] have also reported that excess boron needs to be added to compensate the loss of boron in the form of B_2O_3.

Fig.4.5 presents the XRD patterns of product obtained by stoichiometric and modified charge mixture. It is evident that ZrB and graphite phase are not present and single phase ZrB_2 is obtained by reacting the modified charge mixture (molar ratio, ZrO_2: B_4C: C, 2:1.1:2.7) at 1800 ^oC.

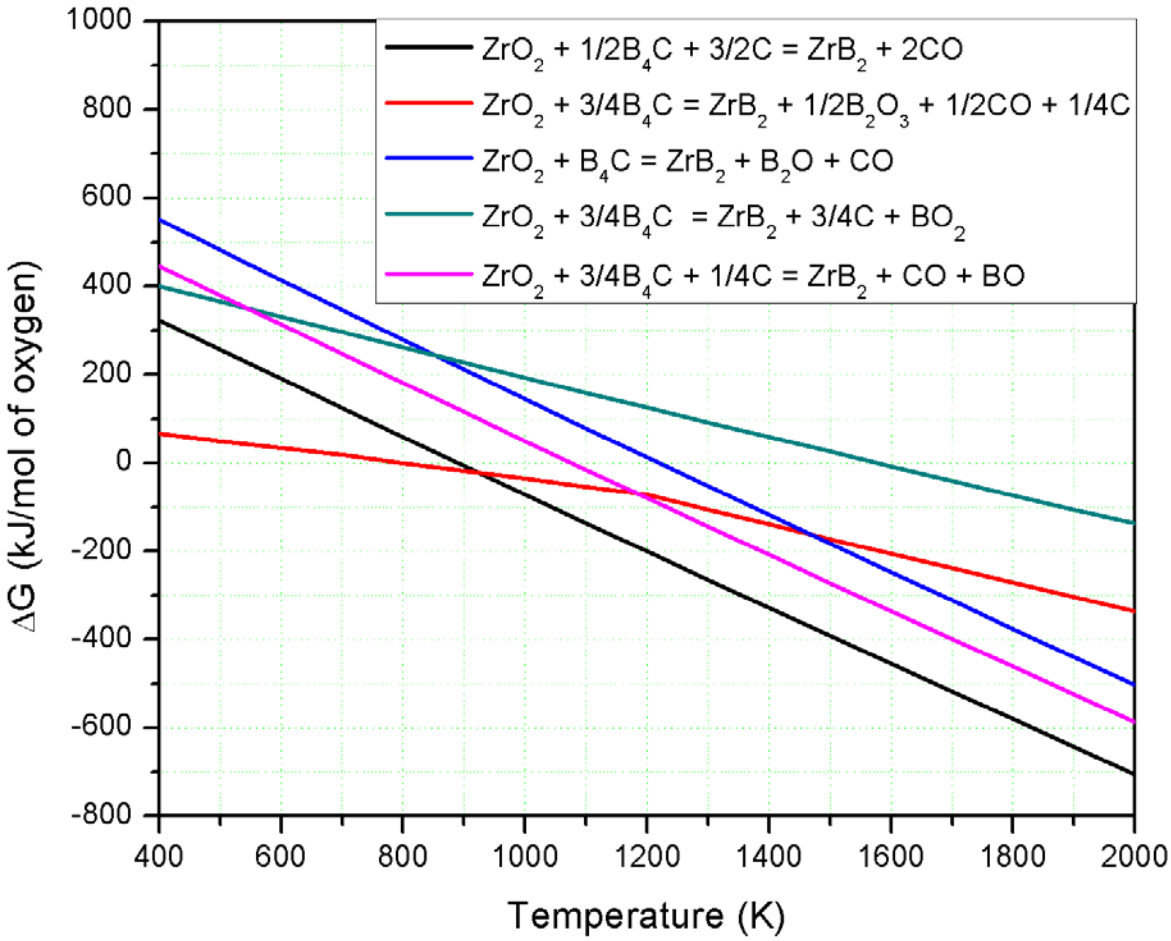

Fig.4.4 Free energy change with temperature for reactions resulting in boron loss

(Calculated by using Factsage software)

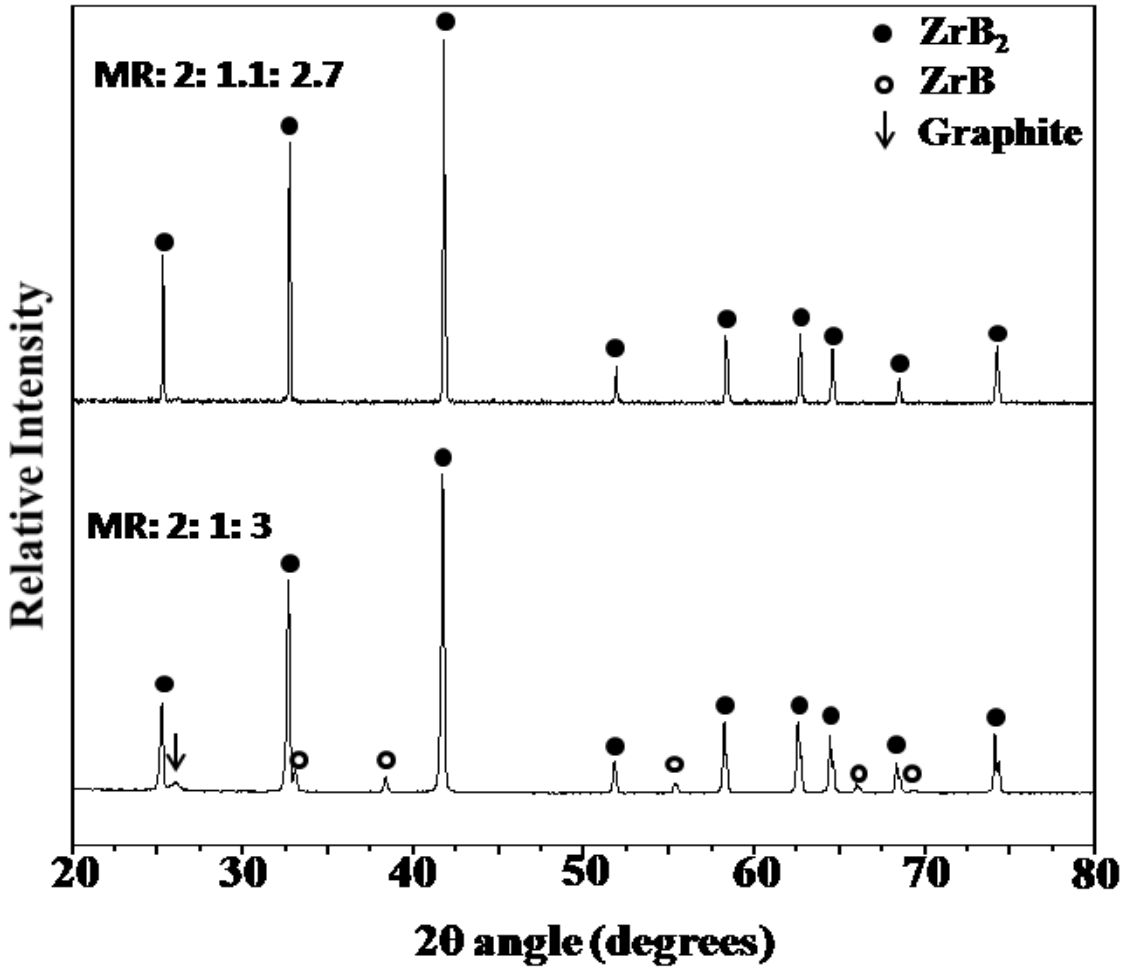

Fig. 4.5. XRD pattern of the products obtained by varying charge composition. MR: molar ratio (ZrO_2:B_4C:C)

Single phase ZrB_2 was formed by heating modified charge at 1825 ^oC but its carbon and oxygen content was still higher The oxygen and carbon content was found to be 1.5 and 1.3% respectively. This product was further purified to low levels of oxygen (0.06 wt%) and carbon (0.5 wt%) by heating to 1875^oC and soaking at this temperature in vacuum for 30 minutes. The progressive removal of carbon and oxygen from the product with reaction temperature and the final purification using modified charge is presented in Fig. 4.6. Oxygen may be present in powder in the form of ZrO_2. Presence of ZrO_2 on powder surface is extremely deleterious for densification as it decreases the specific surface energy of powder particles and thus decreases the driving force of sintering. It also prevents the direct contact between ZrB_2 particles during sintering and thus decreases diffusion rate. Presence of carbon in the final product is deleterious for high temperature properties and should be minimized. Higher oxygen content in the ZrB_2 produced at 1800 ^oC is due to incomplete reaction. Reaction kinetics is very slow as it is a solid state diffusion controlled reaction. High temperature enhanced the kinetics of synthesis reaction and decreased the oxygen and carbon content in the ZrB_2 powder. Guo et al. [29] have prepared ZrB_2 powder by same route at a slightly lower temperature of 1750 ^oC but oxygen content of the powder was higher (0.7 wt.%) compared to present study (<0.5 wt.%).

The obtained ZrB_2 powder was in the form of loosely sintered pellets, which were crushed and ground to obtain powder of desired characteristics. By grinding the powder the specific surface area gets increased which is the driving force for sintering. Properties of densified pellets are a strong function of powder characteristics. To have good mechanical properties the particle shapes should be equiaxed and particle size distribution should be uniform, so that uniform grain size is obtained in the microstructure. To obtain these desired characteristics, ZrB_2 was ground to 2-3 μm range. Longer grinding result in contamination from milling media (Tungsten carbide), which is undesirable. Zirconium diboride is harder than tungsten carbide but there is no other alternate milling media which can be used for grinding ZrB_2. Fig.4.7 presents the particle size distribution of ZrB_2 after grinding. It is seen that particle size distribution is trimodal with peaks around 0.5 μm, 2 μm and 7 μm. Median diameter was determined as 2.7 μm. Fig. 4.8 presents the morphology of the ZrB_2 powder observed in SEM. It is seen that the average particle size is 2.0 -3.0 μm.

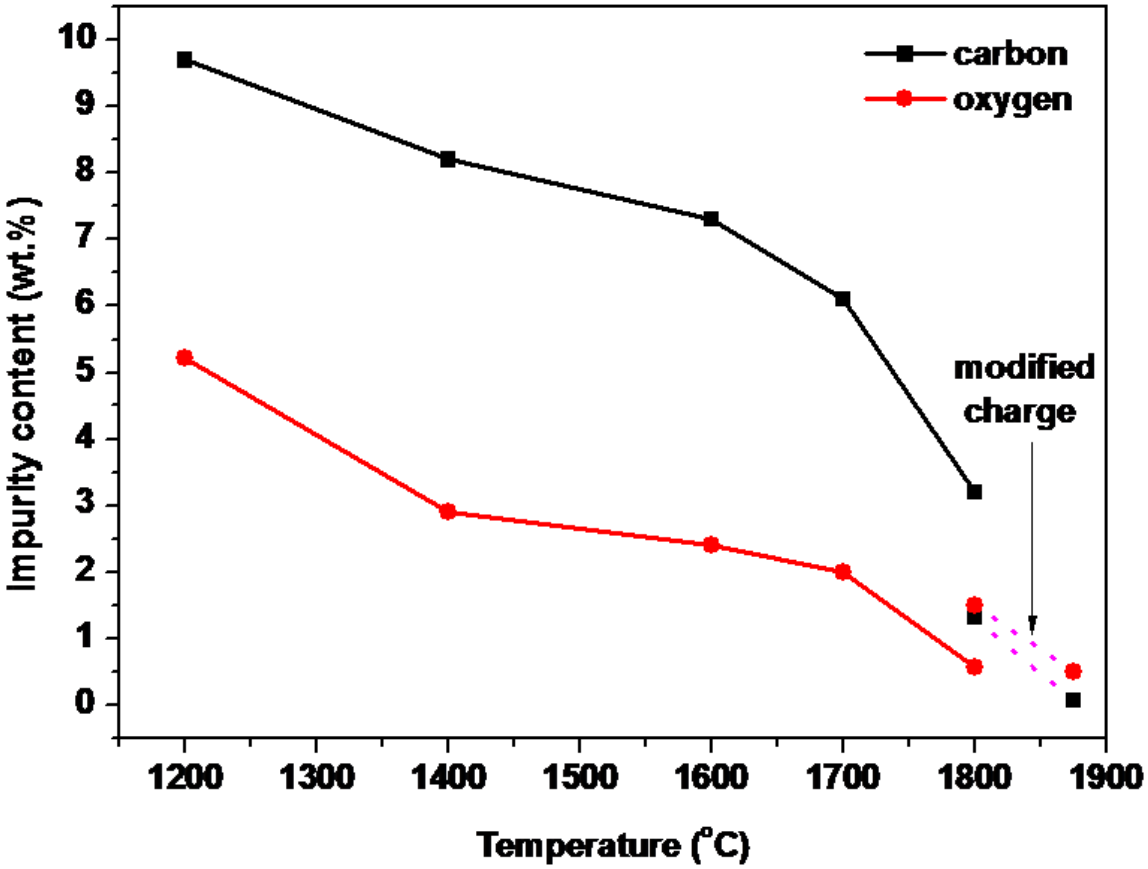

Fig. 4.6 Effect of temperature and charge composition on carbon and oxygen content of the ZrB_2 obtained (solid lines connecting data points are for visual aid only)

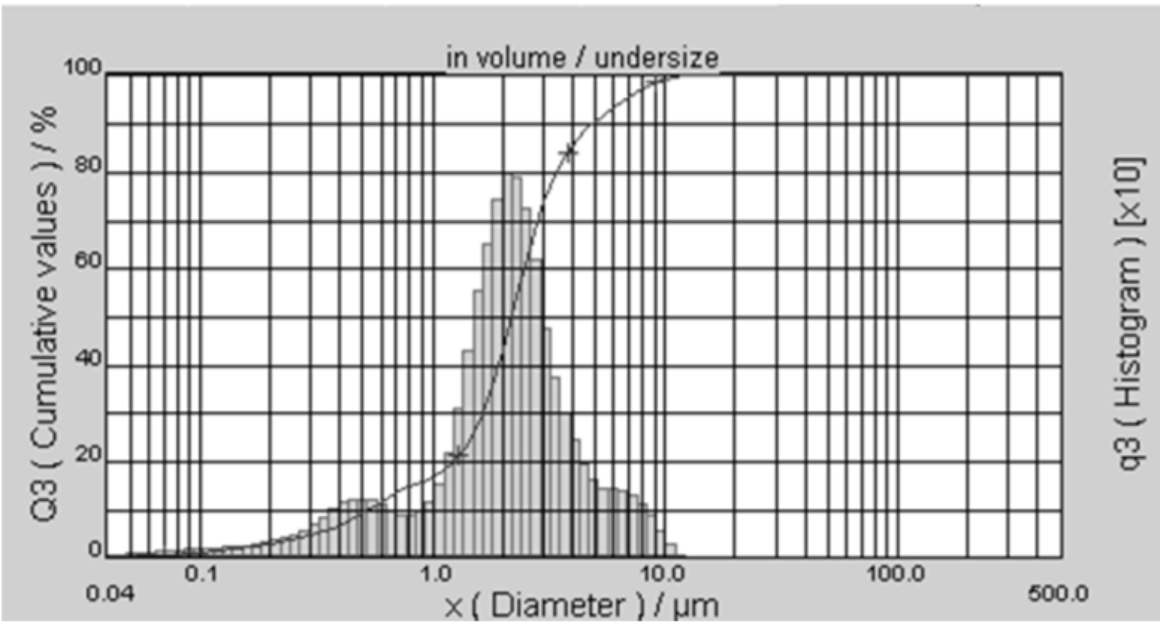

Fig. 4.7 Particle size distribution of ZrB_2 powder synthesized at 1875 ^{o}C using modified charge

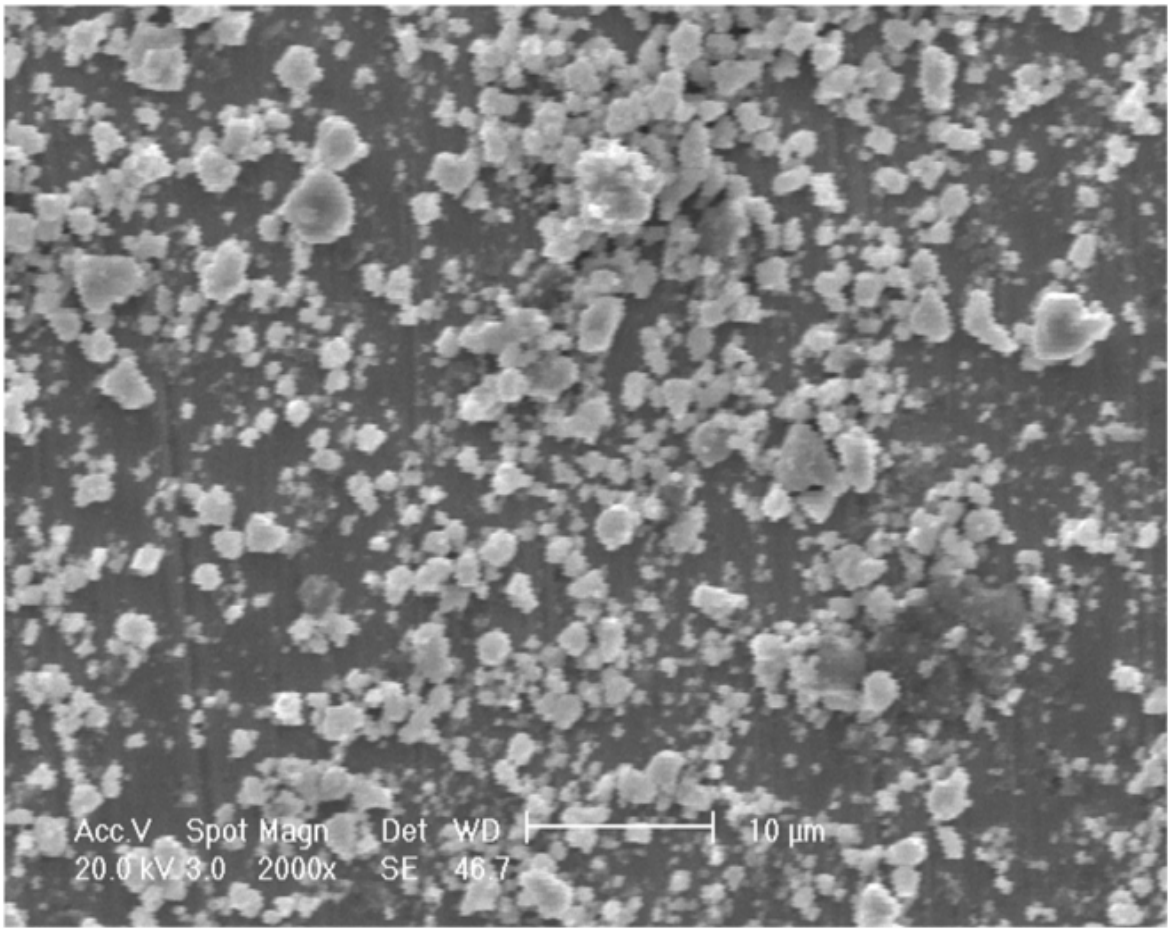

Fig. 4.8 SEM image of ZrB_2 powder synthesized at 1875 ^{o}C using modified charge

In literature, various methods have been reported for synthesis of zirconium diboride. carbothermic reduction in presence of B_4C is indeed an excellent method for producing ZrB_2 powder as it involves the use of easily available raw materials. This study enhances the knowledge available on the understanding of this synthesis route. It was observed that reaction starts at 1200 ^oC, but pure ZrB_2 was obtained at a much higher temperature of 1875 ^oC. It is a solid state reaction in which the product ZrB_2 forms on the surface of reactants and then reactants diffuse through product layer for further reaction. ZrB_2 is a covalently bonded compound and hence diffusion through it is very slow. Therefore high temperature is required to enhance the diffusion kinetics and carry out complete reaction. Subramanian et al.[121] have reported similar observation in case of TiB_2 synthesis by the same route. Thermogravimetry experiment indicated that reaction started at 1092 ^oC itself but the pure TiB_2 could be obtained at much higher temperature (>1800 ^oC).

Furnace atmosphere has a strong influence on progress of reaction. Gibbs free energy change with temperature for ZrB_2 synthesis reaction is calculated for both standard state (1 bar) and vacuum ($1x10^{-5}$ mbar) conditions. The results are presented in Fig.4.9. It shows that free energy change becomes negative at temperature higher than 1700 K (1427 ^oC) when the surrounding pressure is 1 bar whereas at $1x10^{-5}$ mbar, the reaction becomes feasible at 900 K (627^oC). Presence of vacuum decreases the activity (partial pressure) of CO and so free energy change becomes negative at lower temperature. In simple terms, vacuum accelerates the removal of carbon mono-oxide (CO) from reaction zone and according to Le Chatelier's principle the reaction moves faster in forward direction.

One important finding of this study is formation of ZrB phase due to evaporation losses of boron in the form of its oxides. As per author's knowledge there is no report on formation of ZrB during this reaction. Haggerty et al. [122] have noticed the presence of ZrB phase along with ZrB_2 which was prepared by floating zone method. Champian et al. [123] have observed ZrB phase on the interface of Zr - ZrB_2 system.

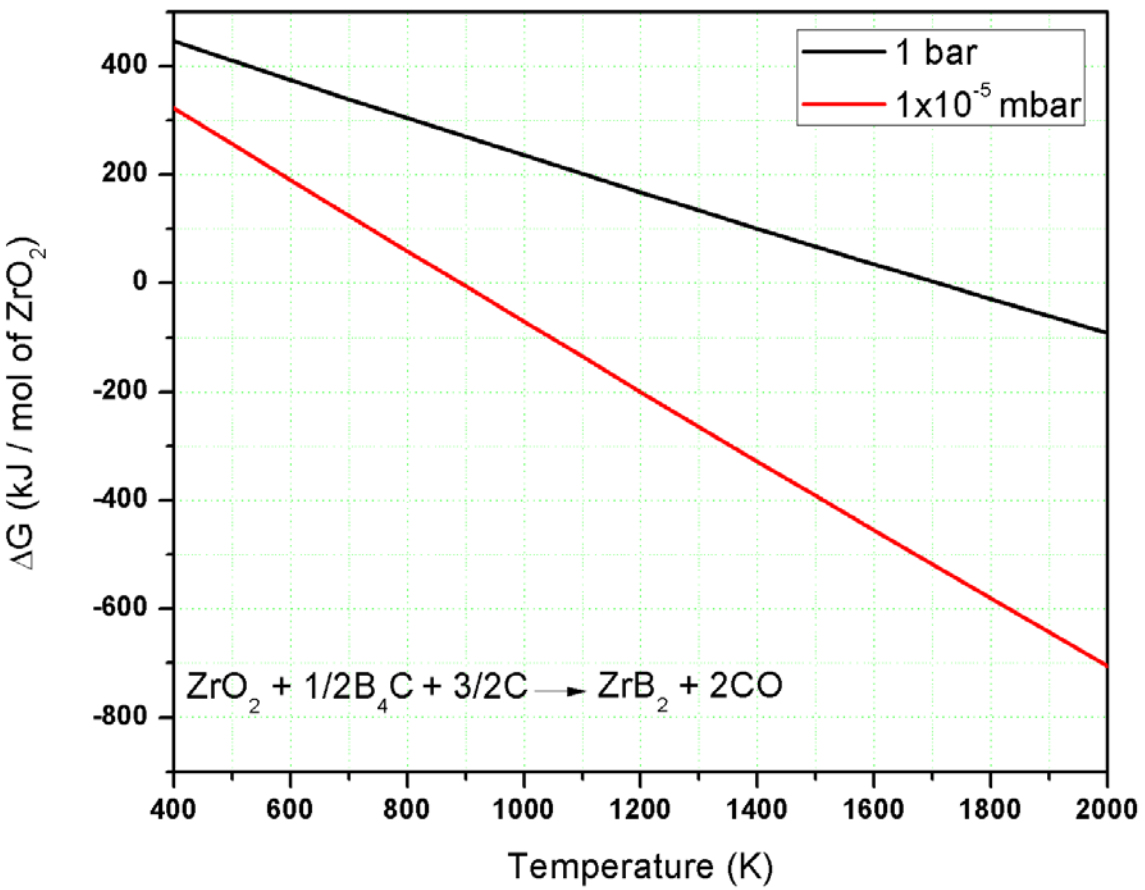

Fig.4.9 Free energy change with temperature for ZrB_2 synthesis (Effect of Vacuum) (Calculated by using FactSage software (version 6.5))

4.1.2 EuB_6 synthesis

EuB_6 was used as sinter additive to ZrB_2. EuB_6 is a boron rich boride and thus can introduce point defects in ZrB_2 lattice on formation of solid solution. Presence of point defects would result in enhanced diffusion and thus may be helpful in densification. EuB_6 was synthesized by reduction of Eu_2O_3 by B_4C according to reaction 4.2.

$$Eu_2O_3 + 3B_4C \rightarrow 2EuB_6 + 3CO \uparrow \quad (4.2)$$

Table 4.2 presents the processing parameters and results of EuB_6 synthesis experiments carried out in vacuum induction furnace. At 1200°C, weight loss is only 2.65% and product is composed of both EuB_6 and Eu_2O_3 phases. Weight loss gradually increases to 4.26 % at 1250°C. At 1300 ^{o}C, loss in weight is 19.56 %, which is higher than the theoretical loss of 16.23%. Though the product contains only EuB_6, its carbon and oxygen content is high at 3.8 and 2.1% respectively. On increasing synthesis temperature to 1400 ^{o}C, weight loss also increased to 21.62% (Fig.4.10), with decrease in carbon and oxygen content of the product (Fig.4.11) and relatively pure EuB_6 is obtained.

Table 4.2: Effect of temperature on synthesis of Europium hexaboride (holding time: 2 hr)

Temperature (^{o}C)	Weight loss (%)	Phases present in XRD Pattern	Carbon (Wt.%)	Oxygen (Wt.%)
1200	2.65	EuB_6, Eu_2O_3	7.4	11.4
1250	4.26	EuB_6	5.9	7.3
1300	19.56	EuB_6	3.8	2.1
1400	21.62	EuB_6	2.6	0.4

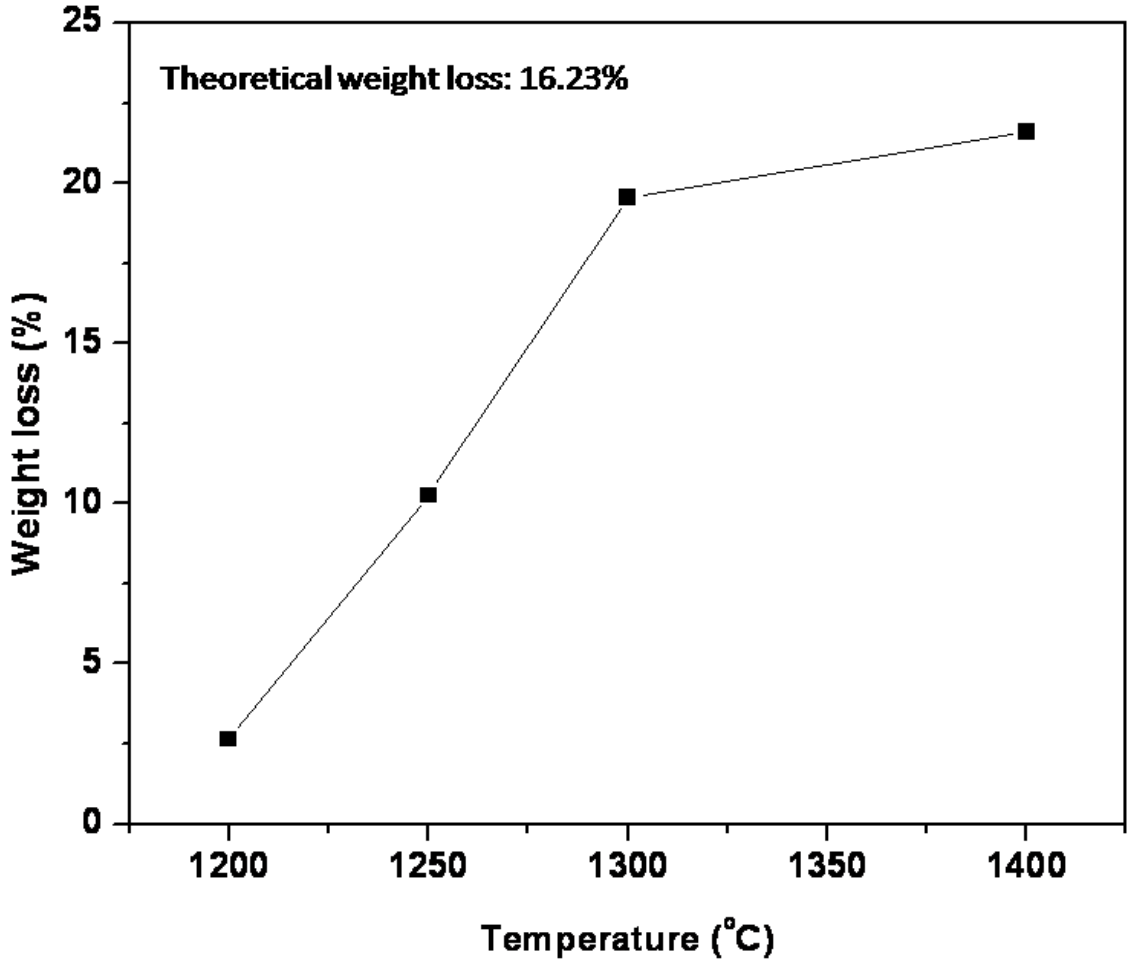

Fig.4.10 Weight loss vs. Temperature during synthesis of EuB_6 (Holding time : 2 h) **(**solid lines connecting data point are for visual aid only)

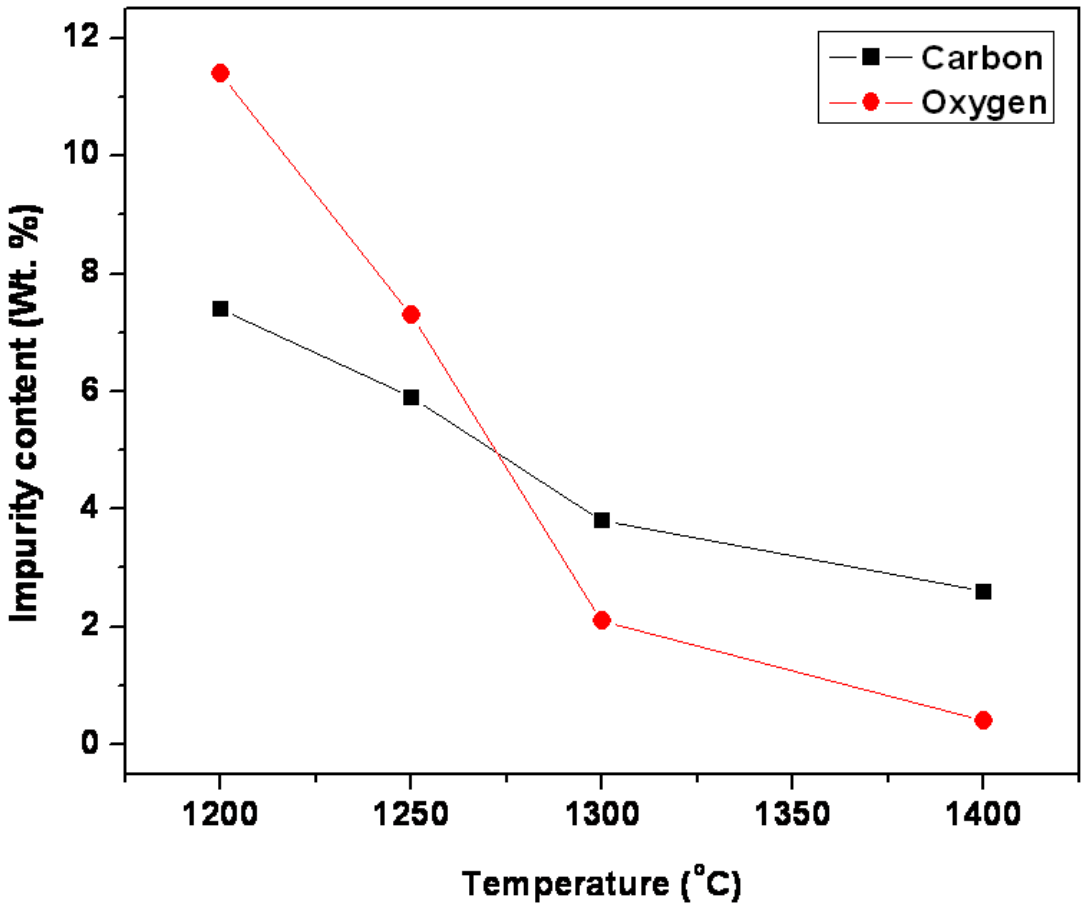

Fig.4.11 Carbon and oxygen content of EuB_6 synthesized at various temperature (solid lines connecting data point are for visual aid only)

Fig. 4.12 presents the XRD pattern indicating changes in the product as a function of temperature. It reveals that intensity of EuB_6 peaks increases with increase in temperature. Product obtained at 1400 ^oC contains 2.6% carbon. The higher carbon content and higher weight loss could be due to the formation of volatile boron oxide during reaction. To reduce carbon in the product, the charge was modified by adding elemental boron and lowering B_4C addition. Table 4.3 presents the effect of charge composition on carbon and oxygen content of the product obtained. Carbon content was reduced to 0.7 % by using modified charge.

Table 4.3 Effect of charge composition on carbon and oxygen content

(Temp.; 1400 ^oC, holding time ; 2 hour)

Charge composition	Phases present	Carbon (Wt.%)	Oxygen (Wt.%)
$Eu_2O_3 + 3B_4C$	EuB_6	2.6	0.4
$Eu_2O_3 + 2.85B_4C + 0.77\ B$	EuB_6	1.3	0.9
$Eu_2O_3 + 2.7B_4C + 1.5\ B$	EuB_6	0.7	0.6

Though the reaction starts at a lower temperature, pure EuB_6 is obtained only at 1400^oC. At the start of the reaction, EuB_6 forms on the surface of starting powders. For completion of reaction, the reactants have to diffuse through EuB_6 surface layer. The diffusion through boride is a slow process and requires high temperature and longer time. Liu et al.[124] have reported that NdB_6 powder is prepared by boron carbide reduction of Nd_2O_3 at 1500^oC in vacuum. Xu et al.[125] have prepared LaB_6 by this route at 1650^oC at atmospheric pressure. Fig. 4.13 presents the morphology of the EuB_6 powder observed in SEM. It shows the particles are of 1-3 μm in size.

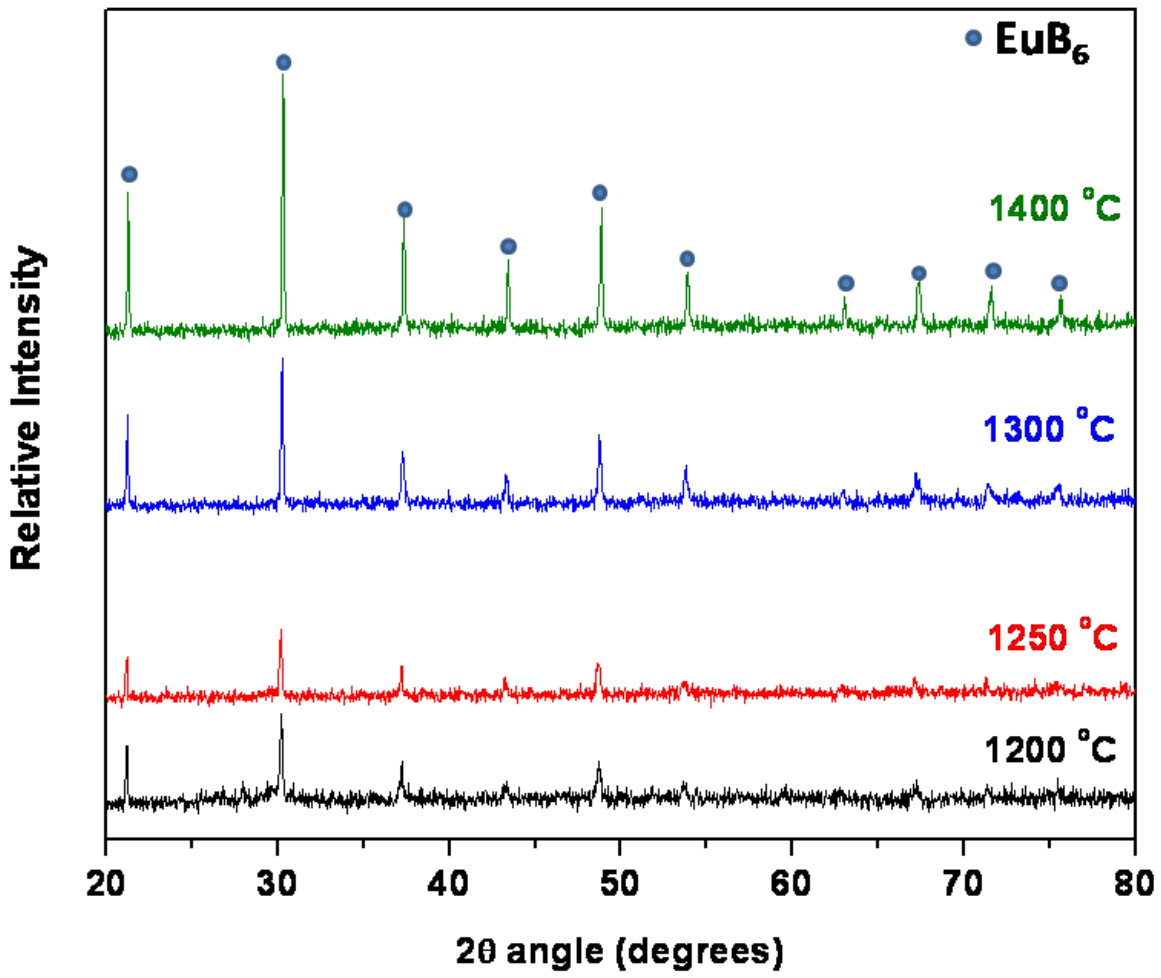

Fig. 4.12 XRD pattern of EuB_6 synthesized at various temperatures

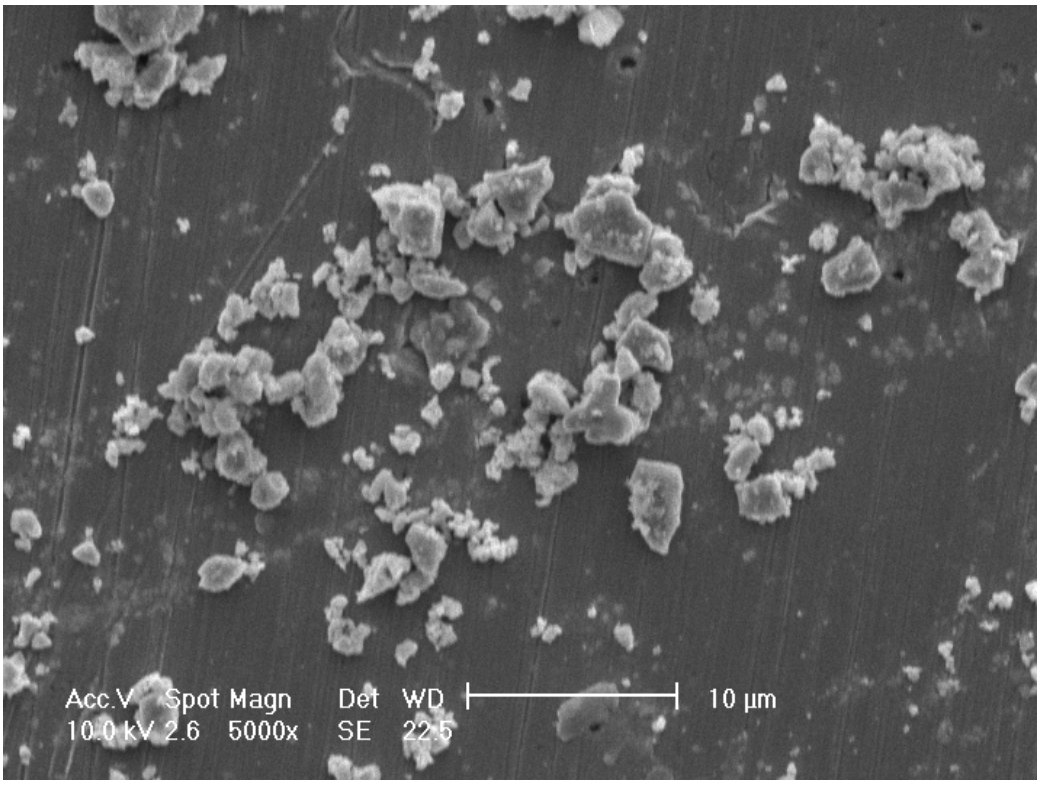

Fig.4.13 SEM image of EuB_6 powder synthesized at 1400 ^{o}C using modified charge

4.1.3 HfB_2 synthesis

HfB_2 was used as additive to ZrB_2. It is expected to enhance the mechanical properties by formation of solid solution. It was synthesized by reduction of HfO_2 by carbon in presence of B_4C according to reaction (4.3).

$$HfO_2 + 1/2B_4C + 3/2C \rightarrow HfB_2 + 2CO\uparrow \quad (4.3)$$

Fig.4.14, 4.15 and 4.16 present the effect of temperature on weight loss, phases present and impurity (O and C) content of the product from synthesis experiments carried out in vacuum induction furnace. At 1200 ^{o}C weight loss is very low at 6.2% and the product is composed of both HfB_2 and HfO_2 phases. Carbon and oxygen content is also high at 7.8 and 9.8 respectively. With increase in temperature, the weight loss increases and the impurity contents decrease. At 1600 ^{o}C, though only HfB_2 phase is present in the product, weight loss is still less than theoretical value, indicating the reaction to be incomplete. At 1875 ^{o}C, weight loss recorded was 26.51% and the carbon and oxygen contents was 0.4 and 0.5 wt.% respectively. Effect of synthesis parameters on weight loss, phase composition and impurity contents are summarized in Table 4.4.

Fig. 4.17 presents the particle size distribution of the HfB_2 powder after grinding in vibratory cup mill. It shows that particle size distribution is di-modal with peaks at 0.8 μm and 2 μm. Fig. 4.18 presents the SEM image of HfB_2 powder.

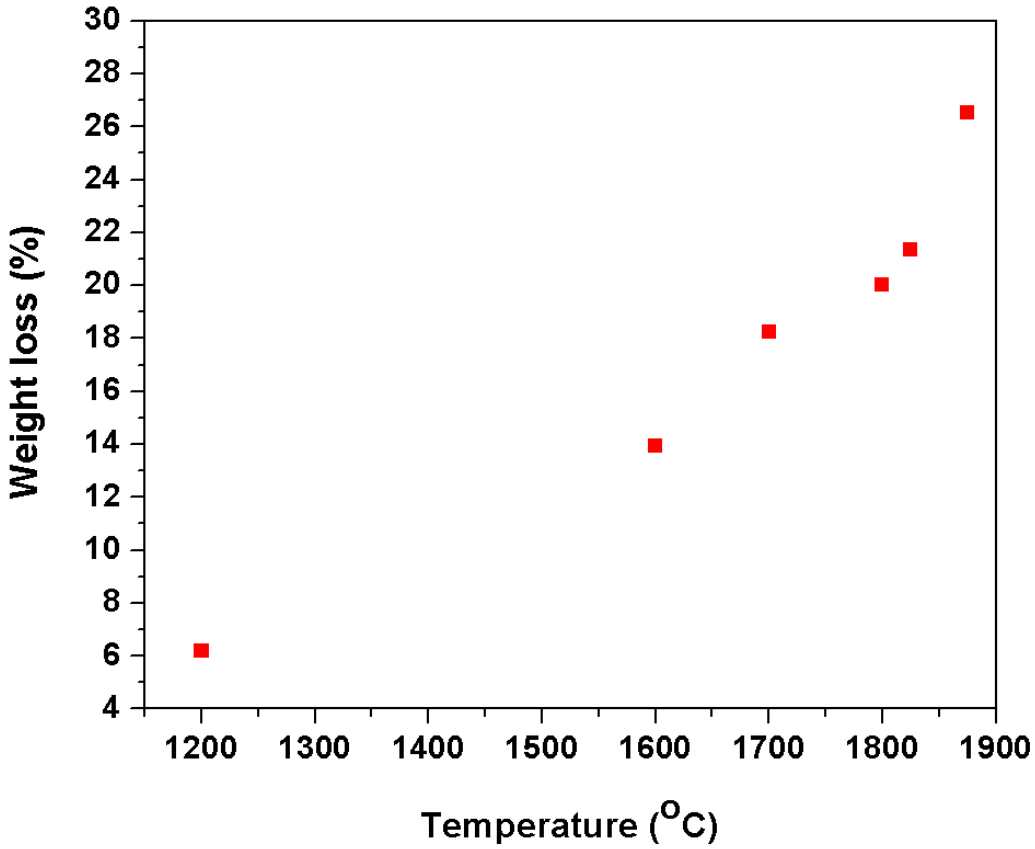

Fig.4.14 Weight loss vs. temperature during synthesis of HfB_2 (time: 2 h)

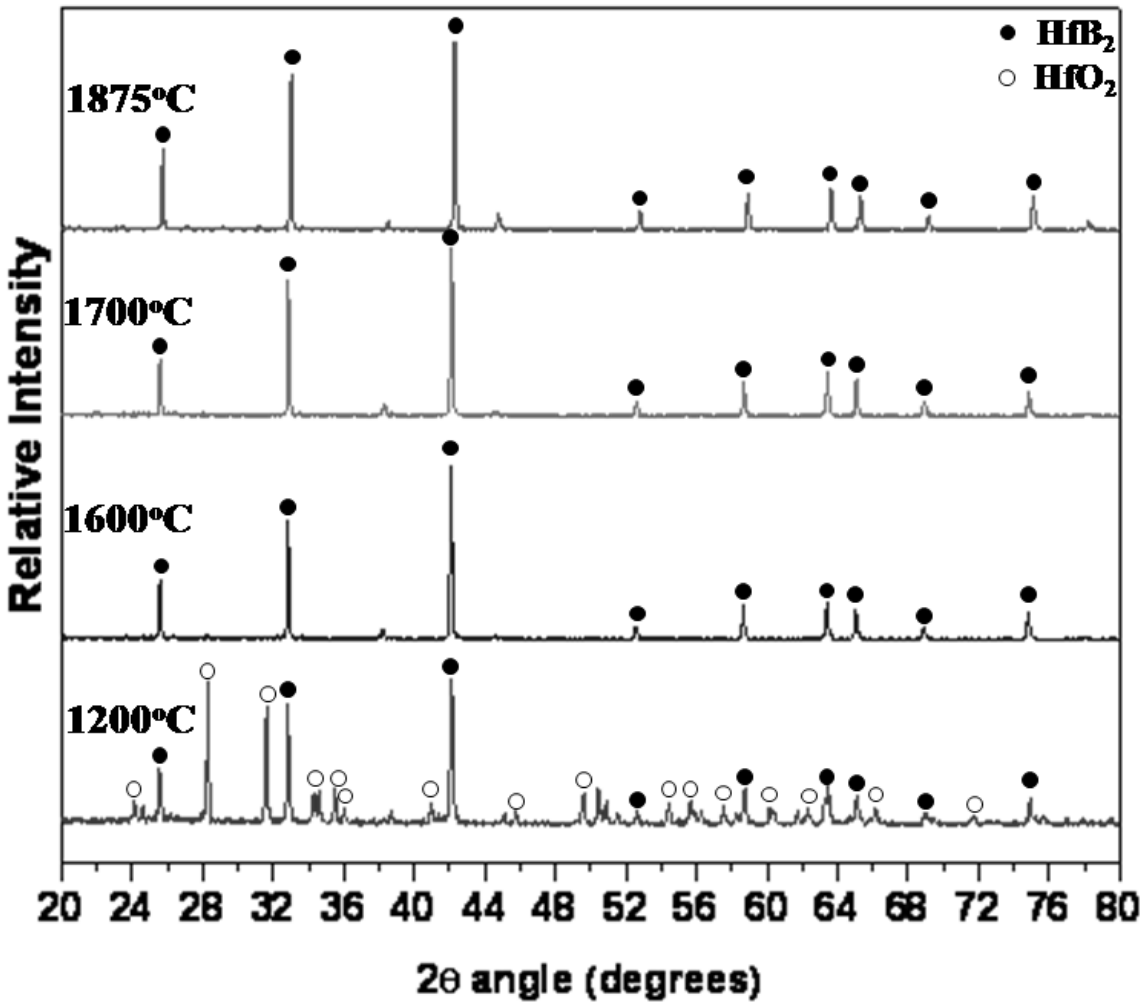

Fig.4.15 XRD of HfB_2 synthesized at various temperatures

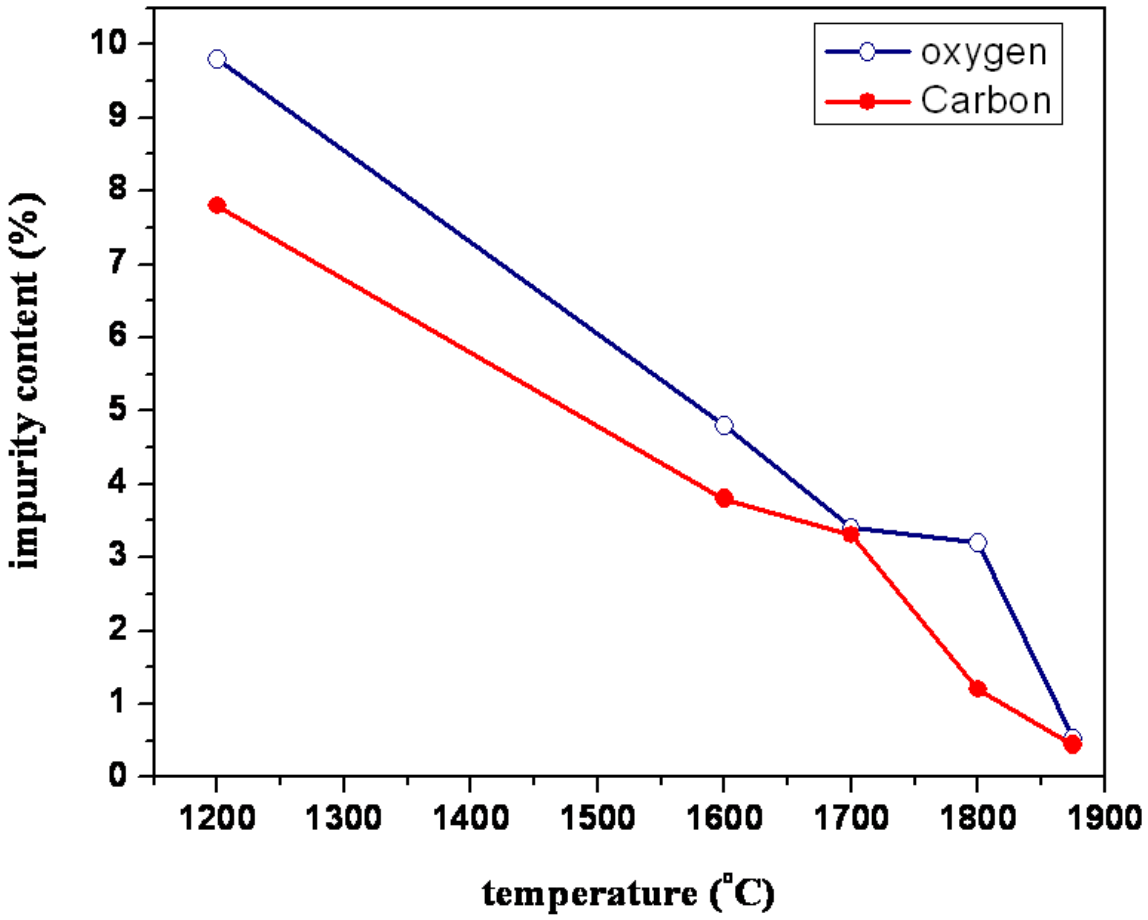

Fig.4.16 Carbon and oxygen content of HfB_2 synthesized at various temperatures (solid lines connecting data point are for visual aid only)

Table 4.4 : Effect of temperature on weight loss, phases present and impurity content on synthesis of HfB_2 **(**charge composition: stoichiometric, time : 2 hour)

S.No.	**Temp. (^oC)**	**Weight loss (%)**	**Phases present**	**O%**	**C %**
1.	1200	6.20	HfB_2, HfO_2	9.8	7.8
2.	1600	13.94	HfB_2	4.8	3.8
2.	1700	18.25	HfB_2	3.4	3.3
3.	1800	20.02	HfB_2	3.2	1.2
4.	1825	21.35	HfB_2	2.4	1.2
5.	1875	26.51	HfB_2	0.5	0.4

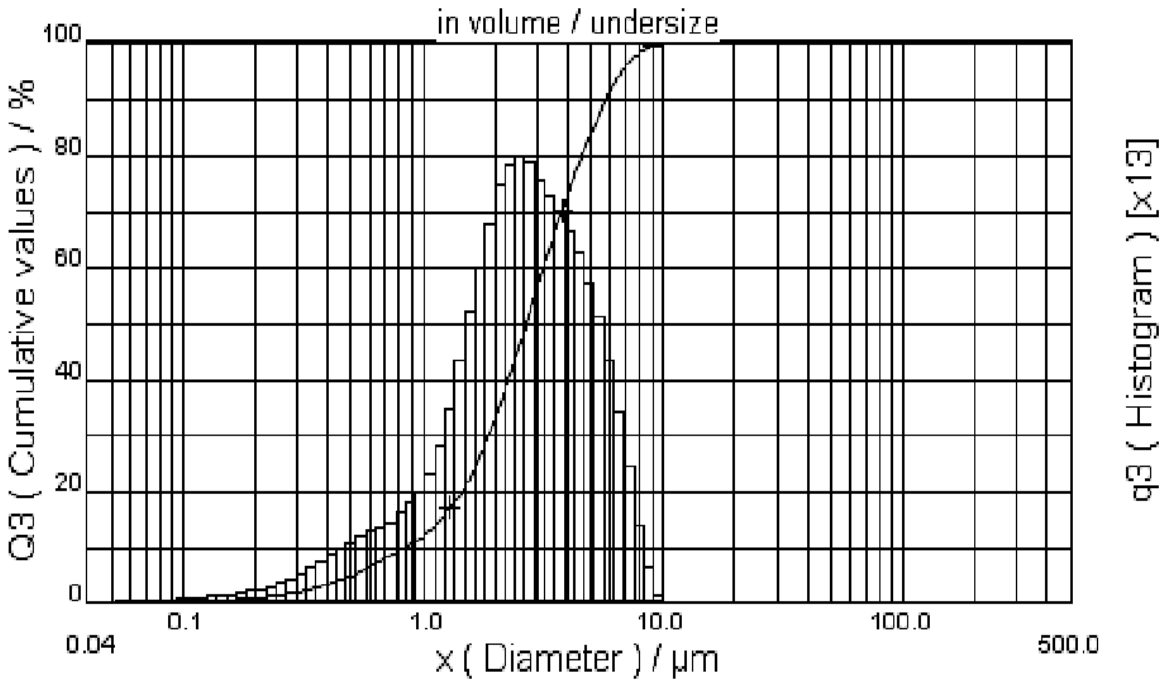

Fig.4.17 Particle size distribution of HfB_2 powder

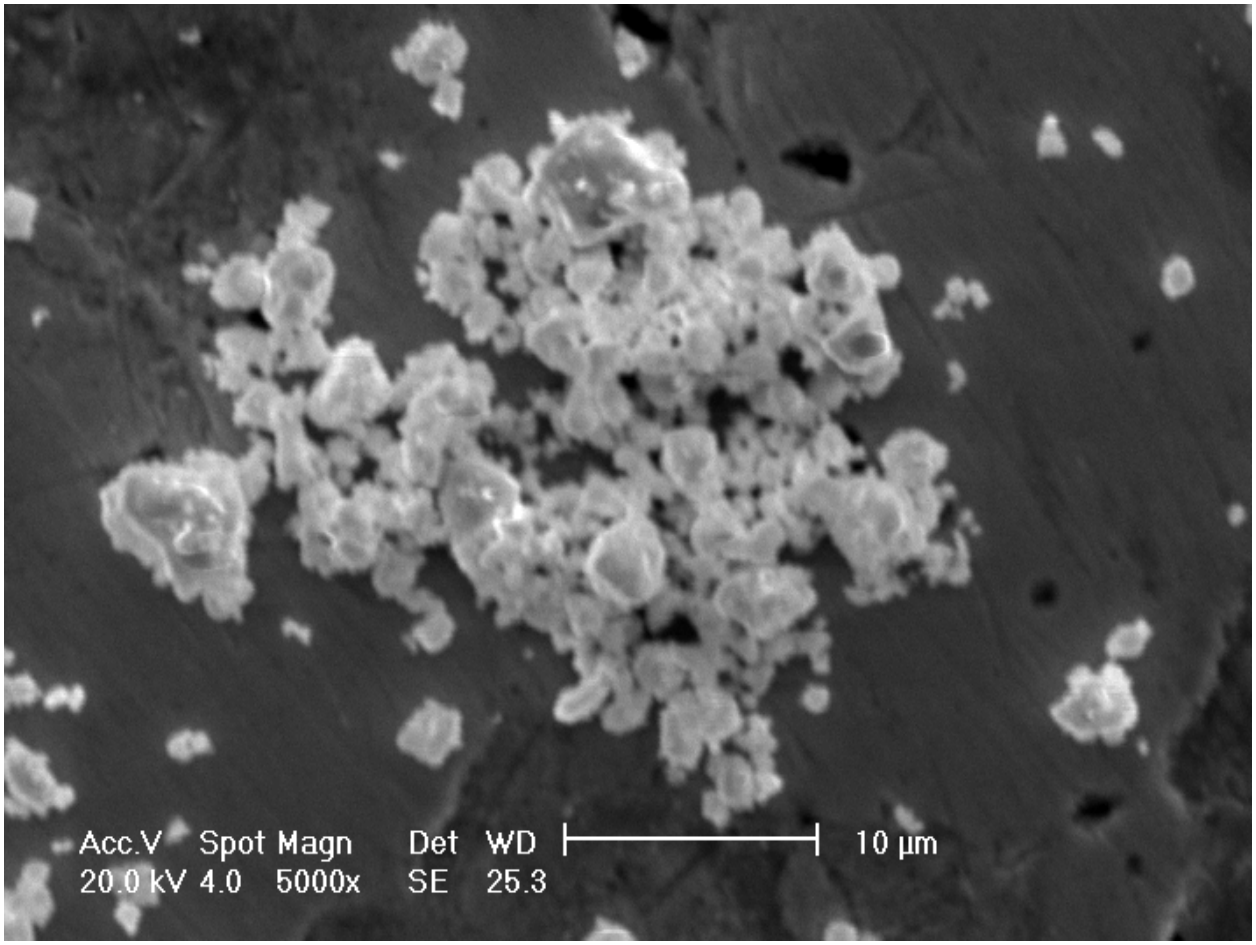

Fig. 4.18 SEM image of HfB_2 Powder particles.

4.2 Densification, mechanical properties and microstructure

This section describes the results on densification, mechanical properties and microstructural characterization of prepared composites. ZrB_2 was used as base material. Densification studies were carried out on mololithic ZrB_2 by pressureless sintering and hot pressing. Effects of sinter additives on densification, mechanical properties were investigated.

4.2.1 Monolithic ZrB_2

Pressureless sintering experiments were carried out in vacuum induction furnace in the temperature range of 1800-2000°C. Pressureless sintering has resulted in maximum density of 78% only. By Hot pressing ZrB_2 was densified to nearly theoretical density at 1850°C and under 35 MPa pressure using graphite die. ZrB_2 has high melting point and low intrinsic self diffusivity, so pressure less sintering of ZrB_2 results in porous bodies [1]. Simultaneous application of pressure and temperature results in better contact between powder particles during the process and thus enhanced diffusion at the particle contact points which in turn helps in densification. At high temperature and pressure diffusional creep takes place which assist in better densification.

Microhardness was measured on the polished surface at a load of 100 gm and dwell time of 10 sec. The indentation fracture toughness (K_{IC}) data were evaluated by crack length measurement of the crack pattern form around Vickers indents (using 10 Kg load). Hardness and fracture toughness values were measured as 23.9 GPa and 3.3 MPa.m$^{1/2}$ respectively. The values obtained are in agreement with values reported in literature [2] Fractured surface of the dense bodies revealed that intergranular fracture is predominant mechanism (Fig. 4.19). Regular faceted grains of 4-6 micron are visible. ZrB_2 has hexagonal crystal structure, which has anisotropic properties in different crystal directions. This may lead to residual stress which in turn causes intergranular fracture.

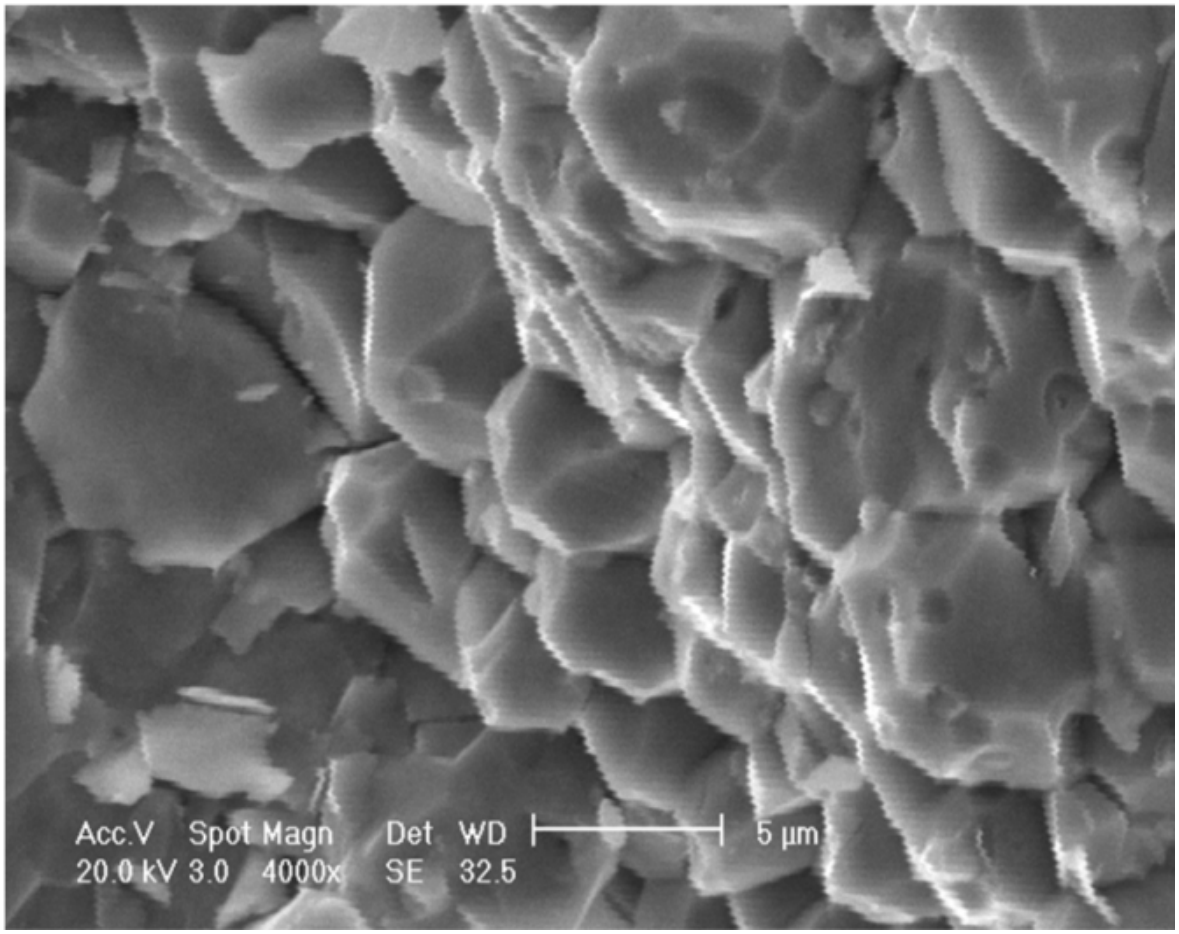

Fig. 4.19 Fractured surface of monolithic ZrB_2

4.2.2 Effect of $TiSi_2$ addition on densification and properties of ZrB_2

4.2.2.1 Densification

Effect of $TiSi_2$ on densification of ZrB_2 was investigated. Table 4.5 presents the comparison of processing conditions and density obtained in monolithic ZrB_2 and composites.

Table 4.5 effect of sinter additives on densification and properties of ZrB_2

sample	Temp. (^oC)	Pressure (MPa)	Bulk density (gm/cc)	Theoretical density (gm/cc)	Relative Density (%)
ZrB_2	1850	35	6.09	6.10	99.8
ZrB_2	1650	35	5.07	6.1	83.1
ZrB_2 + 10 wt.% $TiSi_2$	1650	20	5.76	5.82	98.9
ZrB_2 + 10 wt.% $TiSi_2$	1550	20	5.02	5.82	86.2
ZrB_2 + 10 wt.% $TiSi_2$ + 10% HfB_2	1650	20	6.06	6.09	99.6
ZrB_2 + 10 wt.% $TiSi_2$ + 20% HfB_2	1650	20	6.28	6.38	98.4

Addition of 10% $TiSi_2$ enhanced the density of ZrB_2 pellet from 83.1% to 98.9% at 1650°C and 20 MPa. The enhanced sintering is probably due to liquid phase sintering caused by $ZrSi_2$ which forms by reaction between ZrB_2 and $TiSi_2$. Formation of $ZrSi_2$ phase was observed by XRD analysis (Fig. 4.20) and SEM –EDS analysis (Fig. 4.21) of hot pressed sample. $ZrSi_2$ has low melting point (1620 ^{o}C) and hence results in liquid phase sintering. At 1550 ^{o}C, the density achieved in ZrB_2 + 10%$TiSi_2$ sample was only 86.25 of theoretical value. This is due to the absence of liquid phase $ZrSi_2$ which has a melting point of 1620 ^{o}C. During hot pressing $TiSi_2$ first reacts with ZrB_2 and results in the formation of $ZrSi_2$, which helps in densification by liquid phase sintering. Application of less than 20 MPa pressure also resulted in poor density (less than 90%). Samples with lower than 90% density were not characterized further.

Theoretical density was measured by applying rule of mixture without considering the reaction products as the quantity of reaction product was not known and density difference between reactants (ZrB_2 and $TiSi_2$) and products (($Zr_{0.9}Ti_{0.1}$) B_2) were very less. An effort was made to calculate the theoretical density of ZrB_2+ 10%$TiSi_2$ considering densities of reaction product and assuming that all the $TiSi_2$ gets converted to $ZrSi_2$ and TiB_2 and thus product contains 90% (($Zr_{0.9}Ti_{0.1}$) B_2) and 10% $ZrSi_2$. The calculated density was found 5.76 gm/cc which differes by merely 1% from the density calculated based on the initial raw powders (ZrB_2 + 10% $TiSi_2$). Moreover, If theoretical density is considered to be 5.76 gm/cc then the relative density of the sample is 100% of theoretical which also confirms that $TiSi_2$ addition is very helpful in densification of ZrB_2 at lower temperature.

4.2.2.2 Mechanical properties:

Table 4.6 summarizes the mechanical properties of ZrB_2 based composites. Hardness of ZrB_2 + 10%$TiSi_2$ is measured as 19.5 GPa (at 100 gm load) which is lower than that of monolithic ZrB_2 (23.9 GPa). The lower hardness is due to the presence of relatively soft $ZrSi_2$ phase. To compensate for the reduction in hardness, HfB_2 was added and two more samples of composition (a) ZrB_2+10%$TiSi_2$+10%HfB_2 and (b) ZrB_2+10%$TiSi_2$+20%HfB_2 were also prepared. Near theoretical density was obtained in both the sample at 1650 ^oC and 20 MPa. Hardness of ZrB_2+10%$TiSi_2$+10%HfB_2 was measured as 23.1 GPa, which is comparable to that of monolithic ZrB_2.

Fracture toughness of ZrB_2 + 10%$TiSi_2$ was measured as 6.4 MPa.m$^{1/2}$ which is 50% higher than that of the monolithic ZrB_2. Similar values were obtained in case of ZrB_2+10%$TiSi_2$+10%HfB_2 and ZrB_2+10%$TiSi_2$+20%HfB_2 samples. The increased fracture toughness is attributed to crack deflection. Thermal expansion mismatch between the matrix and second phase results in residual stresses which causes crack deflection. $ZrSi_2$ is having higher thermal expansion coefficient (~9×10^{-6} $^oC^{-1}$) compared to boride (5.9×10^{-6} $^oC^{-1}$) . When thermal expansion coefficient of particulate phase is higher than that of the matrix phase, compressive stress is generated in matrix which increases the fracture toughness.

Table 4.6 Effect of $TiSi_2$ and HfB_2 addition on mechanical properties of ZrB_2

Additive	Hardness (GPa) (100 gm load)	K_{IC} (MPa $m^{1/2}$)
nil	23.9±1.5	3.3±0.2
10 wt.% $TiSi_2$	19.4±1.9	6.4±1.0
10% HfB_2 +10 wt.% $TiSi_2$	23.1±1.3	6.4±1.1
20% HfB_2 +10 wt.% $TiSi_2$	23.7±1.8	6.6±0.7

4.2.2.3 Phase analysis and microstructure

XRD pattern of the dense pellets are shown in Fig. 4.20. All the three samples indicate the presence of crystalline ZrB_2 and $ZrSi_2$. $ZrSi_2$ is formed dur ing sintering by the following reaction.

$$ZrB_2 + xTiSi_2 \rightarrow xZrSi_2 + (Zr_{(1-x)}Ti_x)B_2 \quad (4.4)$$

TiB_2 is not seen in the XRD pattern of sintered product due to the formation of ZrB_2-TiB_2 solid solution. Formation of ZrB_2-TiB_2 solid solution was verified by peak shift observed in XRD pattern of ZrB_2 +10%$TiSi_2$ sample. Interplanar spacing of ZrB_2 phase was found to decrease by $TiSi_2$ addition. This is due to lower atomic radius of Ti (14.5 nm) compared to that of Zr (15.5 nm). HfB_2 also forms solid solution with ZrB_2 and hence not seen as distinct phase in XRD pattern. Post *et al.* [126] have reported that, these borides have complete mutual solubility. $ZrSi_2$ assists in densification by liquid phase sintering as it has low melting point (1620 ^oC).

Fig.4.21 presents the secondary electron image of ZrB_2+10%$TiSi_2$+20%HfB_2 composites. It shows the presence of dark phase in the gray matrix. EDS pattern of the phases are also inserted into the picture. Gray matrix is essentially ZrB_2 in which Ti and Hf have diffused whereas dark phase contains mainly Si with some Zr. Fig.4.22 presents the elemental mapping for Zr, Ti and Si. It shows that Zr and Ti are distributed uniformly whereas Si is present only in the black phase.

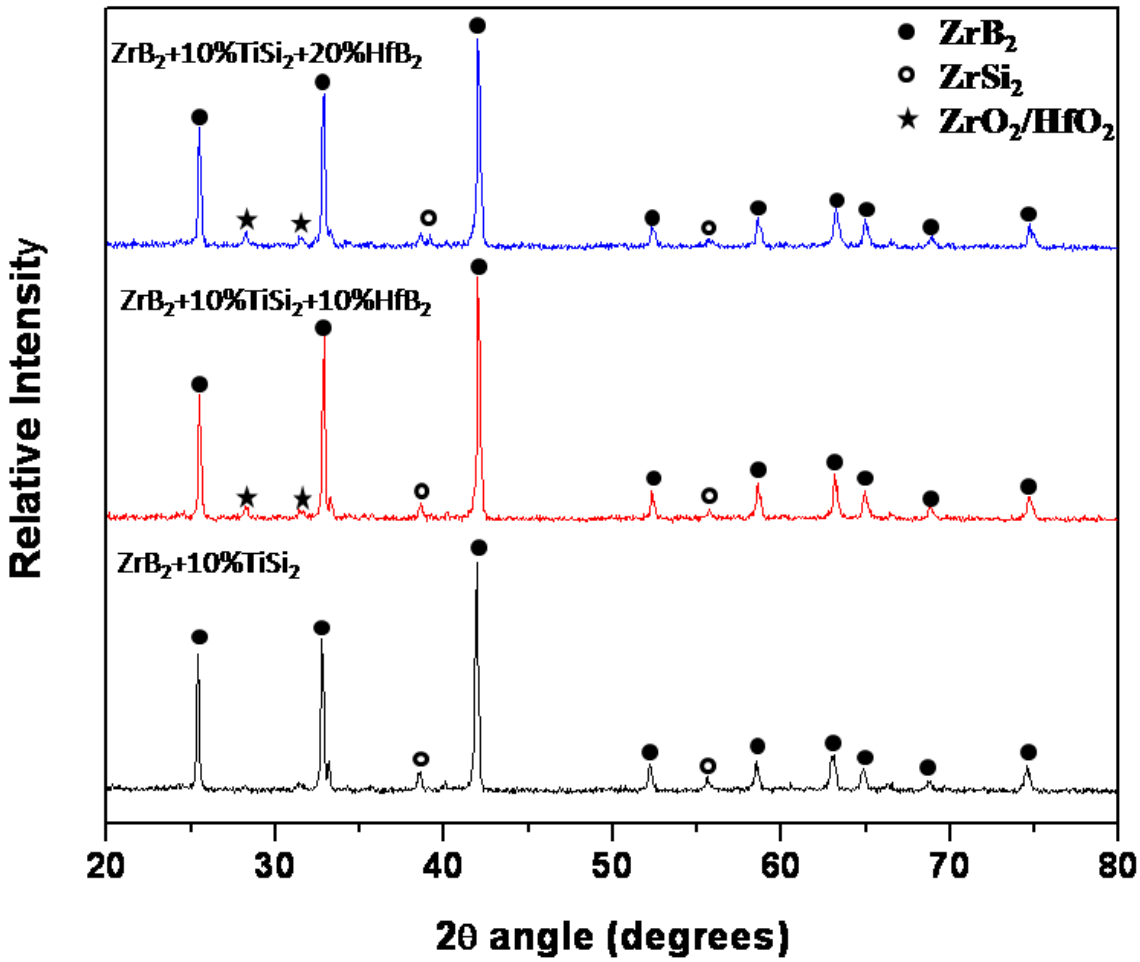

Fig. 4.20 XRD pattern of ZrB_2 based composites

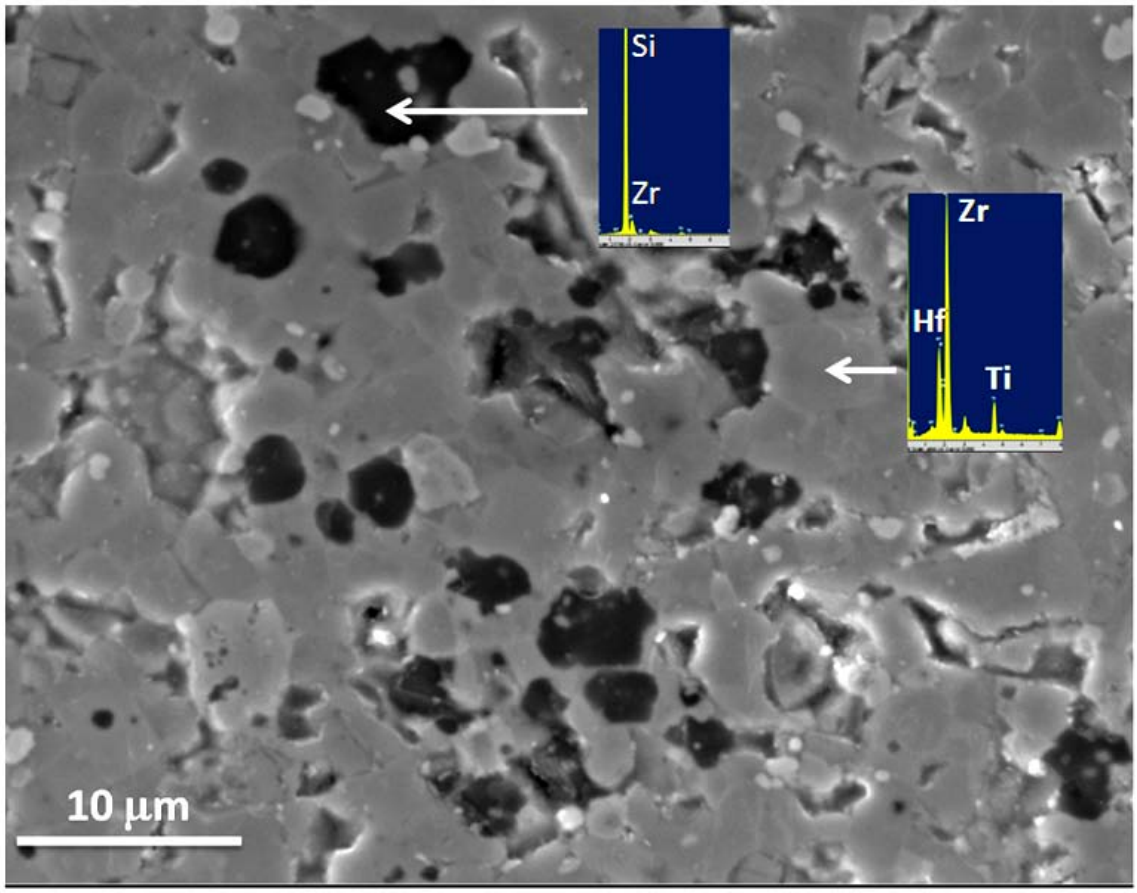

Fig. 4.21 EDS pattern of different phases present in ZrB_2 +10% $TiSi_2$ + 20% HfB_2 composite

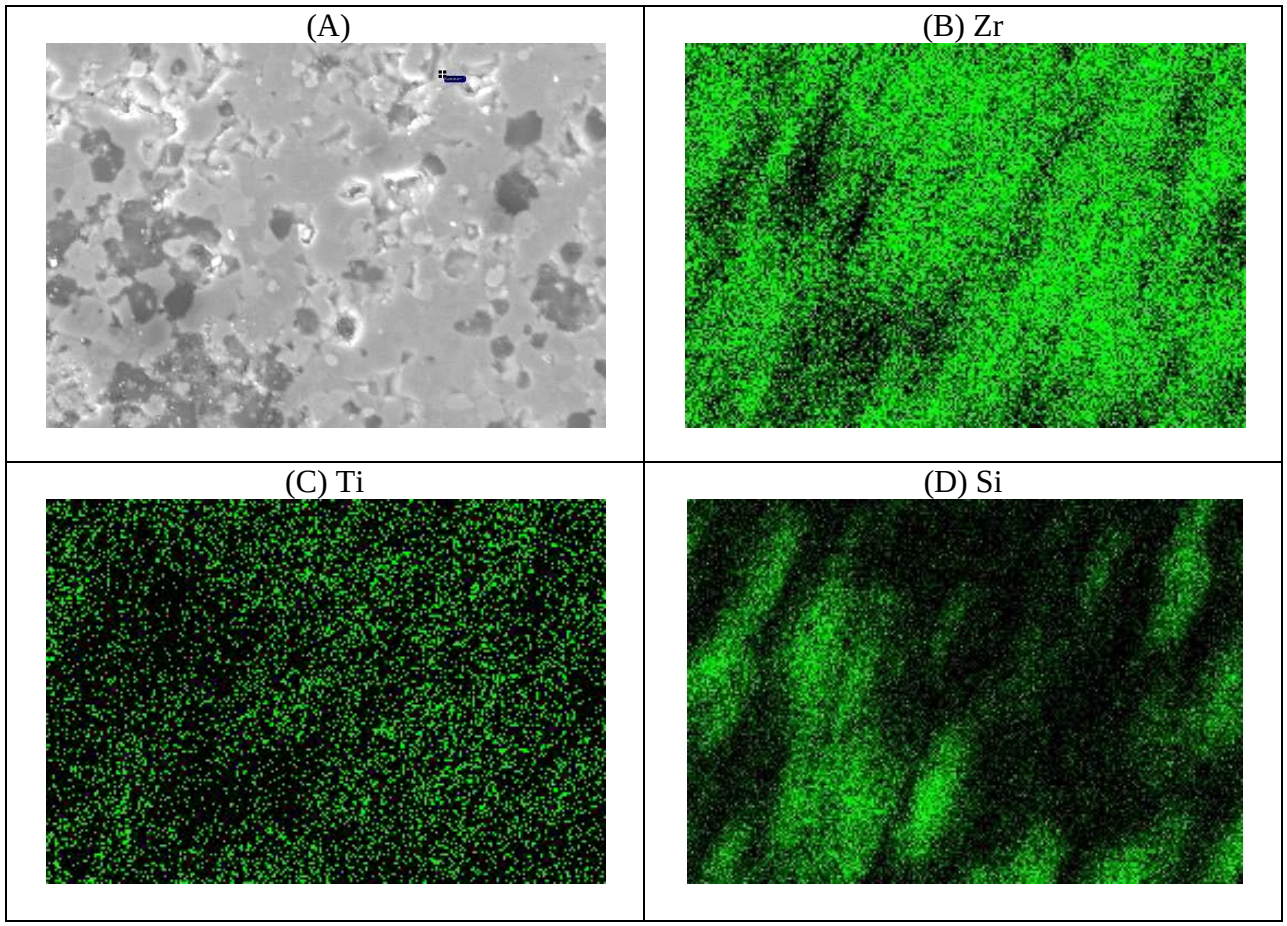

Fig.4.22 Elemental mapping of, Zr, Ti and Si in ZrB_2 +10% $TiSi_2$ + 20% HfB_2 composite

Fig.4.23 present the fracture surfaces of monolithic ZrB_2, ZrB_2+10% $TiSi_2$ and ZrB_2+10%$TiSi_2$+10% HfB_2 composites. The mode of fracture is seen to be predominantly intergranular in all the samples. Regular faceted grains are visible. Fig. 4.24 (a) presents the features of indentation crack in monolithic ZrB_2 and Fig.4.24 (b-d) in composites. The crack propagation in monolithic ZrB_2 shows very few deflections which could be due to intergranular mode of fracture. However deflections are not much due to presence of fine grains. Considerable deflections are observed in the composite samples, which explain the high fracture toughness. These deflections could be due to presence of residual stress in the composite sample.

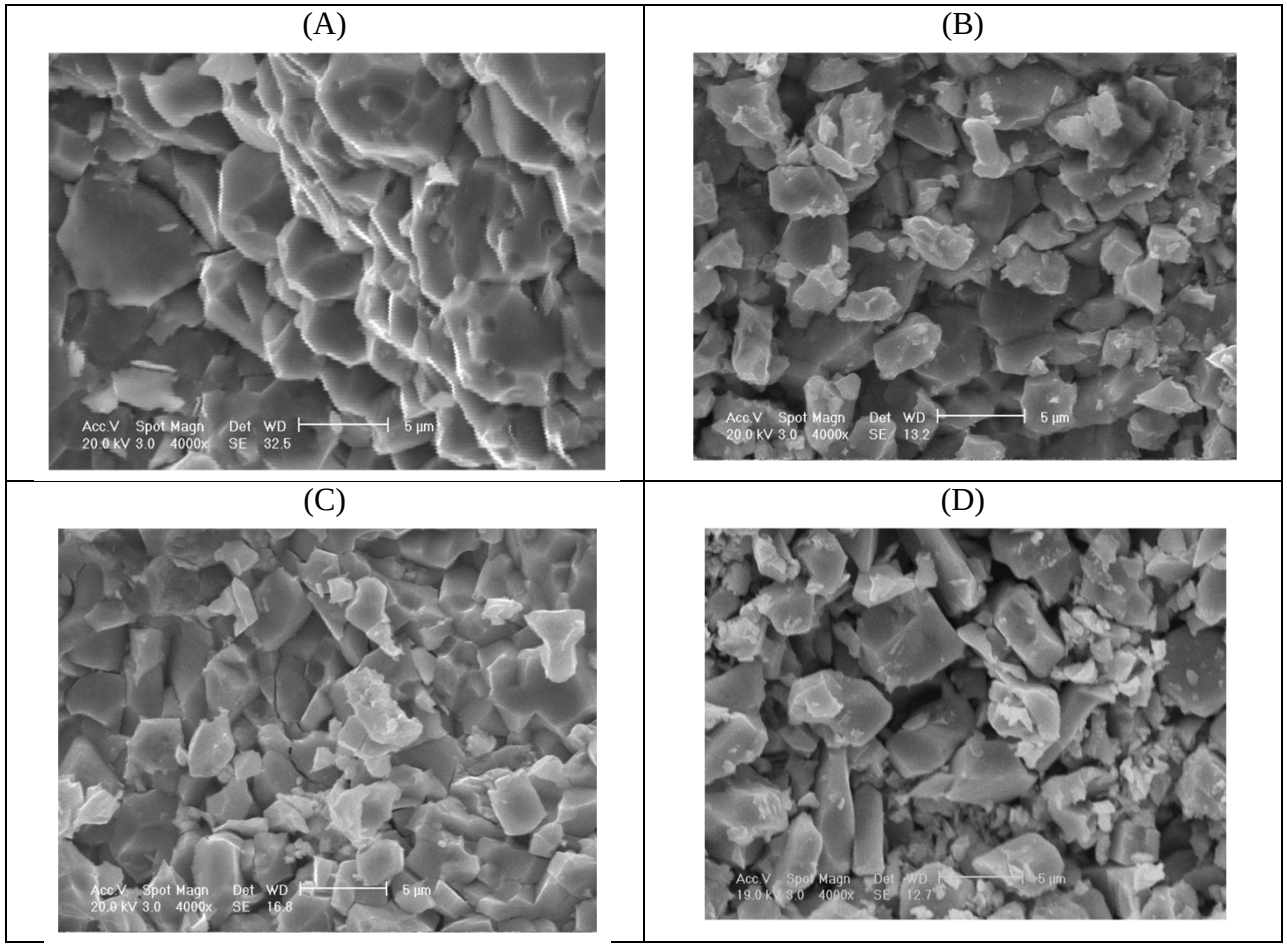

Fig.4.23 Fracture surfaces of (a) monolithic ZrB_2 (b) ZrB_2+10% $TiSi_2$ (c) ZrB_2+10%$TiSi_2$+10% HfB_2 (d) ZrB2+10%$TiSi_2$+20% HfB_2

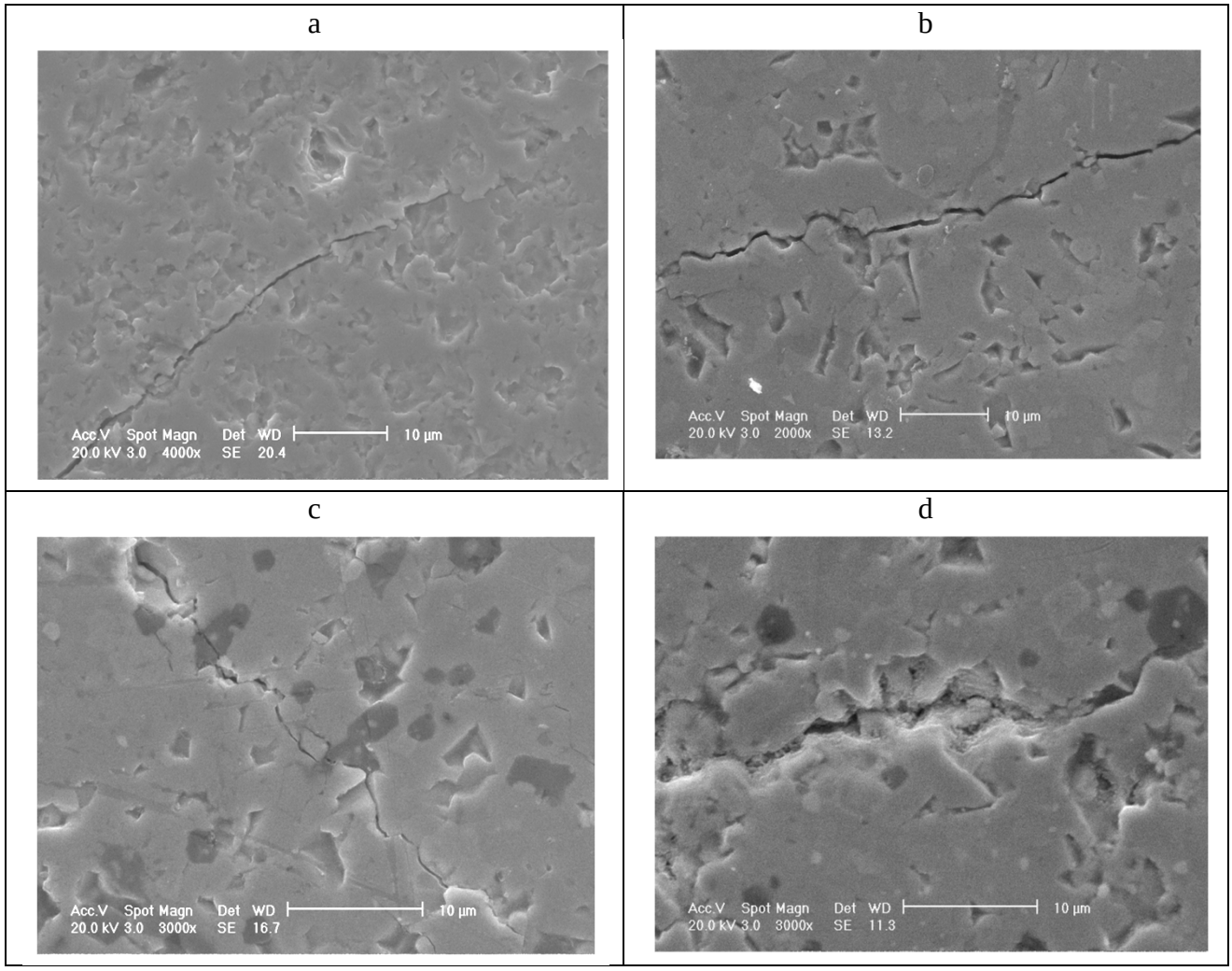

Fig.4.24 Crack propagation in (a) monolithic ZrB_2 (b) ZrB_2+10% $TiSi_2$ (c) ZrB_2+10%$TiSi_2$+10% HfB_2 (d) ZrB_2+10%$TiSi_2$+20% HfB_2

4.2.3 Effect of $CrSi_2$ addition on densification and properties of ZrB_2

4.2.3.1 Densification and characterization

Hot pressing conditions and density obtained in composite as well as monolithic sample is presented in Table.4.7. Addition of 10 weight% $CrSi_2$ resulted in densification of 98.9 % ρ_{th} at a temperature of 1650 ^oC and a pressure of 20 MPa. In case of monolithic ZrB_2, a near full density (99.8% ρ_{th}) was obtained at a higher temperature and pressure of 1850 ^oC and 35 MPa. The enhanced sintering at lower hot pressing temperature and pressure is probably due to the liquid phase sintering with low melting reaction product (1620^oC). $ZrSi_2$ forms by reaction between ZrB_2 and $CrSi_2$.

Table 4.7: Effect of Sinter additives on densification of ZrB_2

Starting material	T (^oC)	Pressure (MPa)	Bulk density (gm/cc)	Theoretical density (gm/cc)	Relative density (%)
ZrB_2	1850	35	6.09	6.10	99.8
ZrB_2	1650	35	5.07	6.10	83.1
ZrB_2+10 wt.% $CrSi_2$	1650	20	5.84	5.91	98.9

4.2.3.2 Mechanical properties

Hardness of ZrB_2 + 10%$CrSi_2$ is measured as 19.8 GPa which is lower than that of monolithic ZrB_2 (23.9 GPa). The lower hardness is due to the presence of relatively soft phase $ZrSi_2$. To compensate the hardness reduction, HfB_2 was added and one more sample of composition ZrB_2+10%$CrSi_2$+10%HfB_2 was prepared. Near theoretical density was obtained for this sample at 1650 ^oC and 20 MPa. Hardness of ZrB_2+10%$CrSi_2$+10%HfB_2 was measured as 23.8 GPa, which is comparable to that of monolithic ZrB_2.

Fracture toughness of ZrB_2 + 10%$CrSi_2$ was measured as 4.1 MPa.m$^{1/2}$ which is relatively higher than that of the monolithic ZrB_2. Similar values were obtained in case of

ZrB_2+10%$CrSi_2$+10%HfB_2 sample. Table 4.8 summarizes the mechanical properties of ZrB_2 based composites. The increased fracture toughness is due to crack deflection as seen in Fig. 4.25 (a) & (b). Thermal expansion mismatch between the matrix and second phase results in residual stresses which causes crack deflection.

Table 4.8 Effect of $CrSi_2$ and HfB_2 addition on mechanical properties of ZrB_2

Additive	**Hardness (GPa)**	**K_{IC} (MPa $m^{1/2}$)**
nil	23.9±1.5	3.3±0.2
10 wt.% $CrSi_2$	19.8±2	4.1±0.5
10% HfB_2 +10 wt.% $TiSi_2$	23.8±2	4.2±0.5

(a)

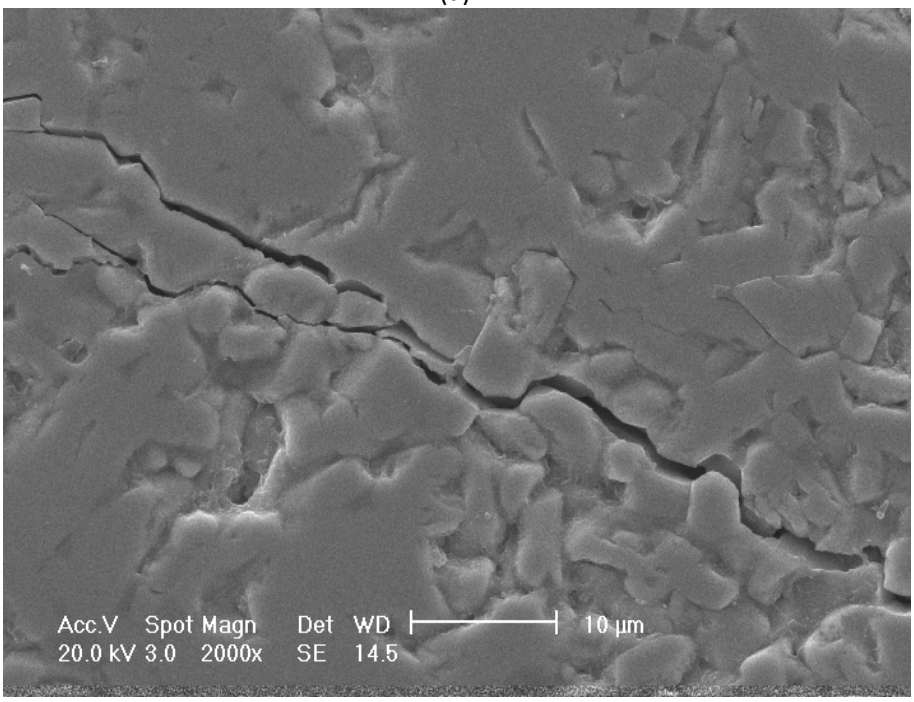

(b)

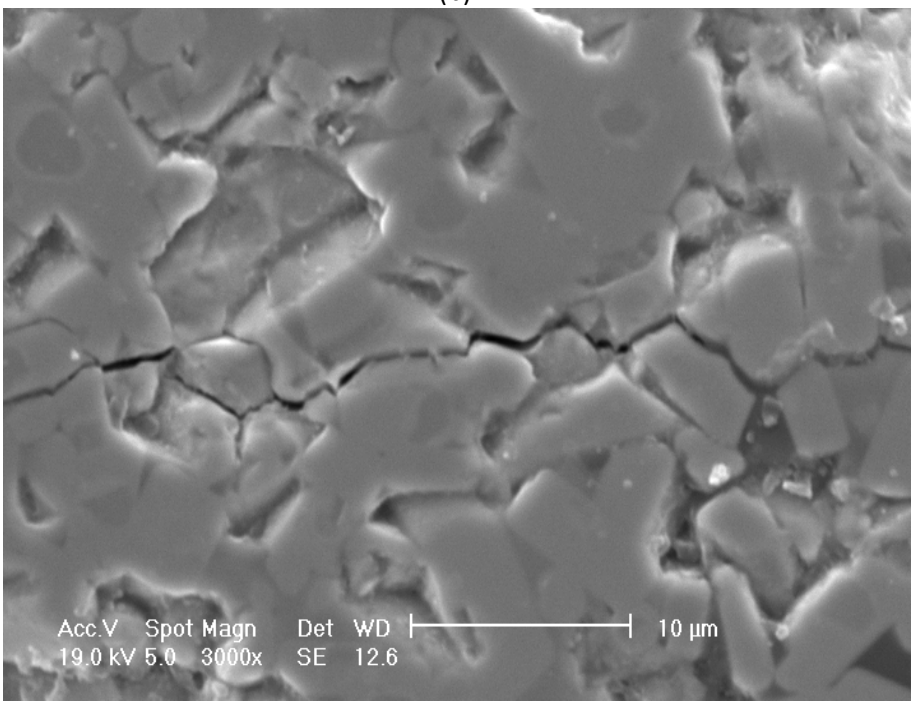

Fig. 4.25 Crack propagation in ZrB_2 based composites (a) ZrB_2 +10%$CrSi_2$ (b) ZrB_2 +10%$CrSi_2$ +10% HfB_2

4.2.3.3 Phase analysis and microstructure

XRD pattern of the dense pellet of ZrB_2+10% HfB_2 +10% $CrSi_2$ sample is shown in Fig. 4.26. It indicates the presence of crystalline ZrB_2 and $ZrSi_2$. $ZrSi_2$ is formed during sintering by the following reaction.

$ZrB_2 + xCrSi_2 \rightarrow xZrSi_2 + (Zr_{(1-x)}Cr_x)\ B_2$……..(4.5)

Formation of $ZrSi_2$ with a melting point of 1620°C would help in densification by liquid phase sintering. Fig.4.27 presents the back scattered image of ZrB_2+10%$CrSi_2$ sample. It shows the presence of black phase, dark gray phase and light gray phase. EDS pattern of the phases are also inserted into the picture. Light gray matrix is essentially ZrB_2. Dark gray phase shows the presence of Zr, Cr and boron which indicates the formation of solid solution of ZrB_2 and CrB_2. Black phase was analysed to contain Zr and Si indicating it is $ZrSi_2$.

Fig. 4.28(a) and (b) present the fracture surfaces of ZrB_2+10% $CrSi_2$ and ZrB_2+10%$CrSi_2$+10% HfB_2 composites. The mode of fracture is seen to be intergranular in both the samples. Regular faceted grains are visible.

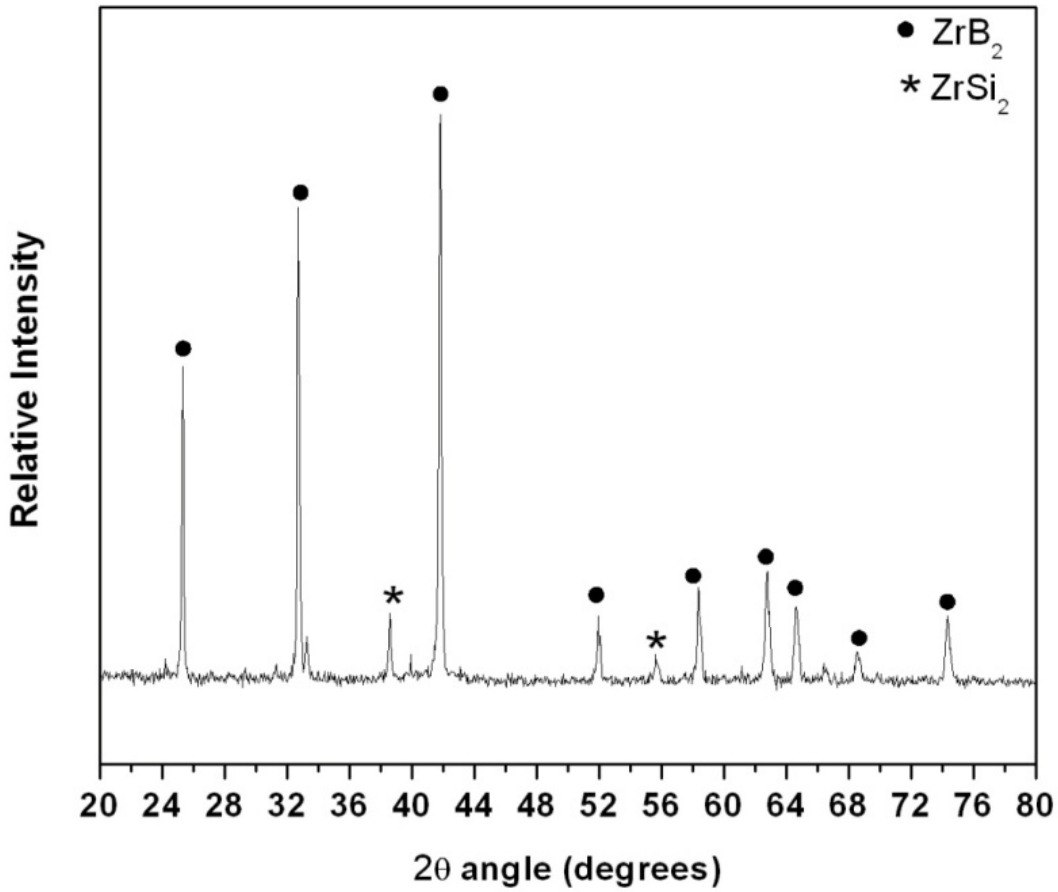

Fig.4.26 XRD Pattern of hot pressed ZrB_2+10%$CrSi_2$ +10%HfB_2

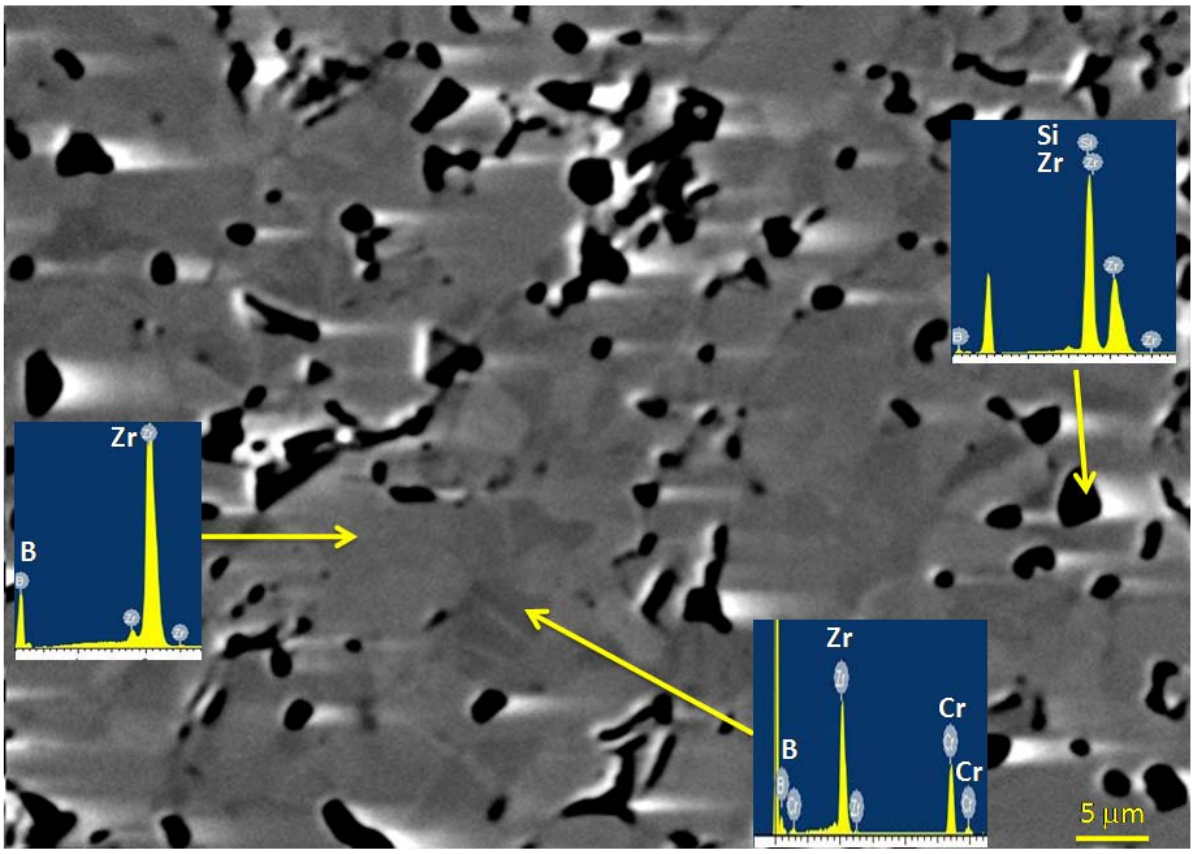

Fig. 4.27 EDS pattern of different phases present in ZrB_2 +10% $CrSi_2$ sample hot pressed at 1650 ^oC

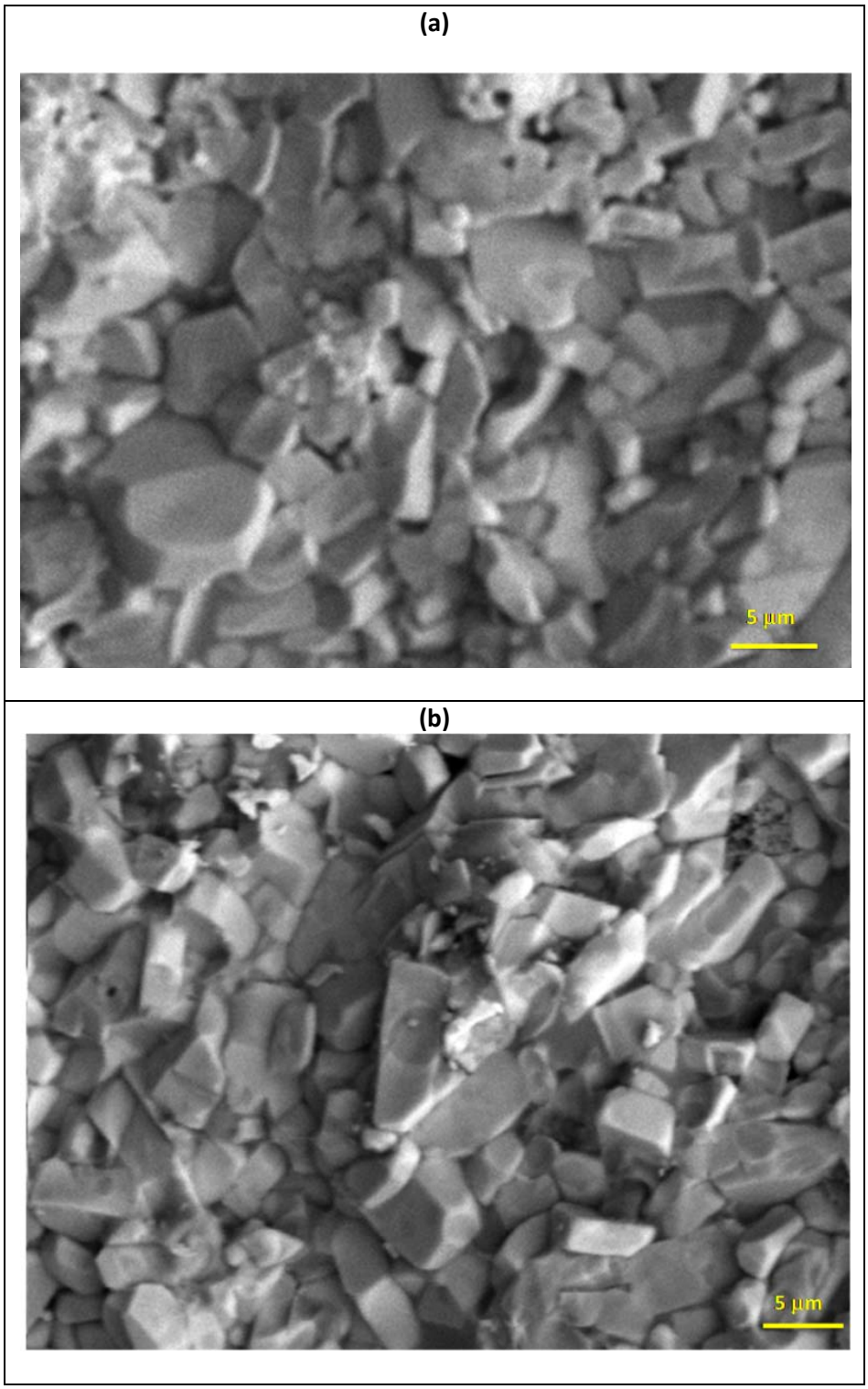

Fig.4.28 Fracture surfaces of (a) ZrB_2 +10%$CrSi_2$ (b) ZrB_2 +10%$CrSi_2$ +10% HfB_2

4.2.4 Effect of EuB_6 addition on densification and properties of ZrB_2

4.2.4.1 Densification

Effect of EuB_6 addition on densification and properties of ZrB_2 was investigated. Hot pressing conditions and properties of the ZrB_2 composites are presented in Table.4.9. Addition of 2.5 weight% EuB_6 resulted in densification of 98.3 % ρ_{th} at a temperature of 1750 ^oC and a pressure of 35 MPa. Composites with 5% EuB_6 was also hot pressed up to 98.1% density at similar processing conditions. A density of 96.0% ρ_{th} was achieved in ZrB_2+10%EuB_6 composite. In case of monolithic ZrB_2, near theoretical density (99.8% ρ_{th}) was obtained at a higher temperature and pressure of 1850 ^oC and 35 MPa. Addition of EuB_6 to ZrB_2 may result the formation of solid solution of ZrB_2 and EuB_6. On the formation of ZrB_2-EuB_6 solid solution, Eu will go to Zr site and boron will go to boron site. Due to large number of boron atoms from EuB_6, there will be formation of point defects in ZrB_2. Point defects could be either interstitials at boron site or vacancies at Zr sites. In any case, diffusional mass transfer gets increased which assist in improved densification. The point defects are known to enhance the and thus assist in densification at slightly lower temperature. Formation of solid solution was confirmed by elemental analysis (EDS) of phases present in microstructure change in lattice parameter measured by XRD. (see 4.3.4.3).

Table 4.9: Effect of EuB_6 addition on densification of ZrB_2

Additive	**Temp (^oC)**	**Pressure (MPa)**	**Bulk density (gm/cc)**	**Theoretical density (gm/cc)**	**Relative Density (%)**
Nil	1850	35	6.09	6.10	99.8
2.5% EuB_6	1750	35	5.97	6.07	98.3
5% EuB_6	1750	35	5.91	6.03	98.0
10% EuB_6	1750	35	5.73	5.97	96.0
2.5%EuB_6	1650	35	5.18	6.07	85.3

4.2.4.2 Mechanical properties

Variation in Vickers hardness and fracture toughness of ZrB_2 composites are presented in Table 4.10. Hardness of monolithic sample was measured as 23.9 GPa, which increased to 24.8 GPa with the addition of 2.5wt% EuB_6. The increase in hardness is due to the formation of solid solution. The hardness value of composite with 5 and 10% EuB_6 addition was measured as 22.6 and 21.9 GPa respectively. The relatively lower hardness is due to the lower density of the hot pressed composite. Hardness of monolithic ZrB_2 has been reported to be in the range of 22-23GPa [1,2, 62]. Chamberlain et al. [62] have reported a hardness of 23 GPa for hot pressed ZrB_2. Akin et al [92] have reported the hardness of ZrB_2- 20-60%SiC composite to be 26 GPa.

Table 4.10: Hardness and fracture toughness of ZrB_2 composite

Additive	**Hardness (GPa)**	**K_{IC} ($MPa.m^{1/2}$)**
Nil	23.9±1.5	3.3±0.2
2.5% EuB_6	24.8±1.6	5.9±0.5
5% EuB_6	22.6±1.7	5.4±0.5
10% EuB_6	21.9±1.6	4.4±0.5

Fracture toughness of ZrB_2 +2.5%EuB_6 sample was measured as 5.9 $MPa.m^{1/2}$. Similar value (5.4 $MPa.m^{1/2}$) was obtained for ZrB_2 + 5%EuB_6 sample. For ZrB_2+10%EuB_6 the fracture toughness is slightly lower. The fracture toughness values obtained in the composite samples are higher than the values reported for monolithic ZrB_2 in literature. Fracture toughness of monolithic ZrB_2 has been reported as 3.5 $MPa.m^{1/2}$[62]. Sun et al [82] have reported the enhancement of fracture toughness to 6.7 $MPa.m^{1/2}$ by 25% Nb addition.

4.2.4.3 Phase analysis and microstructure

Fig.4.29 (a) presents the BSE image and EDS spectra of different phases present in ZrB_2+ 5%EuB_6. It shows the presence of light gray matrix in which dark gray phase and black phase is dispersed. In EDS spectra (fig. 4.29(b-d)), the black phase and dark gray phase was analyzed to contain only Zr and B indicating that it is ZrB_2. The light gray matrix was analyzed to contain Zr, Eu and B indicating the formation of ZrB_2-EuB_6 solid solution.

XRD pattern of the dense pellet of ZrB_2+10%EuB_6 sample is shown in Fig.4.30. It indicates the presence of crystalline ZrB_2, EuB_6 and carbon. Presence of EuB_6 in XRD pattern indicates that the ZrB_2 and EuB_6 do not form complete solid solution and so EuB_6 is also present as second phase in the composite. ZrB_2 has hexagonal crystal structure whereas EuB_6 has cubic crystal structure which does not allow complete solid solution formation. A small peak shift was observed in ZrB_2 peaks towards higher d spacing values compared to d value reported in PCPDF file (PDF # 00-034-0423) indicating the formation of solid solution of ZrB_2 and EuB_6.

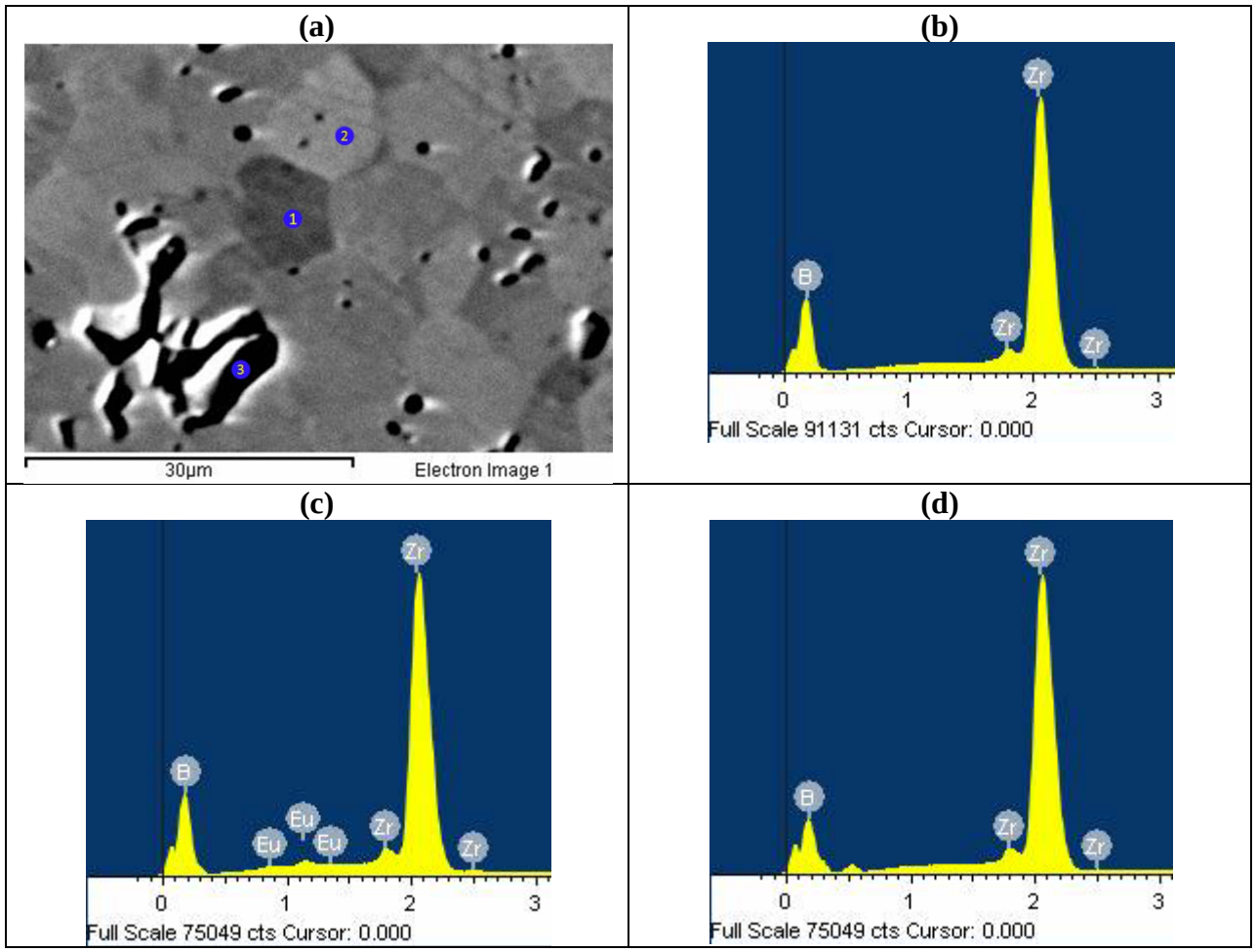

Fig.4.29 (a) BSE image of ZrB_2+ 5%EuB_6 (b) EDS spectra of phase marked as 1 in (a), (c) EDS spectra of phase marked as 2 in (a), and (d) EDS spectra of phase marked as 3 in (a)

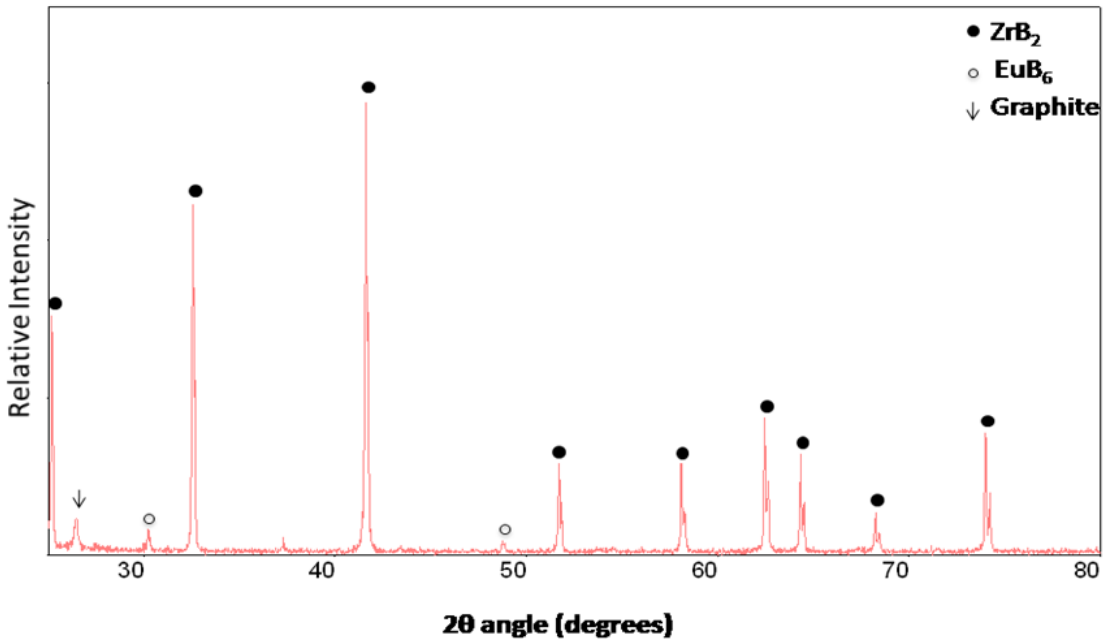

Fig. 4.30 XRD pattern of hot pressed ZrB_2 +10%EuB_6

4.2.5 Discussion on densification and characterization of ZrB_2 composites:

Densification of Zirconium diboride is extremely difficult due to its highly refractory nature, and low self diffusivity. Zirconium diboride is a covalently bonded material. Sintering is a diffusion controlled process and for diffusion to take place bonds need to be broken and reformed. Since covalent bonds are very strong, diffusion is slow in ZrB_2. ZrB_2 particles are also covered with oxide layer which reduces the surface energy and decreases the sinterability of powder.

Maximum density obtained in pressureless sintering method is 78% of theoretical value whereas hot pressing resulted in near theoretical density. In hot pressing, simultaneous application of temperature and pressure causes diffusional creep, which enhances the densification. [127]

In this study, $TiSi_2$, $CrSi_2$ and EuB_6 were selected as sinter additive. Sinter additives were chosen by considering the possible effects on densification as well as on mechanical properties and oxidation resistance. Metal additives can enhance the densification but deteriorate the mechanical properties and oxidation resistance. Silicides are known high temperature materials with better properties than metals at high temperatutre. Some of the studies have reported the use of $MoSi_2$ as sinter additives [51, 65] but there is no report on the $TiSi_2$ and $CrSi_2$ addition on ZrB_2. This study contributes results on the effect of $TiSi_2$ and $CrSi_2$ on densification as well as on mechanical properties and oxidation of ZrB_2 based composites. Europium hexaboride was selected as another sinter additive. EuB_6 has high melting point, high hardness and good oxidation resistance. Since it is also a covalently bonded boride material, its high temperature properties are superior to metals and silicides. Addition of EuB_6 is supposed to enhance the densification by solid solution formation.

Silicide ($TiSi_2$, $CrSi_2$) additions were found to assist in densification and lowered the densification temperature by 200 ^oC. A decrease in densification temperature by 200 ^oC is beneficial in many ways. By decreasing the hot pressing temperature, the grain growth is also prevented and finer microstructure is obtained. The reduction in sintering temperature is due to the liquid phase sintering caused by low melting zirconium silicide phase (1620 ^oC). $ZrSi_2$ is formed by reaction between ZrB_2 and $TiSi_2$ or $CrSi_2$ according to reaction (5.5) and (5.6)

$$ZrB_2 + xTiSi_2 \rightarrow xZrSi_2 + (Zr_{(1-x)}Ti_x)B_2 \quad (5.5)$$

$$ZrB_2 + xCrSi_2 \rightarrow xZrSi_2 + (Zr_{(1-x)}Cr_x B_2 \quad (5.6)$$

The validation of the formation of liquid phase, resulting in liquid phase sintering, can be obtained by results obtained at 1650 ^oC and 1550 ^oC. At lower temperature, the achieved density is only 86.25% due to absence of liquid phase.

Application of pressure results in better contact between ZrB_2 and $TiSi_2/CrSi_2$, thus promotes reactions between them. During chemical reaction the diffusion is enhanced and helps in densificaton. After reaction the $ZrSi_2$ phase is formed and helps in densification by liquid phase sintering. Presence of liquid phase assists in rearrangement of particles, enhances the mass transfer by solution and re-precipitation and fills the remaining pores.

EuB_6 addition decreased the densification temperature by formation of solid solution. When EuB_6 and ZrB_2 forms solid solution, Eu occupy Zr sites and B occupy boron sites in the structure of ZrB_2. Since EuB_6 has more number of boron atoms there is a possibility of formation of point defects in the form of boron interstitials or metal vacancy. Diffusional mass transfer increases in presence of vacancies and interstitials and thus densification is enhanced.

Literature on effect of other sinter additives is discussed below. Sciti et al [51]. have reported that addition of 20% $MoSi_2$ results in 98.1% TD on hot pressing at 1800^oC and 30MPa. It was reported that $MoSi_2$ phase has ductility at high temperature and thus can be accommodated among the ZrB_2 particles by hot pressing process. This process results in filling the voids left by ZrB_2 and favors the formation of a porosity free material. Silica present on the silicide phase also assisted in densification by reacting with surface oxide layer. Guo et al. [77] have reported that addition of 5% Re_2O_3 (Re= Y,Yb,La,Nd) to ZrB_2-20%SiC results in >99%TD on hot pressing at 1900^oC. La_2O_3 and Nd_2O_3 react with surface oxides to form a liquid phase and promote densification of ZrB_2–SiC ceramics. Wang et al.[83] have reported that 10% Mo addition gives a density of 98.9%TD on hot pressing at 1950^oC and 20MPa.Zhu *et al* [73] have reported that addition of 3-10% Al_2O_3 and Y_2O_3 and 20% SiC_w to ZrB_2 gives a density > 97% TD on hot pressing at 1800^oC.

Hardness and fracture toughness are two important mechanical properties for ceramic materials. Hardness is resistance to indentation damage and thus related to resistance to plastic deformation. In crystalline material, plastic deformation takes place by movement of dislocations. In metals, metallic bonds are present which are non directional and thus movement of dislocation is easier and hardness is low (~ 1GPa). In ceramic material, the bonds are either ionic or covalent which prevents the motion of dislocations and results in high hardness compared to metals. Hardness of borides is very high (20-30 GPa) compared to oxide ceramic (10-20 GPa). This high hardness is due to strong covalent bond present in the boride materials.

In this study, hardness of monolithic ZrB_2 was found as 23.9 GPa which is in agreement with literature vaules. Hardness is sensitive to microstructure and gets strongly affected by presence of pores, second phases or residual stresses. The presence of silicide phase, which is softer (~ 10GPa) decreased the hardness of composites. HfB_2 addition to the composite increased the hardness. This increase is due to solid solution formation. Addition of EuB_6 also increases the hardness by solid solution formation. Hardness values of less dense samples were found less due to presence of pores. Hardness values reported in literature for ZrB_2 based material is discussed in the next paragraph.

Hardness is strongly affected by processing conditions and by the additive used. Chamberlain et al. [17] have reported a hardness of 23 GPa for hot pressed ZrB_2. Akin et al [92] have reported the hardness of ZrB_2- 20-60%SiC composite to be 26 GPa. Sciti et al. [64] have reported a hardness of 17.8 GPa for ZrB_2+15%$TaSi_2$ composite. The lower hardness is due to presence of silicide phase. Sun et al. [82] have reported the hardness of ZrB_2 + 25% Nb as 16.3 GPa. It was observed in literature that soft phases such as metals and silicides decrease the hardness, whereas phases such as SiC increase the hardness.

Fracture toughness is an important property of ceramic materials. Ceramics have cracks in their microstructure. Under stress, crack propagation takes place and results in fracture of material. Fracture toughness is a measure of resistance to crack propagation. Fracture toughness is also a microstructure sensitive property and gets influenced by presence of porosity, second phase, defects etc. Fracture toughness of ceramics are generally low (1-5 $MPa.m^{1/2}$) whereas metals have high fracture toughness (~50 $MPa.m^{1/2}$). In this study, fracture toughness of monolithic ZrB_2 was measured as 3.3 $MPa.m^{1/2}$, which gets increased by addition of silicides. In

composite material, there is a mismatch of thermal expansion coefficient in matrix phase and dispersed phase. Due to this mismatch, residual stress gets generated during processing of composites. These residual stresses causes crack deflection which is responsible for increased fracture toughness. Crack propagation is faster when it progresses normal to the tensile stress. After crack deflection, the crack is no longer normal to tensile stress and hence stresses intensity at the crack tips reduced and crack propagation slow down. Fracture toughness values reported in literature for ZrB_2 based material is discussed in the next paragraph.

Fracture toughness of monolithic ZrB_2 has been reported as 3.5 $MPa.m^{1/2}$[62]. Sciti et al. [64] have reported the fracture toughness of ZrB_2 + 15% composites as 3.8 $MPa.m^{1/2}$. Rezaie et al. [86] have reported the fracture toughness of ZrB_2+ 30%SiC to be 3.9 $MPa.m^{1/2}$. Zhu et al [73] have reported the fracture toughness of 6.7 $MPa.m^{1/2}$ for ZrB_2+20%SiC_w+3%YAG. The higher fracture toughness is due to crack deflection and crack bridging by whiskers. Sun et al. [82] have reported the fracture toughness value of ZrB_2 + 25% Nb composite as 6.7$MPa.m^{1/2}$. The increase in toughness may be due to the ductile Nb, weak interface bonding and pores, which could enhance crack deflection and bridging as well as stress relaxation near the crack tip. Table 4.11 presents a summary of mechanical properties of composites prepared in this study as well as reported in literature. It concludes that $TiSi_2$, $CrSi_2$ and EuB_6 addition helped in development of boride composites with superior property.

Table 4.11: Mechanical properties of Boride based composites.

Material	Density (%)	Hardness (GPa)	Fracture toughness ($MPa.m^{1/2}$)	Reference
ZrB_2	99.8	23.9	3.3	Present study
ZrB_2+10%$TiSi_2$	98.9	19.4	6.4	Present study
ZrB_2+10%$TiSi_2$ +10%HfB_2	99.6	23.1	6.4	Present study
ZrB_2+10%$TiSi_2$ +20%HfB_2	98.4	23.7	6.6	Present study
ZrB_2 +2.5% EuB_6	98.3	24.8	5.9	Present study
ZrB_2+5%EuB_6	98.0	22.6	5.4	Present study
ZrB_2 +4%Ni	98.0	14.4	2.8	79
ZrB_2 +5%Si_3N_4	98.0	13.4	3.7	78
ZrB_2 +25%Nb	97.2	16.3	6.7	82
ZrB_2 +10%Mo	98.9	-	6.7	83
ZrB_2 +20%SiC	99.7	24.0	4.4	62
ZrB_2 +30%ZrO_2	98.9	22.0	7.9	74
ZrB_2 + 20% SiC + 3% Y_2O_3	99.3	17.6	5.6	76
ZrB_2 +20%$MoSi_2$	98.1	15.0	-	51
ZrB_2 +20vol%SiC+20%C_{fiber}	98.4	-	6.3	72

4.3 Oxidation study

Non oxide ceramics are susceptible for oxidation at high temperatures. For any application in air, the material must be resistant to oxidation. Oxidation test were carried out at 900 ^{o}C in air for different time intervals. Following sub-sections describe the results obtained by oxidation test of different composites.

4.3.1 Monolithic ZrB_2

The weight gain data obtained during oxidation at 900 ^{o}C as a function of time for monolithic ZrB_2 is presented in Fig 4.31. It shows that weight gain is linear indicating non-protective nature of oxide formed. The test was stopped after 32 hours as the oxide layer was broken and spalled off from the sample.

4.3.2 Effect of $TiSi_2$ and HfB_2 addition

The weight gain data obtained during oxidation at 900 ^{o}C as a function of time for ZrB_2 composites containing $TiSi_2$ and HfB_2 are presented in fig.4.32. Continuous weight gain with time is observed in all the samples. In case of composites, the rate of oxidation was found to decrease with increase in time which indicates the formation of protective layer. In monolithic ZrB_2, oxidation rate was high and found to remain constant up to 32 hour. Samples containing HfB_2 has shown highest oxidation resistance.

Better oxidation resistance of the composite samples having silicide phase is attributed to the formation of silica based glassy layer. SEM microstructures (Fig.4.33) of oxidized surfaces evidently show the formation of protective glassy phase. The glassy phase was analysed by EDS to contain mainly silicon (~ 46 at%) and oxygen (~52 at%). Zirconium (~ 0.8 at%) and titanium (~0.2 at%) are also present in very small quantity. A typical EDS pattern from the oxidized surface is shown in Fig.4.34. SEM microstructure and elemental analysis of cross section of oxidized sample is presented in fig.4.35. It shows presence of oxidized layer which is composed mainly of silicon and oxygen.

Fig.4.36 presents the XRD pattern of oxidized surface. The major crystalline phase in all the composites is confirmed as ZrO_2. Peaks of $ZrSiO_4$ and TiO_2 are also present. Oxidation of ZrB_2 +$TiSi_2$ +HfB_2 composite may involve following reactions.

$2/5ZrB_2 + O_2 \rightarrow 2/5ZrO_2 + 2/5B_2O_3$ ……..…...(5.7)

$2/5TiB_2 + O_2 \rightarrow 2/5TiO_2 + 2/5B_2O_3$

$2/5HfB_2 + O_2 \rightarrow 2/5HfO_2 + 2/5B_2O_3$…….……(5.8)

$1/3ZrSi_2 + O_2 \rightarrow 1/3\ ZrO_2 + 2/3SiO_2$ ……..……..(5.9)

$1/3TiSi_2 + O_2 \rightarrow 1/3\ TiO_2 + 2/3SiO_2$ ……..……..(5.10)

Free energy change for all the above reactions are calculated and presented in Fig.4.37. The calculation was done for one mol of oxygen. Thermodynamic calculations were carried out by considering the species in standard condition (1 atm). It shows that free energy change is negative for all the above reaction in the temperature range from 300 to 2000 K. In the present study oxidation test was carried out at 900 ^{o}C (1173 K) and hence all these reaction takes place during oxidation. Free energy change is more negative for oxidation of silicides as compared to that of borides. It indicates the higher affinity of silicides for oxygen. Silicides react with oxygen preferentially and forms silica based protective oxide layer on surface of ZrB_2 composite.

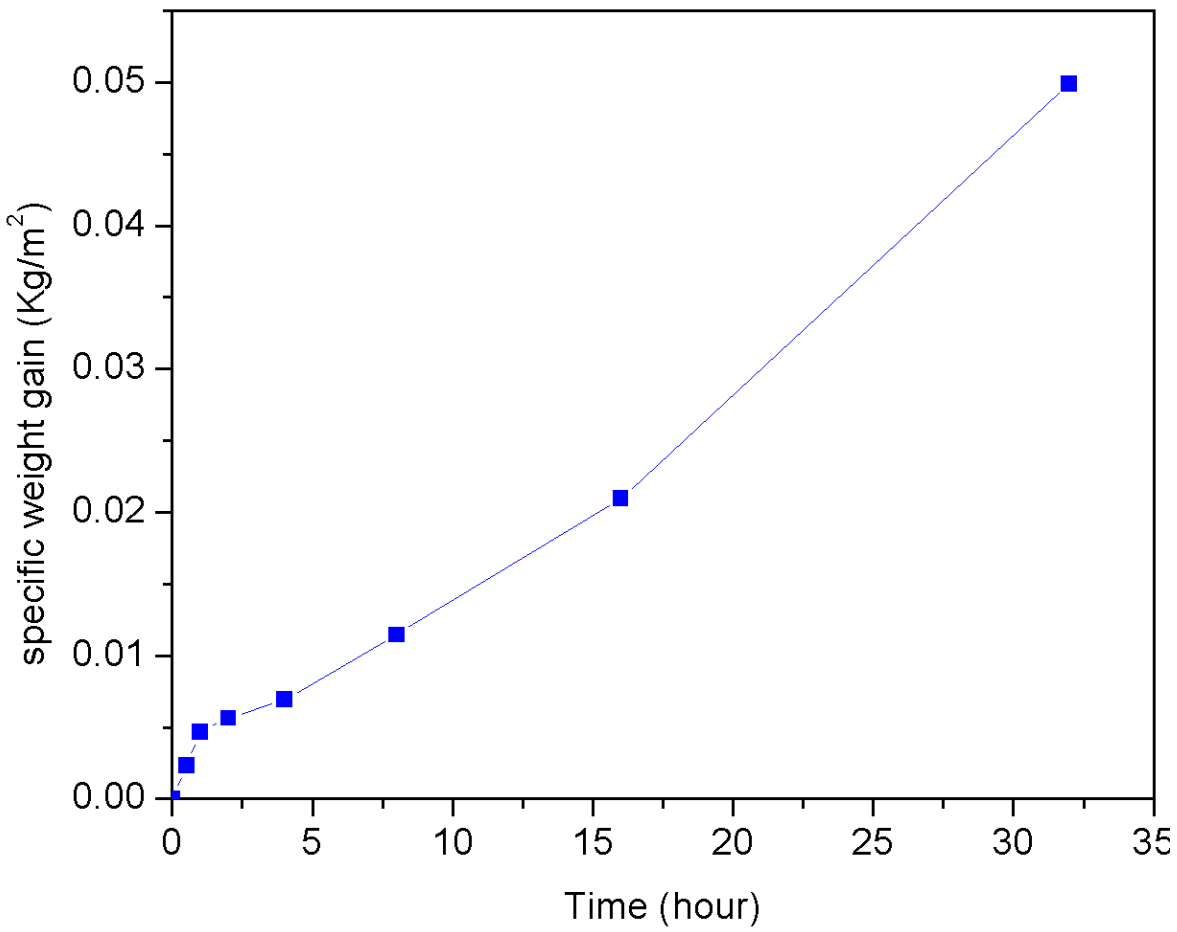

Fig. 4.31 Specific weight gain vs time plot for monolithic ZrB_2 at 900 ^oC in air

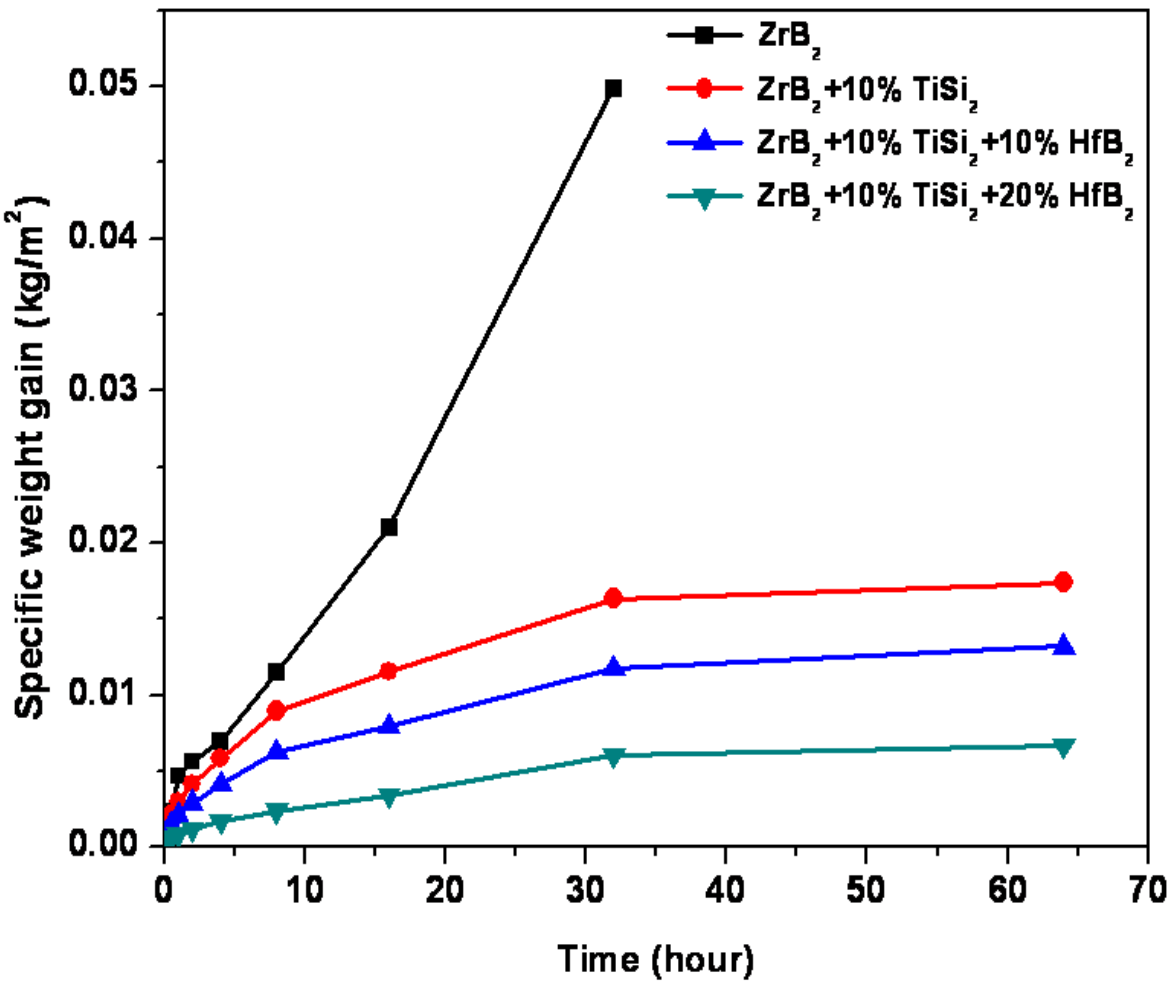

Fig. 4.32 Specific weight gain vs time plot for ZrB_2 based composites.

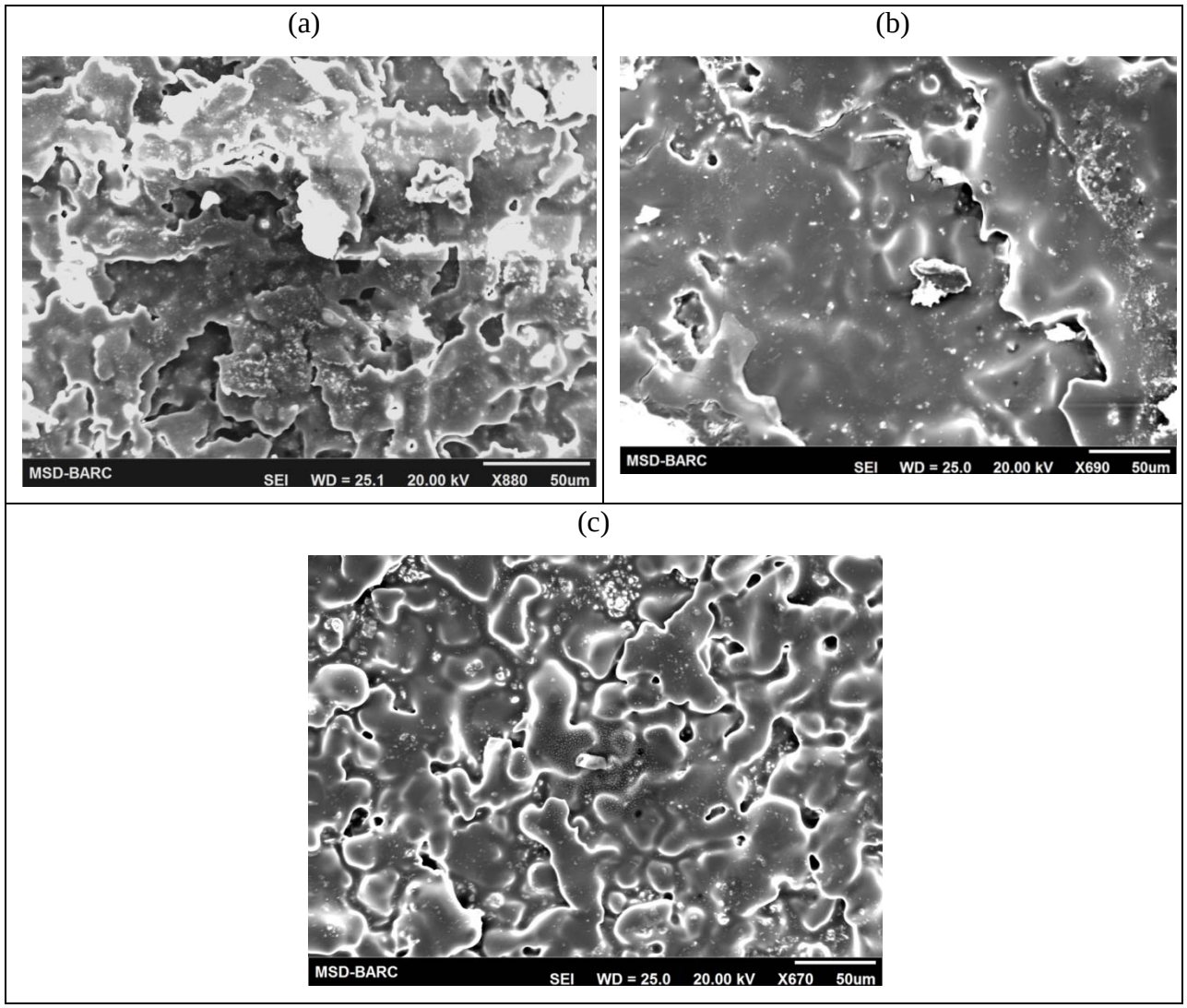

Fig. 4.33 SEM of the oxidized (900 ^{o}C, 64 h) surface of ZrB_2 with (a)10% $TiSi_2$, (b) 10%$TiSi_2$+10%HfB_2, and (c) 10%$TiSi_2$+20%HfB_2

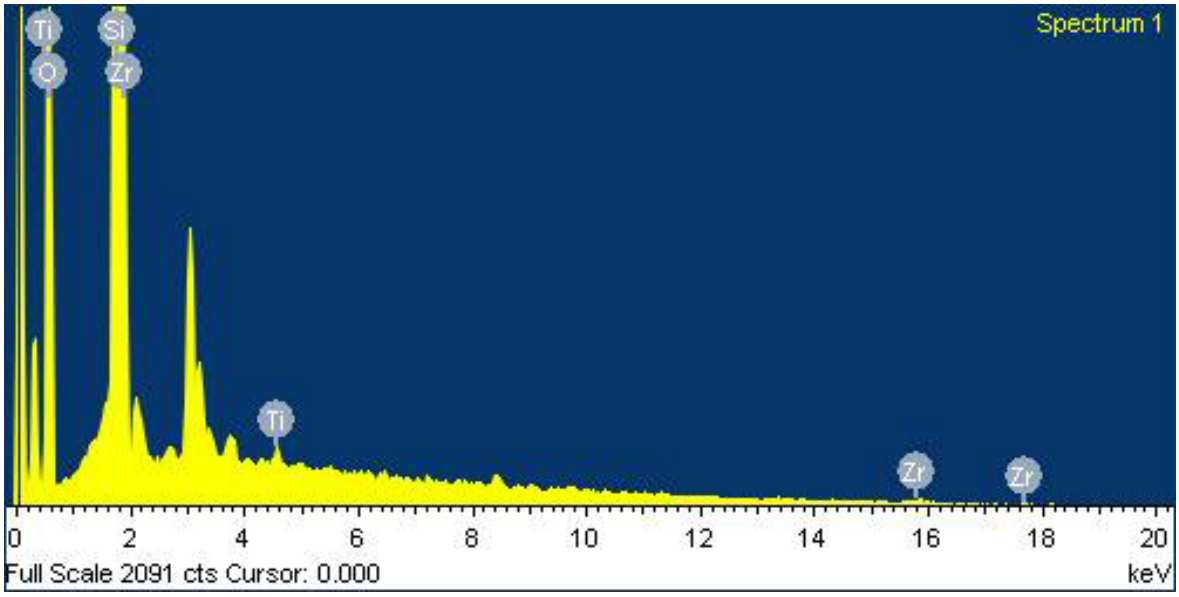

Fig. 4.34 Typical EDS pattern of the oxidized surface in ZrB_2 + 10%$TiSi_2$ + 20%HfB_2 composites.

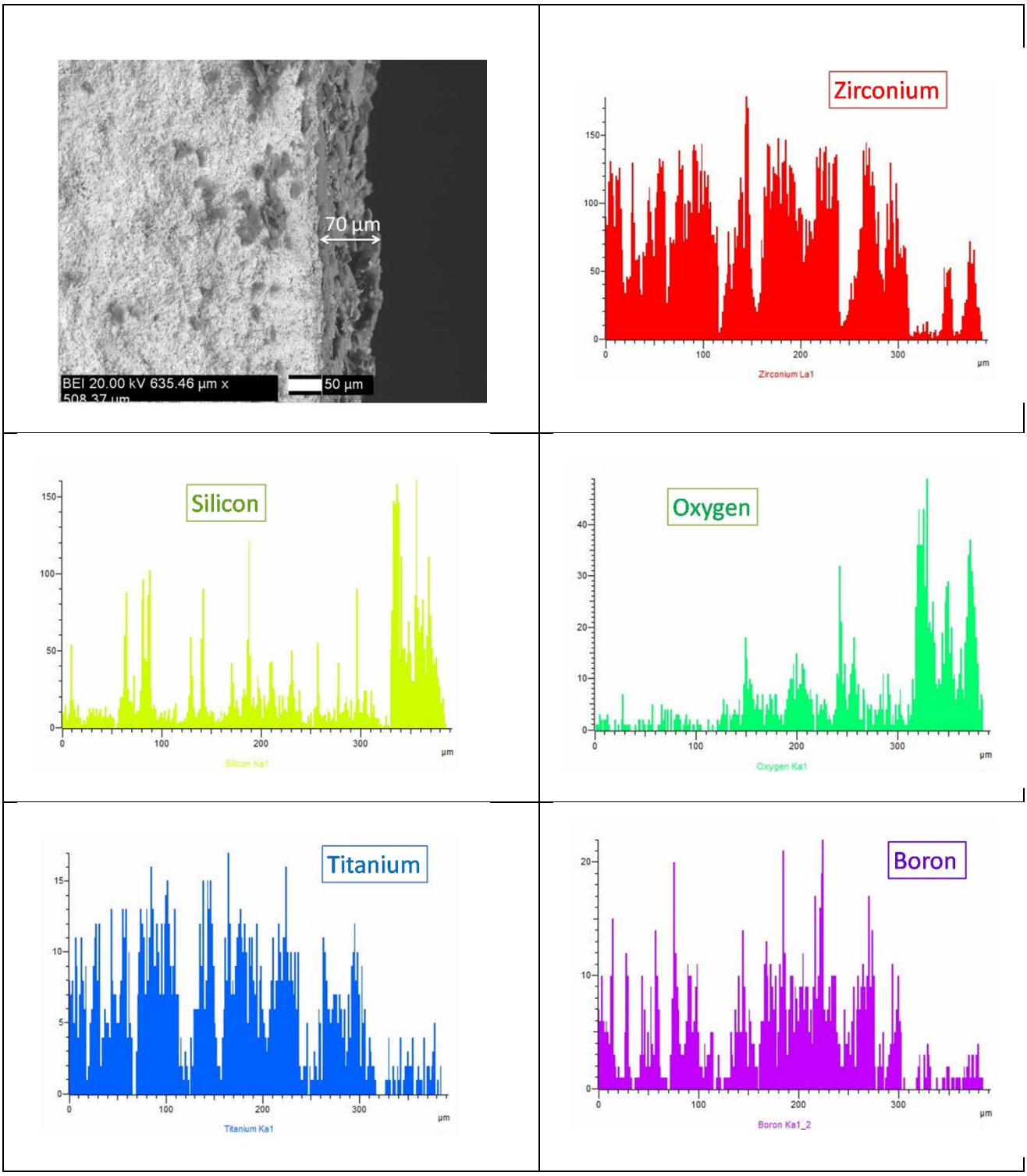

Fig. 4.35 SEM microstructure and elemental distribution of cross section of oxidized sample ZrB_2+$TiSi_2$ sample.

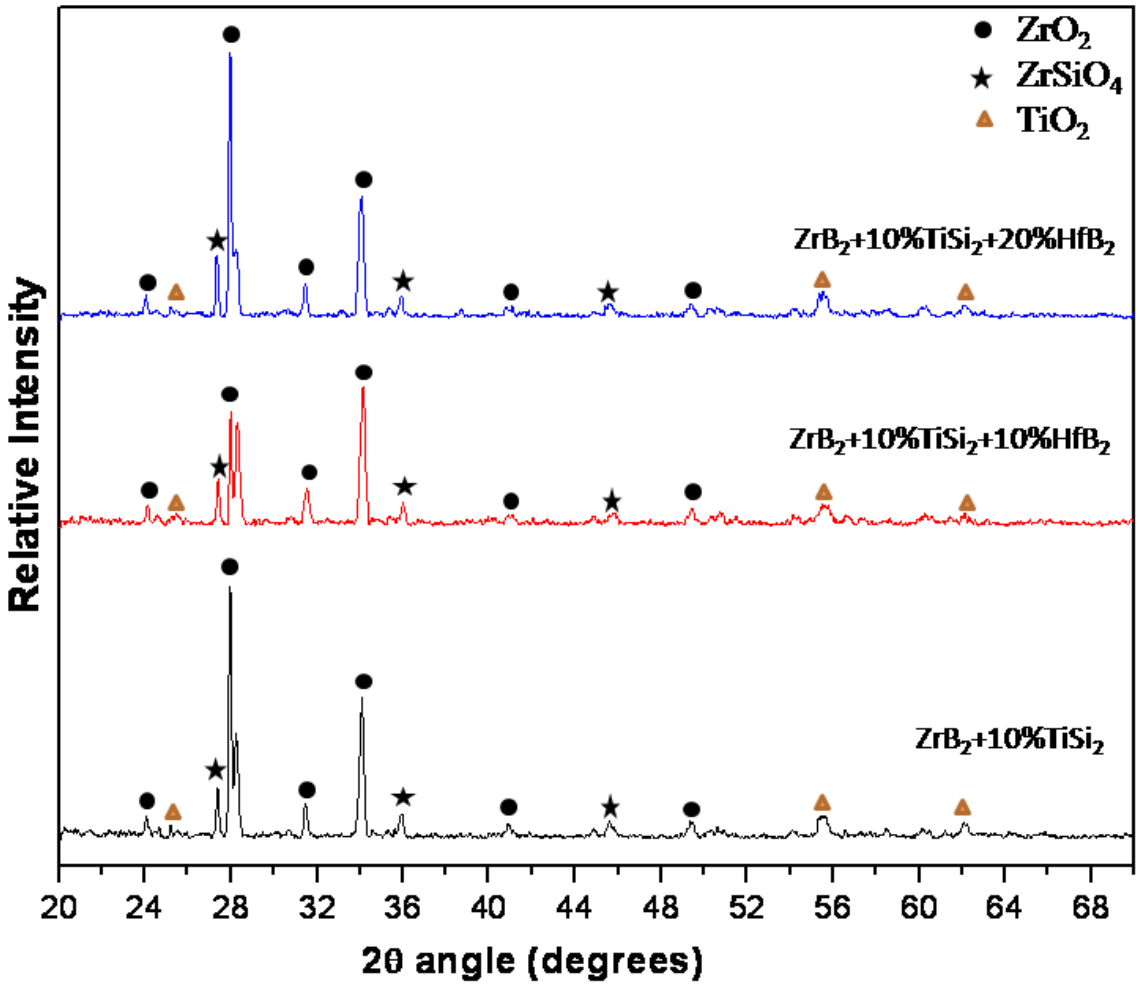

Fig. 4.36 XRD pattern of oxidized surfaces of ZrB_2 based composites

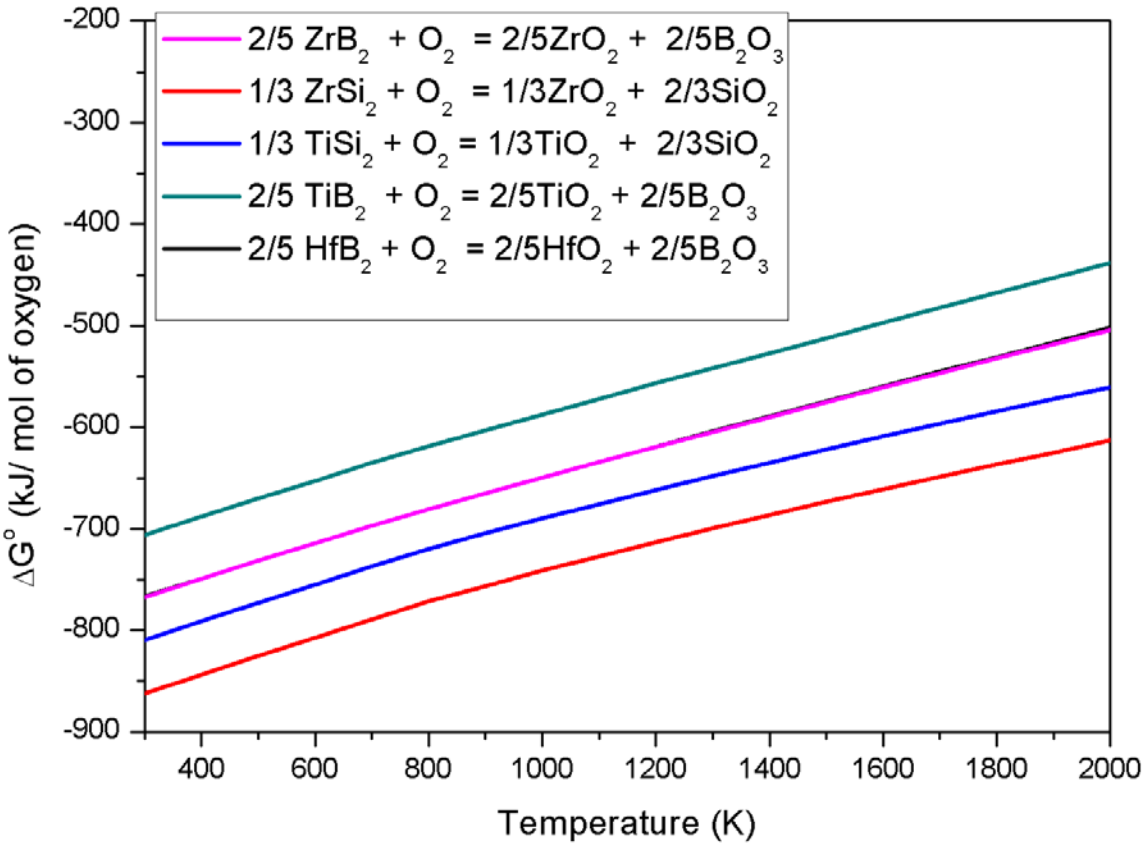

Fig.4.37 Free energy change with temperature plot for the reactions involved in oxidation of ZrB_2 +$TiSi_2$ +HfB_2 composites (Calculated by using Factsage software)

4.3.3 Effect of $CrSi_2$ and HfB_2 addition

The weight gain data obtained during oxidation at 900 ^oC as a function of time for ZrB_2 +10%$CrSi_2$ and ZrB_2+10%$CrSi_2$+10%HfB_2 samples are presented in Fig 4.38. Single sample of each composition was used for oxidation study. Both the samples have shown continuous weight gain with time. However, the rate of oxidation is found to decrease with increase in time which indicates the formation of protective layer. The final weight gain in ZrB_2+10%$CrSi_2$ sample is 0.0397 kg/m^2 after 64 hours whereas in ZrB_2+10%$CrSi_2$+10%HfB_2 sample is 0.0171 kg/m^2 which is lower. The lower weight gain in the HfB_2 containing sample could be attributed to lower diffusivity of oxygen ion through HfO_2 [128, 129]. There was a large difference in weight gain of both the samples even after the short exposure time of 30 minutes, which could be due to the faster formation of protective layer in HfB_2 containing sample. Monolithic ZrB_2 has shown continuous oxidation and higher weight gain of 0.0513 kg/m^2 even after a shorter duration of 32 hour at 900^oC.(fig. 4.28)

The oxidation products were analyzed by X-ray diffraction and SEM with energy dispersive spectroscopy (EDS). Fig.4.39 (a) presents the SEM image of oxide layer formed in ZrB_2 +10%$CrSi_2$ composite at 900^oC after 64 hour of exposure. The microstructure consists of cluster of bright particles in dark matrix. EDS analysis of the phases are presented in Fig.4.39 (b,c). Dark phase is rich in SiO_2 whereas bright phase is rich in ZrO_2.

SEM image of ZrB_2+ 10%$CrSi_2$+ 10%HfB_2 sample is shown in Fig. 4.40(a). It shows the presence of three phases: dark flakes and bright particle agglomerates dispersed in glassy matrix. EDS analysis of these phases are presented in Fig. 4.40 (b-d). The analysis indicates that the glassy matrix contains mainly Zirconium, Silicon and Oxygen with some Hafnium and Chromium content. The flakes were analyzed to be ZrO_2 rich phase whereas the bright phase was analyzed to contain Zr, Hf and O, indicating $(Zr,Hf)O_2$.

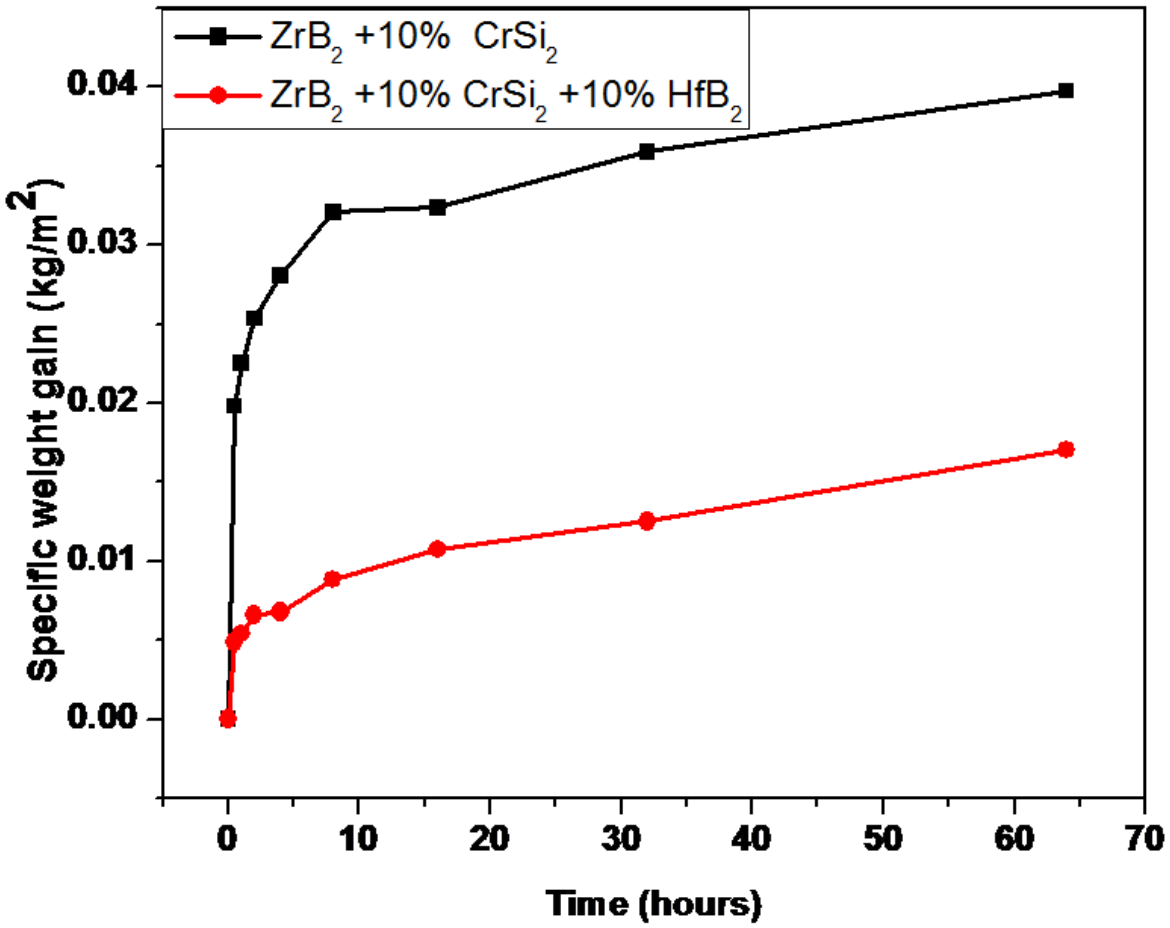

Fig. 4.38 Specific weight gain vs time in the ZrB_2 +10%$CrSi_2$ and ZrB_2 +10%$CrSi_2$ +10% HfB_2 sample at 900 ^oC

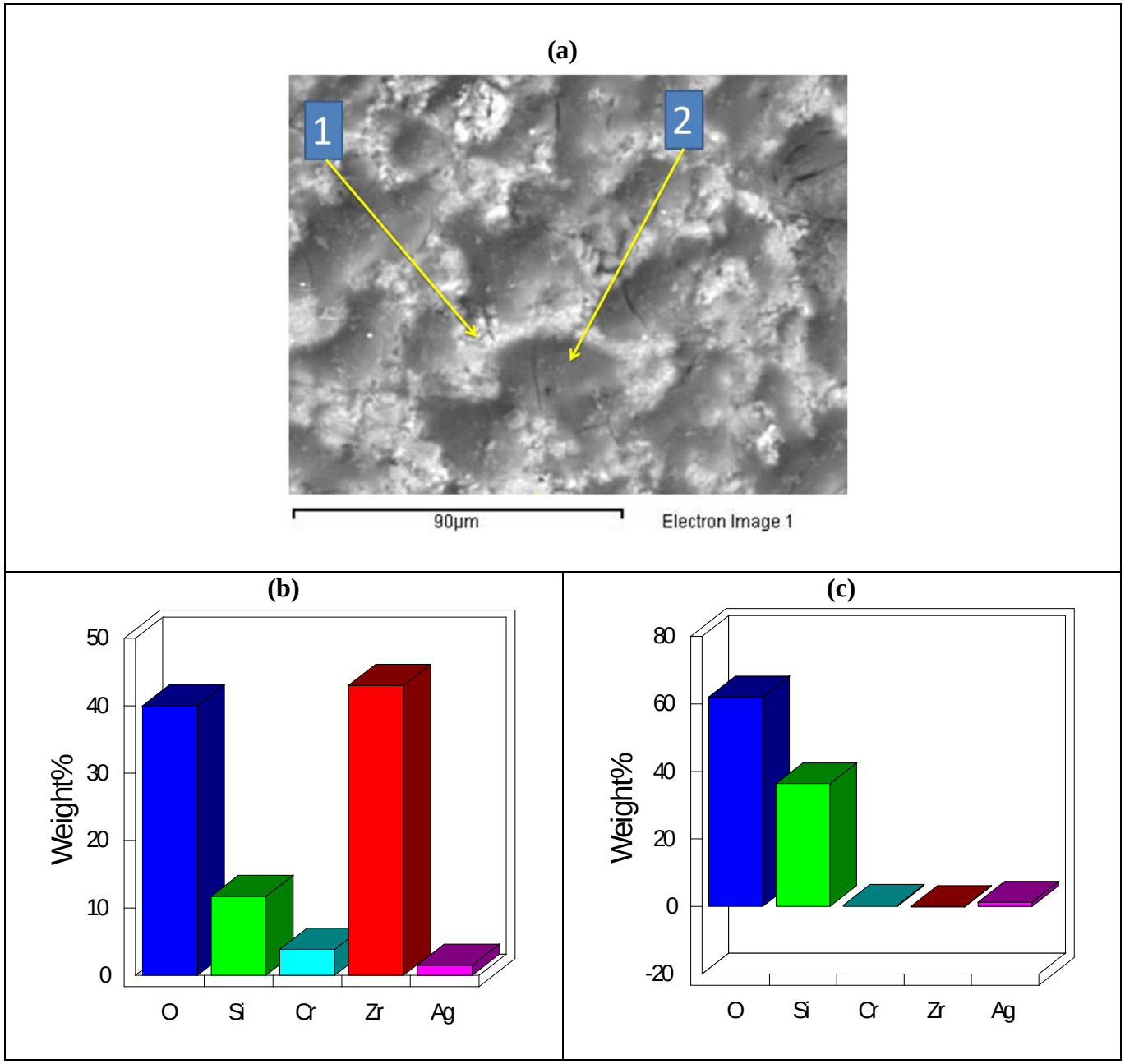

Fig.4.39 (a) BSE image of ZrB_2 +10%$CrSi_2$ oxidized at 900°C for 64 hours (b) EDS analysis of phase marked as 1 in (a), (c) EDS analysis of phase marked as 2 in (a)

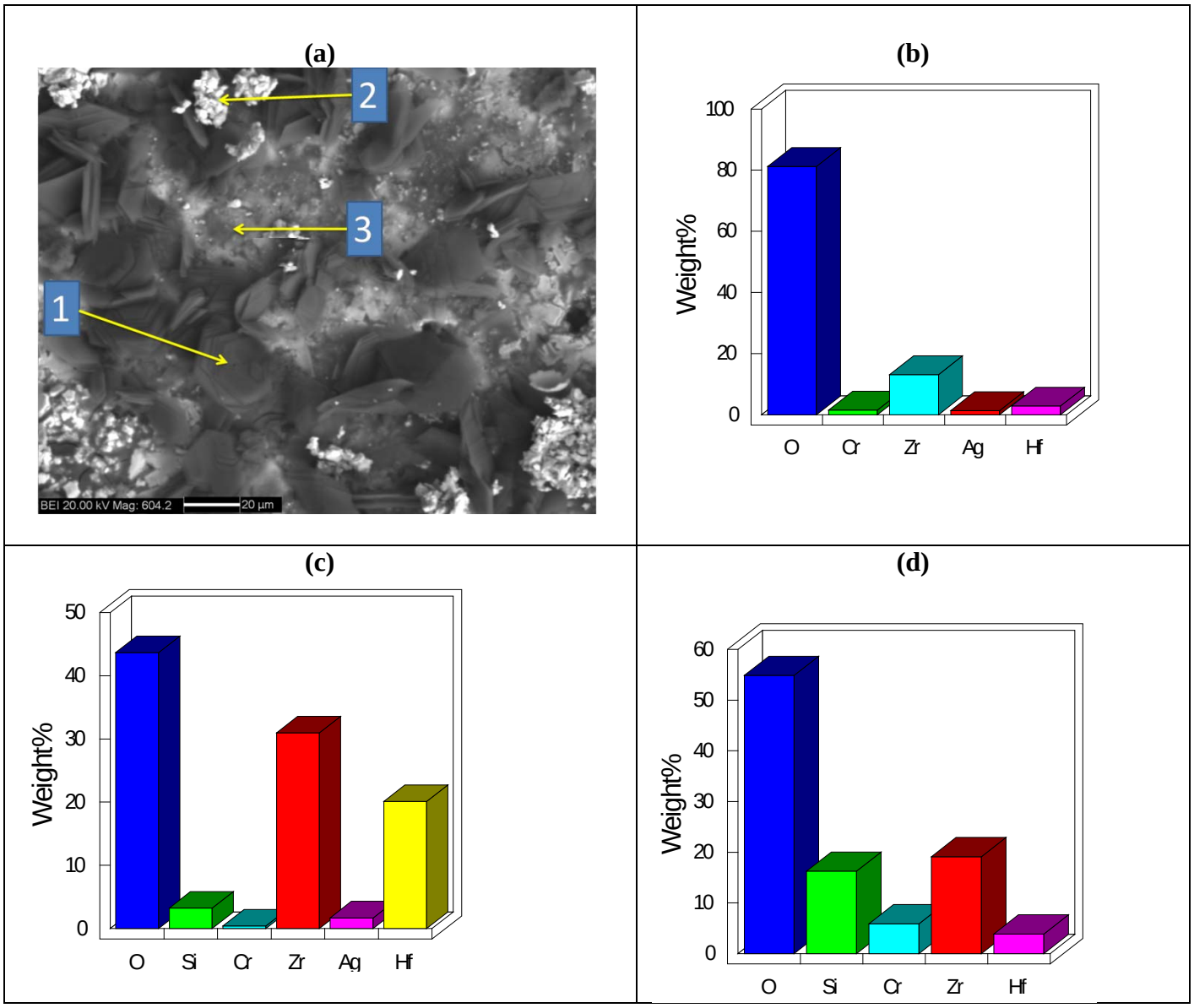

Fig.4.40 (a) BSE image of ZrB_2 +10% $CrSi_2$ +10% HfB_2 oxidized at 900°C for 64 hours (b) EDS spectra of phase marked as 1 in BSE image, (c) EDS spectra of phase marked as 2 in (a) (d) EDS spectra of phase marked as 3 in BSE image

XRD pattern obtained from the oxide scales of ZrB_2+10%HfB_2+10%$CrSi_2$ sample after oxidation at 900^oC for 64 hour is presented in Fig. 4.41. It showed that ZrO_2 and Cr_2O_3 are the only crystalline phases present in the oxide layer. SiO_2 and B_2O_3 have not been identified due to their amorphous nature.

Following reactions are possible during the oxidation process.

$2/5ZrB_2 + O_2 \rightarrow 2/5ZrO_2 + 2/5B_2O_3$ ……..…...(4.6)

$4/9CrB_2 + O_2 \rightarrow 2/9Cr_2O_3 + 4/9B_2O_3$……..…..(4.7)

$2/5HfB_2 + O_2 \rightarrow 2/5HfO_2 + 2/5B_2O_3$…….……(4.8)

$1/3ZrSi_2 + O_2 \rightarrow 1/3\ ZrO_2 + 2/3SiO_2$ ……..……..(4.9)

$4/11CrSi_2 + O_2 \rightarrow 2/11Cr_2O_3 + 8/11SiO_2$……(4.10)

Free energy change with temperature plot for reactions involved in oxidation of ZrB_2 +$CrSi_2$ +HfB_2 composite is presented in Figure 4.42. This shows that all the reactions listed in the plot are thermodynamically feasible at the test temperature of 1173 K (900 ^oC). Thermodynamic calculations were carried out by considering the species in standard condition (1 atm).

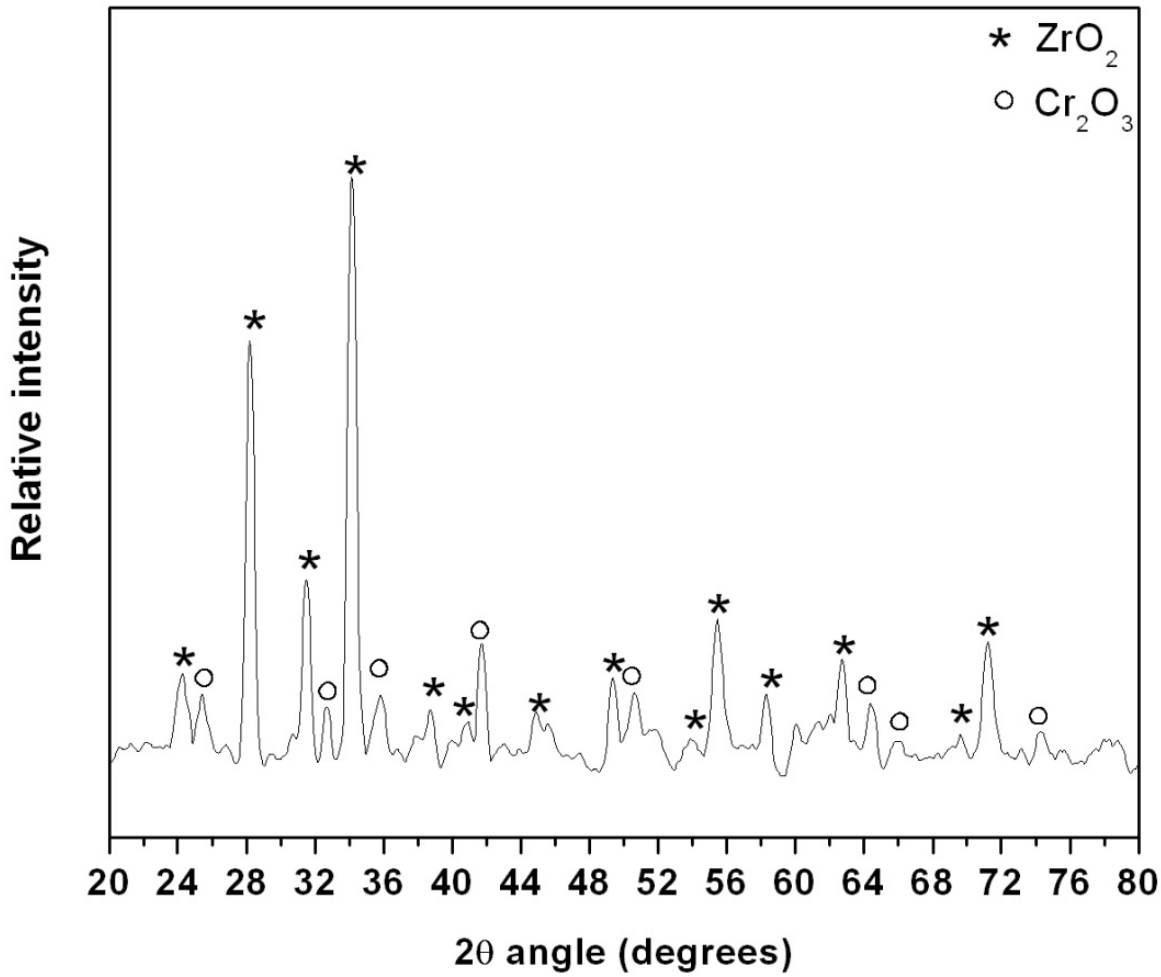

Fig.4.41 XRD Pattern of ZrB_2 +10%$CrSi_2$ +10% HfB_2 after oxidation at 900° C for 64 hour

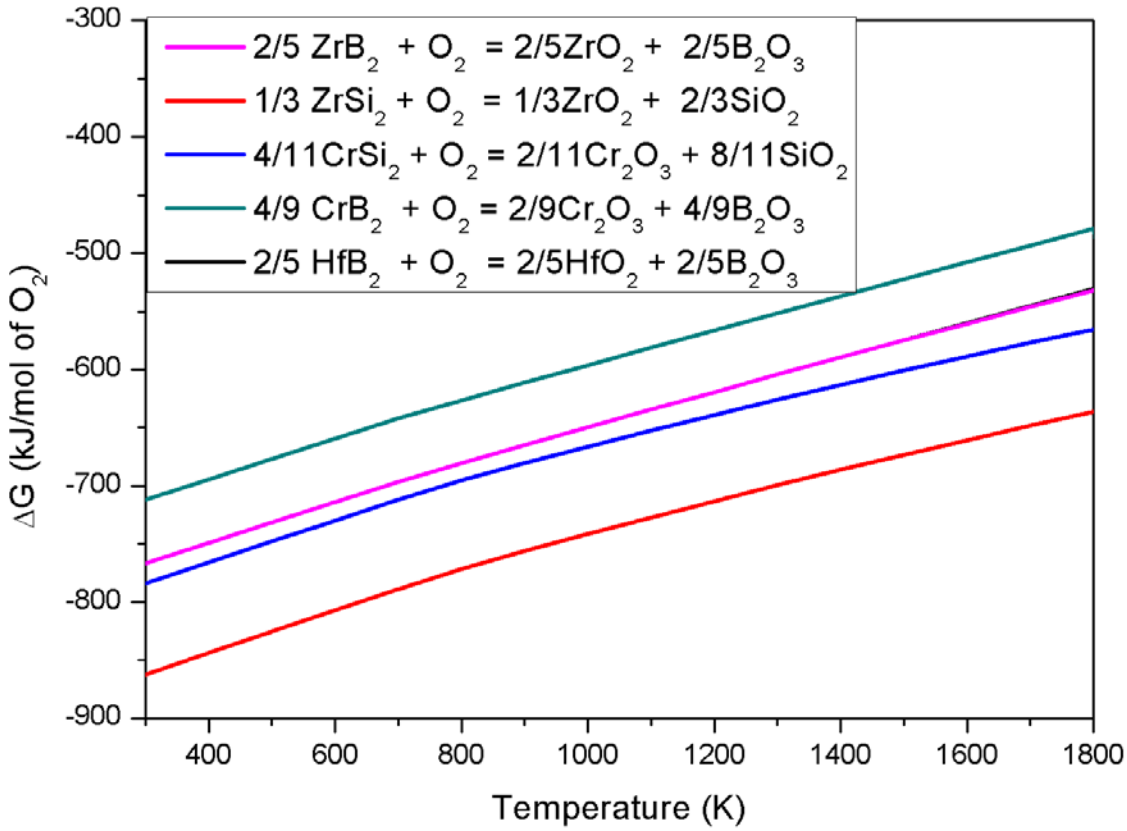

Fig.4.42 Free energy change with temperature plot for the reactions involved in oxidation of ZrB_2 +$CrSi_2$ +HfB_2 composites (Calculated by using Factsage software)

4.3.4 Effect of EuB_6 addition

The weight gain data obtained during oxidation at 900 ^oC as a function of time for ZrB_2 +2.5%EuB_6, ZrB_2 +5%EuB_6 and ZrB_2 +10%EuB_6 samples are presented in Fig 4.43. All the three samples have shown continuous weight gain with time. In the initial 8 hours, the weight gain is very small which increases during the exposure at 8-16 hour and then the rate of oxidation (slope of the curve) gets decreased. The decrease in rate of oxidation after 16 hour is due to the formation of a protective layer. In case of monolithic ZrB_2, oxidation rate was found to be constant.

There is a possibility of the formation of protective layer by combined effect of Eu_2O_3 and ZrO_2. ZrO_2 layer alone is not protective and results in linear weight gain but Eu_2O_3 may probably help in stabilizing the layer and making it protective by formation of solid solution between ZrO_2 and Eu_2O_3. EuB_6 has been reported to have good oxidation resistance by formation of protective layer based on Eu_2O_3 [130].

In order to understand the nature of oxidation, the oxidation data was fitted in the general rate equation for all the composites.

$$(\Delta w/A)^m = K_m.t \quad \ldots\ldots\ldots\ldots\ldots\ldots\ldots\ldots \quad (4.12)$$

Where Δw- is the change in weight, A- surface area of the sample, t- oxidation time and K_m- rate constant. Rate constant values are presented in Table 4.12. The composite samples have shown a near parabolic pattern of oxidation.

Fig. 4.44 presents the SEM microstructures of the oxidized surface. It shows the presence of protective layer. The oxidized layer was analyzed by EDS to contain mainly zirconium (~21.67 at%) Europium (6.49 at %) and oxygen (~71.84 at%). A typical EDS pattern from the oxidized surface is shown in fig.4.45.

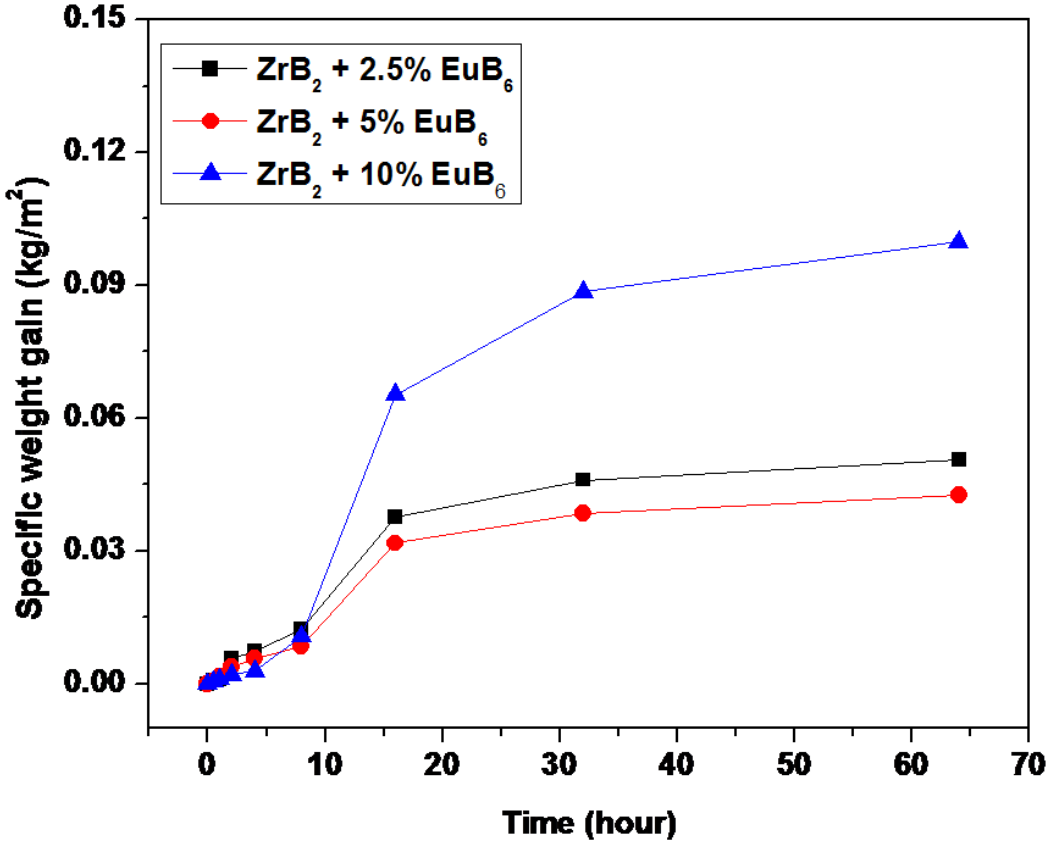

Fig. 4.43 Specific weight gain vs time in ZrB_2 based composite samples oxidized at 900°C

Table 4.12: Rate constants for ZrB_2 +EuB_6 composites after 64h of oxidation at 900 ^oC

Sample	$^*K_p$ ($kg^2m^{-4}s^{-1}$)	$^\$K_m$	$^\#m$
ZrB_2 + 2.5% EuB_6	1.1 x10^{-4}	6.0x10^{-5}	1.79
ZrB_2 + 5% EuB_6	1.0 x10^{-4}	4.0x10^{-5}	1.74
ZrB_2 + 10% EuB_6	2.1 x10^{-4}	3.0x10^{-5}	1.47

(**$^*K_p$** – Parabolic rate constant, $^\$K_m$ – Rate constant of general rate equation, $^\#m$- Slope of general rate equation)

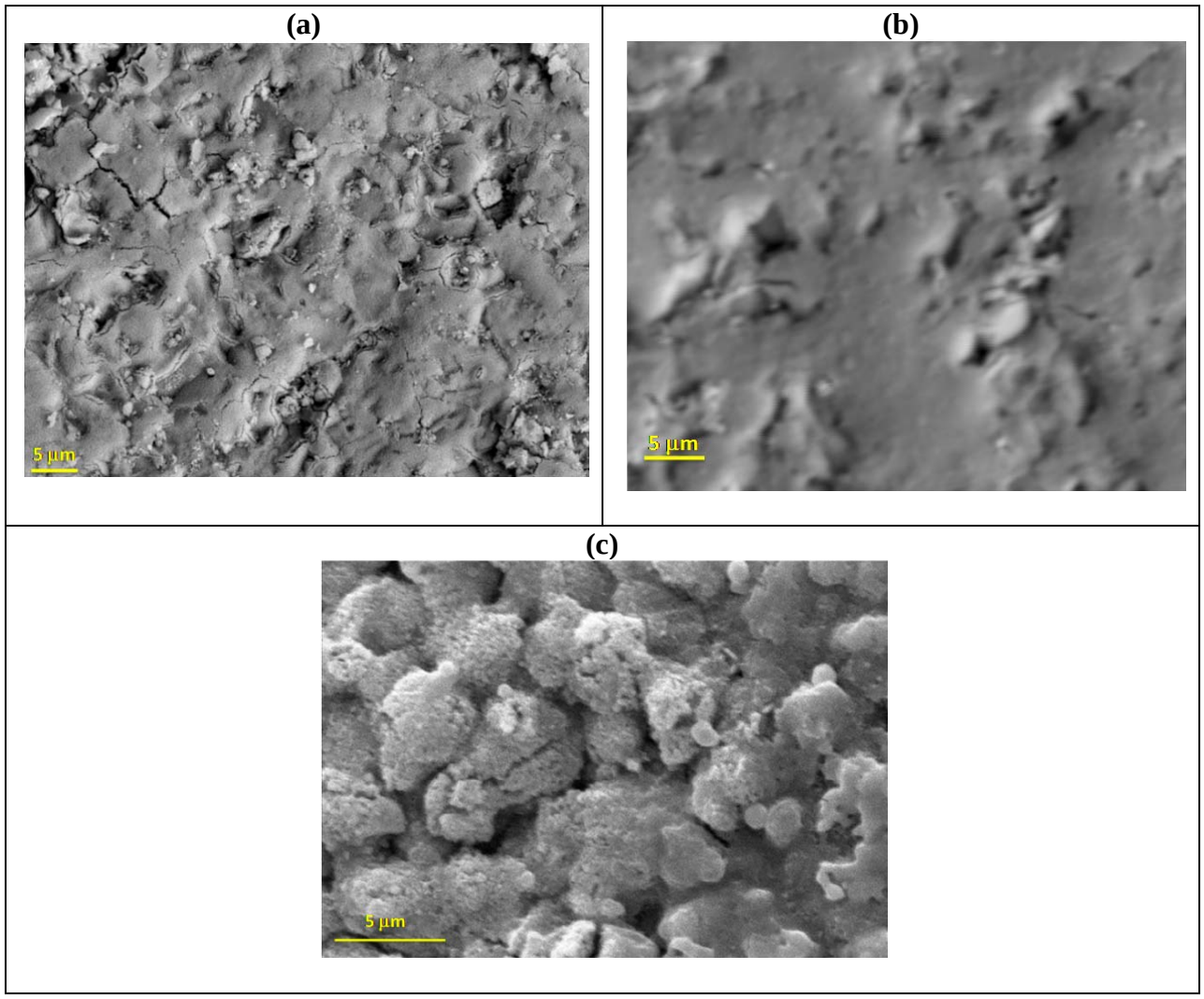

Fig.4.44 SEM images of oxidized (900°C, 64 hr) surface of ZrB_2 with (a) 2.5%EuB_6 (b) 5%EuB_6 and (c) 10%EuB_6

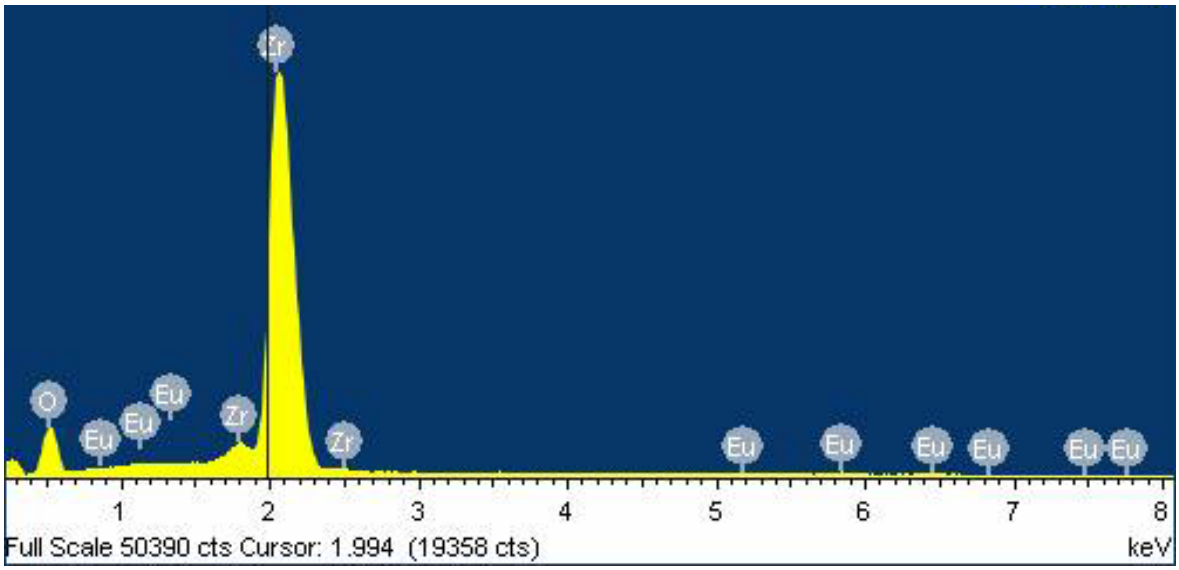

Fig.4.45 Typical EDS pattern of the oxidized surface in ZrB_2+ 5% EuB_6 composite

ZrB_2 is a non-oxide ceramic material and hence is susceptible for oxidation in air at high temperature. Oxidation of material changes the material properties completely. Chemistry of materials gets changed and the material is no longer suitable for the high temperature application**.** Mechanical and physical property degradation also takes place due to oxidation. Oxidation behavior of ceramic depends on reaction product obtained during oxidation. The reaction product can be solid, liquid or gas. Gaseous oxidation product is highly undesirable as it gets removed from reaction zone and oxidation continues. For good oxidation resistance, the oxide layer formed should be adherent to material and should act as diffusion barrier for oxygen. Thus it prevents the further oxidation of material and provides oxidation resistance.

In this study, it was observed that ZrB_2 is not resistant to oxidation at 900 ^{o}C in air. The oxide layer was not protective and hence the rate of weight gain was constant. Silicide addition

improved oxidation resistance by formation of borosilicate glassy layer. The glassy layer covers the complete surface of ZrB_2 composite and prevents further oxidation.

The observations of other researchers on oxidation of ZrB_2 based material is discussed below. Guo et al. [131] have reported that oxidation of ZrB_2 powder follows para-linear kinetics in air at 650–800 ◦C, where the dominating term is the parabolic one which indicates that oxidation takes place by oxygen diffusion in the oxide scale. Karlsdottir et al. [132] have studied the oxidation behavior of ZrB_2+SiC composite at 1500°C and observed the formation of ZrO_2 islands in the borosilicate glass based protective layer. Wang et al. [133] have noticed the formation of silica rich layer on the top of oxidized surface of ZrB_2-SiC-ZrC ceramic on oxidation at 1750°C. Monteverde et al. [107] have observed that oxidation of monolithic ZrB_2 starts at 420°C. Introduction of SiC particles markedly improves oxidation resistance due to the formation of an adherent and protective borosilicate glass layer that coats the sample surface, effectively limiting the inward diffusion of oxygen toward the reaction interface. Mallik et al. [128] have reported that oxidation of ZrB_2 +20%SiC starts at 740°C. Guo et al. [134] have observed that addition of Si improves the oxidation resistance of ZrB_2 at 1500°C whereas Zr addition decreases the oxidation resistance.

One important finding of this study is improvement in oxidation resistance with rare earth additive. Addition of EuB_6 also improved oxidation resistance by formation of protective layer based on Eu_2O_3 and ZrO_2. Europium oxide and zirconium oxide forms solid solution and this solid solution impart the oxidation resistance to the material. Thermodynamic data for EuB_6 is not available and hence free energy calculation for oxidation reaction could not be done for this system. Table 4.13 compares the oxidation kinetics data of developed composites with the values reported for other boride composites in literature. It reveals that composites developed in this study have good oxidation resistance.

Table: 4.13 Oxidation kinetics parameters of boride based composites

material	Temperature (^oC)	Parabolic rate constant (**Kg^2 m^{-4} s^{-1}**)	(m): exponent value in general rate equation.	Reference
ZrB_2	900	$1.25x10^{-8}$	0.9	Present study
ZrB_2+10%$TiSi_2$	900	$1.80x10^{-9}$	2.5	Present study
ZrB_2+10%$TiSi_2$ +10%HfB_2	900	$9.53x10^{-10}$	2.4	Present study
ZrB_2+10%$TiSi_2$ +20%HfB_2	900	$2.22x10^{-10}$	2.0	Present study
ZrB_2+10%$CrSi_2$ +20%HfB_2	900	$6.08x10^{-10}$	2.1	Present study
ZrB_2+2.5%EuB_6	900	$1.1\ x10^{-4}$	1.8	Present study
ZrB_2+5%EuB_6	900	$1.0\ x10^{-4}$	1.7	Present study
ZrB_2+10%EuB_6	900	$2.1\ x10^{-4}$	1.5	Present study
TiB_2 +10%WSi_2	850	$2.5x10^{-8}$	1.8	135
TiB_2 +10% CrB_2	850	$1.31x10^{-9}$	2.5	136
TiB_2 +10%$CrSi_2$	850	$6.73x10^{-8}$	2.7	137
TiB2 +2.5%$TiSi_2$	850	$1.38x10^{-9}$	1.8	138
TiB_2 + 20%$MoSi_2$	850	$5.9x10^{-5}$	1.4	139
TiB2 +10%$TiSi_2$	1200	$2.9x10^{-2}$	1.9	140
TiB_2 +10% $MoSi_2$	1200	$2.1x10^{-2}$	1.8	141
ZrB_2 + SiC +ZrC	1750	$7.8x10^{-5}$	~2	133
ZrB_2 + 20% SiC	1627	$3x10^{-1}$	~2	111
ZrB_2 +20%SiC +20%$TaSi_2$	1627	$8x10^{-3}$	~2	111

Chapter –5

Summary and Conclusions

Content

Chapter -5

Summary and Conclusions

5.1 Summary and Conclusion

In this study, experiments were carried out to investigate the process for synthesis and densification of borides. Synthesis of pure borides suitable for sintering is a challenge and requires high temperature, high vacuum operations. For synthesis, solid state reaction of charge mixture containing oxides, B_4C and carbon was chosen. Effect of process parameters were studied for synthesis of ZrB_2. Based on the results the parameters were optimized for synthesis of these boride powders. Densification of boride materials is extremely difficult due to their covalent bonding and highly refractory nature. In this study, ZrB_2 was selected as base material and EuB_6, HfB_2 and silicides were selected as additives for densification experiments. Dense pellets were characterized by XRD and SEM to analyze the possible sintering mechanism. Effect of sinter additives on densification, microstructure, mechanical properties and oxidation resistance of ZrB_2 was investigated.

The major findings of the present study are summarized below.

- Heating of stoichiometric charge for synthesis of ZrB_2 by boron carbide reduction of zirconia in presence of carbon results in formation of ZrB phase along with ZrB_2. This boron deficient phase is formed due to loss of boron in the form of its volatile oxides.

- The boron deficient phase ZrB can be avoided and single phase ZrB_2 can be obtained by adjusting the molar ratio of charge by increasing B_4C and reducing carbon.
- Synthesis of pure ZrB_2 by this method requires a temperature of 1875 ^oC. The High temperature is required due to low diffusivity of all the elements through boride phase which is predominantly covalently bonded.
- Synthesis of single phase EuB_6 is possible by using the stoichiometric charge but the product contains around 2% carbon which can be reduced by addition of elemental boron in the charge mixture.
- Synthesis of pure EuB_6 is possible at temperature of 1400 ^oC, which is relatively lower than that required for ZrB_2.
- Pressureless sintering of Monolithic ZrB_2 results in maximum density of 78% at 2000 ^oC. Near theoretical density of Monolithic ZrB_2 can be obtained by hot pressing at 1850 ^oC and 35 MPa pressure for 2 hour.
- Addition of $TiSi_2$ or $CrSi_2$ lowers the hot pressing temperature by 200 ^oC. This decrease is attributed to liquid phase sintering caused by reaction product $ZrSi_2$ which has low melting point of 1620 ^oC. Reaction sintering is also responsible for better densification.
- Addition of EuB_6 lowers the hot pressing temperature by 100 ^oC. This is due to the formation of solid solution of ZrB_2 and EuB_6 which in turn results in the formation of point defects and diffusion is enhanced.
- $TiSi_2$ and $CrSi_2$ addition results in formation of $ZrSi_2$ which is also responsible of liquid phase sintering.
- EuB_6 is only partially soluble in ZrB_2 and also exist as a distinct phase in the material.

- $TiSi_2$ and $CrSi_2$ addition has resulted in lower hardness whereas EuB_6 addition has increased the hardness.
- Fracture toughness of all the composite samples is higher than the monolithic sample. This is due to crack deflection caused by the presence of second phase in microstructure.
- Monolithic ZrB_2 does not have good oxidation resistance at 900 ^oC. Linear oxidation kinetics was observed in case of monolithic ZrB_2.
- Silicide addition as well as EuB_6 addition has improved the oxidation resistance of ZrB_2 in the temperature range of 900 ^oC. The good oxidation resistance is due to the formation of protective oxide layer.

5.2 Future Scope:

In this study, it was found that EuB_6 addition helps in densification of ZrB_2 by formation of solid solution. In literature phase diagram of ZrB_2-EuB_6 is not available. In future, studies could be carried out on generation of binary phase diagram on ZrB_2-EuB_6 system. Similarly for other boride systems, phase diagrams could be generated. In synthesis studies, it was found that thermodynamic data for Europeum hexaboride (EuB_6) and zirconium monoboride (ZrB) is not available. In future studies, the thermodynamic data for these compounds could be generated which will be very useful for scientific studies. Till now there is no report on formation of ZrB as single phase. Efforts could be made to synthesize this compound in the single phase form. Effects of other rare earth borides could also be studied in future. In this study the oxidation test was carried out at 900 ^oC. Future studies may focus on oxidation studies at higher temperatures.

Chapter-6

References

References

1. WG Fahrenholtz and GE Hilmas: 'Refractory diborides of zirconium and hafnium', *J. Am. Ceram. Soc.*, 2007, 90(5), 1347-1364.
2. ML Bauccio: 'ASM Engineered Materials Reference book', *United States of America: ASM International*, 1994.
3. K Upadhyay, JM Yang and WP Hoffman: 'Materials for ultrahigh temperature structural application'. *Am. Ceram. Soc. Bull.*, 1997,76, 51-56.
4. MM Opeka,. IG Talmy and JA Zaykoski: 'Oxidation-based materials selection for 2000°C + hypersonic aerosurfaces: Theoretical considerations and historical experience', *J. Mater. Sci.*, 2004, 39, 5887-5904.
5. SR Levine, EJ Opila, MC Halbig, JD Kiser, M Singh and JA Salem: 'Evaluation of ultra-high temperature ceramics for aeropropulsion use', *J. Euro. Ceram. Soc.*, 2002, 22, 2757-2767.
6. C Mroz: 'Annual Mineral review: zirconium diboride', *Am. Ceram. Soc. Bull.*, 1995, 74, 164-165.
7. C Mroz: 'Annual Mineral review: zirconium diboride', *Am. Ceram. Soc. Bull.*, 1994, 73, 141-142.
8. HM Zaw, JYH Fuh, AYC Nee and L Lu: 'Formation of a new EDM electrode material using sintering techniques', *J. Mater, Process. Techno.*, 1999, 89-90, 182-186.
9. AK Khanra, BR Sarkar, B Bhattacharya, LC Pathak and MM Godkhindi: 'Performance of ZrB_2-Cu composite as an EDM electrode', *J Mater. Process. Techno.*, 2007, 83, 122-126.
10. VI Matkovich: 'Boron and refractory borides', *New York: Springler – Verlag*,1977.
11. P Peshev and G Bliznakov: 'On the borothermic preparation of titanium, zirconium and hafnium diborides', *J. Less Com. Met.*, 1968,14, 23-32.
12. H Zhao, Y He and Z Jin: 'Preparation of zirconium boride powder', *J. Am. Ceram. Soc.* 1995, 78(9), 2534-2536.
13. N Setoudeh and NJ Welham: 'Formation of zirconium diboride (ZrB_2) by room temperature mechanochemical reaction between ZrO_2, B_2O_3 and Mg', *J. Alloy and Compounds* , 2006, 420, 225-228.

14. K Nishiyama, T Nakamur, S Utsumi, H Sakai and M Abe: 'Preparation of ultrafine boride powders by metallothermic reduction method', *Journal of Physics*, 2009, Conference Series 176, 012043-1-8.
15. SK Mishra, S Das and LC Pathak: 'Defect structures in zirconium diboride powder prepared by self-propagating high-temperature synthesis', *Mater. Sci. & Engg. A*, 2004, 364, 249–255.
16. S Motojima, K Funahashi and K Kurosawa: 'ZrB_2 coated on copper plate by chemical vapour deposition, and its corrosion and oxidation stabilities', *Thin Solid Films*, 1990, 189, 73- 79.
17. A Wang and G Male: 'Experimental system investigation of the Zr-B-C1-H CVD', *Journal of the European Ceramic Society*, 1993, 11, 241-251.
18. L Chen , Y Gu, Z Yang , L Shi, J Ma and Y Qian: 'Preparation and some properties of nanocrystalline ZrB_2 powders', *Scripta Materialia* 2004, 50, 959–961.
19. EJ Frazer, KE Anthony and BJ Welch: 'Electrodeposition of zirconium diboride from oxides dissolved in molten cryolite' *Electrodeposition and Surface Treatment*, 1975, 3**,** 169 – 177.
20. Y Yan, Z Huang, S Dong, and D Jiang: 'New route to synthesize ultra-fine zirconium diboride powders using inorganic–organic hybrid precursors' *J. Am. Ceram. Soc.*, 2006, 89, (11), 3585–3588.
21. K Su and LG Sneddon: 'Polymer-precursor routes to metal borides: Syntheses of TiB_2, and ZrB_2', *Chem. Mater.* 1991, 3, 10-12.
22. HE Camurlu, F Maglia:, 'Preparation of nano-size ZrB_2 powder by self-propagating high-temperature synthesis', *J. Euro. Ceram. Soc*., 2009, 29, 1501–1506.
23. AL Chamberlain, WG Fahrenholtz, GE Hilmas: 'Reactive hot pressing of zirconium diboride', *J. Euro. Ceram. Soc.* 2009, 29, 3401–3408.
24. T Tsuchida, S Yamamoto: 'Mechanical activation assisted self-propagating high-temperature synthesis of ZrC and ZrB2 in air from Zr/B/C powder mixtures', *J. Euro. Ceram. Soc.*, 2004, 24, 45–51.
25. DD Radev and M Marinov: 'Properties of titanium and zirconium diborides obtained by self-propagated high-temperature synthesis', *J. Alloys and Compounds*, 1996, 244, (1-2), 48-51.
26. M Brochu , BD Gauntt, L Boyera,, RE Loehmanb: 'Pressureless reactive sintering of ZrB_2 ceramic', *J. Euro. Ceram. Soc.*, 2009, 29, 1493–1499.
27. P Millet, T Hwang: 'Preparation of TiB_2 and ZrB_2- Influence of a mechanochemical

treatment on the borothermic reduction of titania and zirconia', *J. Mater. Sci.*, 1996, 31, 351- 355.

28. S Ran, OV Biest and J Vleugels: 'ZrB_2 powders synthesis by borothermal reduction' J. Am. Ceram. Soc., 2010, 93, (6), 1586–1590.
29. WM Guo and GJ Zhang: 'Reaction processes and characterization of zrb_2 powder prepared by boro/carbothermal reduction of ZrO_2 in vacuum', *J. Am. Ceram. Soc.*, 2009, 92, (1), 264–267.
30. GJ Zhang, WM Guo, DW Ni and YM Kan: 'Ultrahigh temperature ceramics (UHTCs) based on ZrB_2 and HfB_2 systems: powder synthesis, densification and mechanical properties', *Journal of Physics: Conference Series*, 2009, 176, 012041
31. AK Khanra, LC Pathak, SK Mishra and MM Godkhindi: 'Sintering of ultrafine zirconium diboride powder prepared by modified SHS technique', *Advances in Applied Ceramics*, 2005, 104, (6), 282-284.
32. SK Mishra and SK Das: 'Sintering and microstructural behaviour of SHS produced zirconium diboride powder with the addition of C and TiC', *Mater. Letters*, 2005, 59, 3467-3470
33. SK Mishra and LC Pathak: 'Effect of carbon and titanium carbide on sintering behavior of zirconium diboride', *Journal of Alloys and Compounds*, 2008, 465, 547–555.
34. SK Mishra, SK Das, P Ramachandrarao, DY Belov and S Mamyan: 'Synthesis of zirconium diboride-alumina composite by the self-propagating, high-temperature synthesis process', *Metallurgical and Materials Transactions A*, 2003, 34,1979.
35. SK Mishra, SK Das and V Sherbacov: 'Fabrication of Al_2O_3–ZrB_2 in situ composite by SHS dynamic compaction: A novel approach', *Composites Science and Technology*, 2007, 67, 2447–2453.
36. YB Lee, HC Park, KD Oh, CR Bowen and R Stevens: 'Self-propagating high-temperature synthesis of ZrB_2 in the system ZrO_2-B_2O_3-Fe_2O_3-Al', *J Mater. Sci. Let.* 2000, 19, 469– 471.
37. AK Khanra, LC Pathak and MM Godkhindi: 'Carbothermal synthesis of zirconium diboride (ZrB2) whiskers', *Advances in Applied Ceramics*, 2007,106, (3), 155-60.
38. Y Xie, T.H. Sanders and R.F. Speyerw: 'Solution-based synthesis of submicrometer ZrB_2 and ZrB_2–TaB_2', *J. Am. Ceram. Soc*., 2008, 91, (5), 1469–1474.

39. SV Devyatkin: 'Electrosynthesis of zirconium boride from cryolite-alumina melts containing zirconium and boron oxides', *Russian Journal of Electrochemistry*, 2001, 37, (12), 1308-1311
40. K Su and LG Sneddon: 'A polymer precursor route to metal borides', *Chem. Mater.* 1993, 5, 1659-1668.
41. JF Pierson, T Belmonte, T Czerwiec, D Hertz and H Michel: 'Low temperature ZrB_2 remote plasma enhanced chemical vapor deposition', *Thin Solid Films*, 2000, 359, 68-76.
42. S Berthon and G Male: 'Infiltration of zirconium diboride by ICVI in porous materials', *Composite science and technology*, 1997, 57, 217-227.
43. AL Wayda, F Scnneemeyer and RL Oplla: 'Low temperature deposition of zirconium and hafnium boride films by thermal decomposition of the metal borohydrides (M $[BH_4]_4$)', *Appl. Phys. Lett.* 1988, 53 (5).
44. S Reich, S Hnrald, H Klhra, and S Laszlri: 'Deposition of thin films of zirconium and hafnium boride by plasma enhanced chemical vapor deposition', *Adv. Mater*. 1992, 4, (10), 650-653.
45. S.Randich and DD Allred: 'Chemically vapor-deposited ZrB_2 as a selective solar absorber', *Thin Solid Films*, 1981, 83, 393-398.
46. WG Fahrenholtz, GE Hilmas, SC Zhang and S Zhu: 'Pressureless sintering of zirconium diboride: Particle size and additive effects', *J Am Ceram Soc* 2008, 91, (5), 1398-1404.
47. AL Chamberlain, WG Fahrenholtz and GE Hilmas: 'Pressureless sintering of zirconium diboride', *J Am Ceram Soc*, 2006, 89, (2), 450-456.
48. S Zhu, WG Fahrenholtz, GE Hilmas and SC Zhang: 'Pressureless sintering of carbon-coated zirconium diboride powders', *Mater Sci Eng A*, 2007, 459,167-171.
49. SC Zhang, GE Hilmas and WG Fahrenholtz: 'Improved oxidation resistance of zirconium diboride by tungsten carbide additions', *J. Am. Ceram. Soc.*, 2008, 91, (11), 3530–3535.
50. H Zhang, Y Yan, Z Huang, X Liu and D Jiang: 'Properties of ZrB_2–SiC ceramics by pressureless sintering', *J. Am. Ceram. Soc*., 2009, 92, (7), 1599–1602.
51. D Sciti, F Monteverde, S Guicciardi, G Pezzotti and A Bellosi: 'Microstructure and mechanical properties of ZrB_2-$MoSi_2$ ceramic composites produced by different sintering techniques', *Mater. Sci. Eng. A*, 2006, 434, 303-309.

52. XG Wang, WM Guo and GJ Zhang: ‘Pressureless sintering mechanism and microstructure of ZrB_2–SiC ceramics doped with boron’, *Scripta Materialia*, 2009, 61, 177–180.
53. SK Mishra, SK Das, AK Ray and P Ramachandrarao: ‘Effect of Fe and Cr addition on the sintering behavior of ZrB_2 produced by self-propagating high-temperature synthesis’ *J. Am. Ceram. Soc.*, 85 [11] 2846–48 (2002)
54. YM Cheng and AM Gadalla: ‘Synthesis and analysis of ZrB_2-based composites’, *Materials and Manufacturing Processes*, 1996, 11, (4), 575-587.
55. Y Yan, Z Huang, S Dong, and D Jiang. ‘Pressureless sintering of high-density ZrB_2–SiC ceramic composites’, *J. Am. Ceram. Soc.*, 2006, 89 (11), 3589–3592.
56. AK Khanra and MM Godkhindi: ‘Effect of Ni additives on pressureless sintering of SHS ZrB_2’, *Advances in Applied Ceramics*, 2005, 104, (6), 273.
57. D Sciti, M Brach and Alida Bellosi. ‘Long-term oxidation behavior and mechanical strength degradation of a pressurelessly sintered ZrB_2–$MoSi_2$ ceramic’, *Scripta Materialia*, 2005, 53,1297–1302.
58. J Zou, GJ Zhang, YM Kan, PL Wang: ‘Pressureless densification of ZrB_2-SiC composites with vanadium carbide’, *Scripta Materialia*, 2008, 59 (3), 309-312.
59. SQ Guo, Y Kagava, T Nishimura and H Tanaka: ‘Pressureless sintering and physical properties of ZrB_2- based composites with $ZrSi_2$ additive’, *Scripta Materialia*, 2008, 58, 579-582.
60. M Zhu and Y Wang: ‘Pressureless sintering ZrB_2–SiC ceramics at low temperatures’, *Mater. Let.*, 2009, 63, 2035–2037.
61. M Brochu, B Gauntt, T Zimmerly, A Ayala and R Loehman: ‘Fabrication of UHTCs by conversion of dynamically consolidated Zr + B and Hf +B powder mixtures’, *J. Am. Ceram. Soc.*, 2008, 91, (9), 2815–2822.
62. AL Chamberlain, WG Fahrenholtz and GE Hilmas: ‘High strength zirconium diboride based ceramics’, *J. Am. Ceram. Soc.*, 2004, 87,(6), 1170-1172 .
63. F Monteverde, A Bellosi and S Guicciardi: ‘Processing and properties of zirconium diboride-based composites’, *J. Eur. Ceram. Soc.*, 2002, 22, 279-288.
64. D Sciti, L Silvestroni, G Celotti, C Melandri and S Guicciardi: ‘Sintering and mechanical properties of ZrB_2–$TaSi_2$ and HfB_2–$TaSi_2$ ceramic composites’, *J. Am. Ceram. Soc.*, 2008, 91, (10), 3285–3291.
65. SQ Guo, T Nishimura, T Mizuguchi, Y Kagawa: ‘Mechanical properties of hot-pressed ZrB_2–$MoSi_2$–SiC composites’, *J. Euro. Ceram. Soc.*, 2008, 28, 1891–1898.

66. F Monteverde and A Bellosi: ‘Effect of the addition of silicon nitride on sintering behaviour and microstructure of zirconium diboride’, *Scripta Materialia,* 2002, 6, 223-228.
67. W Han, G Li, X Zhang, J Han: ‘Effect of AlN as sintering aid on hot-pressed ZrB_2–SiC ceramic composite’, *Journal of Alloys and Compounds,* 2009, 471, 488–491.
68. F Monteverde: ‘Beneficial effects of an ultra-fine α-SiC incorporation on the sinterability and mechanical properties of ZrB_2’ *Appl. Phys. A,* 2006, 82, 329–337.
69. SQ Guo, JM Yang, H Tanaka, Y Kagawa. ‘Effect of thermal exposure on strength of ZrB_2-based composites with nano-sized SiC particles’. *Composites Science and Technology* , 2008, 68, 3033–3040.
70. S Zhou, Z Wang, X Sun, J Han: ‘Microstructure, mechanical properties and thermal shock resistance of zirconium diboride containing silicon carbide ceramic toughened by carbon black’. *Materials Chemistry and Physics,* 2010, 122, 470–473.
71. WB Tian, YM Kan, GJ Zhang and PL Wang: ‘Effect of carbon nanotubes on the properties of ZrB_2–SiC ceramics’, *Materials Science and Engineering A,* 2008, 487, 568–573.
72. F Yang , X Zhang, J Han, S Du: ‘Processing and mechanical properties of short carbon fibers toughened zirconium diboride-based ceramics’, *Materials and Design,* 2008, 29, 1817–1820.
73. T Zhu, L Xua, X Zhang , W Hana, P Hua and L Weng. ‘Densification, microstructure and mechanical properties of ZrB_2–SiC_w ceramic composites’, *J Euro. Ceram. Soc.,* 2009, 29 2893–901.
74. W Li, X Zhang, C Hong, W Han and J Han: ‘Preparation, microstructure and mechanical properties of ZrB_2–ZrO_2 ceramics’, *Journal of the European Ceramic Society,* 2009, 29, 779–786.
75. X Zhang, W Li, C Hong and W Han: ‘Microstructure and mechanical properties of ZrB_2-based composites reinforced and toughened by zirconia. *Int. J. Appl. Ceram. Technol.*, 2008, 5 (5), 499–504.
76. X Zhang , X Li, J Hana, W Hana, C Honga: ‘Effects of Y_2O_3 on microstructure and mechanical properties of ZrB_2–SiC ceramics’, *Journal of Alloys and Compounds* 2008, 465, 506–511.
77. WM Guo, J Vleugels, GJ Zhang, PL Wang and OV Biest. ‘Effects of Re_2O_3 (Re = La, Nd, Y and Yb) addition in hot-pressed ZrB2–SiC ceramics’. *J Euro Ceram Soc,* 2009, 29, 3063–3068.

78. F Monteverde, S Guicciardi and A Bellosi. Advances in microstructure and mechanical properties of zirconium diboride based ceramics. *Materials Science and Engineering A*, 2003, 346, 310-319.
79. JJM Martinez, AD Rodriguez, F Monteverde, C Melandri and GD Portu: 'Characterization and high temperature mechanical properties of zirconium diboride based materials', *J. Euro. Ceram. Soc.*, 2002, 22, 2543-2549.
80. X Zhang, WLC Hong, W Han, J Han: 'Microstructure and mechanical properties of hot pressed ZrB2–SiCp–ZrO2 composites', *Materials Letters*, 2008, 62, 2404–2406.
81. X Zhang, P Hu, J Han, L Xu and S Meng: 'The addition of lanthanum hexaboride to zirconium diboride for improved oxidation resistance', *Scripta Materialia*, 2007, 57, 1036–1039.
82. X Sun, W Han, P Hu, Z Wang and X Zhang: 'Microstructure and mechanical properties of ZrB_2–Nb composite'. *Int. J. of Refract. Met. & Hard Mater.* 2010, 28, 472–474.
83. H Wang, D Chen, CN Wang, R Zhang, and D Fang: 'Preparation and characterization of high-toughness ZrB_2 /Mo composites by hot pressing process', *Int. J. Refract. Met. & Hard Mater*, 2009, 27, 1024-1026.
84. H Wu and W Zhan: 'Fabrication and properties of ZrB_2–SiC–BN machinable ceramics', *Journal of the European Ceramic Society*, 2010,30, 1035–1042.
85. W Li, X Zhang, C Hong, W Han and J Han. 'Microstructure and mechanical properties of zirconia-toughened ZrB_2–$MoSi_2$ composites prepared by hot-pressing', *Scripta Materialia* 2009, 60, 100–103.
86. A Rezaie, WG Fahrenholtz and GE Hilmas: 'Effect of hot pressing time and temperature on the microstructure and mechanical properties of ZrB_2–SiC', *J. Mater. Sci.*, 2007, 42, 2735–2744.
87. WG Fahrenholtz, GE Hilmas, AL Chamberlain, JW Zimmermann: 'Processing and characterization of ZrB_2-based ultra-high temperature monolithic and fibrous monolithic ceramics', *Journal of Materials Science*, 2004, 39, 5951 – 5957.
88. G Liu, S Meng, J An, S Sun, X Ding. 'The evaluation of reliability for zirconium diboride composite with additives of graphite', *Int. Journal of Refractory Metals & Hard Materials*, 2009, 27, 868–871.
89. A Spring, WM Guo, GJ Zhang, PL Wang, and VD Krsticy: 'Fabrication and characterization of ZrB_2-based ceramic using synthesized ZrB_2–LaB_6 powder', *J. Am. Ceram. Soc.*, 2008, 91, (8), 2763–2765.

90. SQ Guo, T Nishimura, Y Kagawa and JM Yang: 'Spark plasma sintering of zirconium diborides', *J. Am. Ceram. Soc.*, 2008, 91, (9), 2848–2855.
91. T Venkateswaran, B Basu , GB Raju, DY Kimb: 'Densification and properties of transition metal borides-based cermets via spark plasma sintering', *Journal of the European Ceramic Society*, 2006, 26, 2431–2440.
92. I Akin, M Hotta, FC Sahin, O Yucel, G Goller and T Goto: 'Microstructure and densification of ZrB_2–SiC composites prepared by spark plasma sintering', *J. Euro. Ceram. Soc.*, 2009, 29, 2379–2385.
93. CM Carney, P Mogilvesky and TA Parthasarathy: 'Oxidation behavior of zirconium diboride silicon carbide produced by the spark plasma sintering method'. *J. Am. Ceram. Soc.*, 2009, 92, (9), 2046–2052.
94. J Song, J Li, J Song and L Zhang: ' Mechanism of sintering YAG/ZrB2 multiphase ceramics with spark plasma sintering', *Materials and Manufacturing Processes*, 2008, 23, 475–478.
95. A Balbo and D Sciti: 'Spark plasma sintering and hot pressing of ZrB_2–$MoSi_2$ ultra-high-temperature ceramics', *Materials Science and Engineering A*, 2008, 475, 108–112.
96. D Sciti, L Silvestroni , M Nygren. 'Spark plasma sintering of Zr- and Hf-borides with decreasing amounts of $MoSi_2$ as sintering aid', *Journal of the European Ceramic Society*, 2008, 28, 1287–1296.
97. C Hu, Y Sakka ,H Tanaka, T Nishimura, S Guo, S Grasso: 'Microstructure and properties of ZrB_2–SiC composites prepared by spark plasma sintering using $TaSi_2$ as sintering additive', *Journal of the European Ceramic Society*, 2010, 30, (12), 2625-2631.
98. Y Zhao, LJ Wang, GJ Zhang, W Jiang and LD Chen: 'Effect of holding time and pressure on properties of ZrB_2-SiC composite fabricated by the spark plasma sintering reactive synthesis method', *International Journal of Refractory Metals and Hard Materials*, 2008, 27, (1), 177-180.
99. M Cao, S Wang and W Han: 'Influence of nanosized SiC particle on the fracture toughness of ZrB_2-based nanocomposite ceramic', *Materials Science and Engineering A*, 2010, 527, 2925–2928.
100. A Bellosi, F Monteverde and D Sciti: 'Fast densification of ultra-high-temperature ceramics by spark plasma sintering'. *Int. J. Appl. Ceram. Technol.*, 2006, 3, (1), 32–40.

101. WM Guo, J Vleugels, GJ Zhang, PL Wang and OV Biest: 'Effect of heating rate on densification, microstructure and strength of spark plasma sintered ZrB_2-based ceramics', *Scripta Materialia*, 2010, 62, 802–805.

102. M Ikegami, K Matsumura, SQ Guo, Y Kagawa and JM Yang. 'Effect of SiC particle dispersion on thermal properties of SiC particle-dispersed ZrB_2 matrix composites', *J Mater. Sci.*, 2010, 45, (19), 5420-5423.

103. R Licheri, R Orru, C Musa & G Cao: 'Fabrication of fully dense ZrB_2 and HfB_2 based ultra high temperature ceramics by combining self propagating high temperature synthesis and spark plsma sintering', *Chemical Engg. Trans*., 2009, 17, 1705-1710.

104. S Zhu, WG Fahrenholtz, GE Hilmas, SC Zhang, EJ Yadlowsky and MD Keitz: 'Microwave sintering of a ZrB_2–B_4C particulate ceramic composite', *Composites: Part A*, 2008, 39, 449–453.

105. CN Sun and MC Gupta: 'Laser Sintering of ZrB_2', *J. Am. Ceram. Soc.*, 91 [5] 1729–1731 (2008)

106. CN Sun, T Baldridge, MC Gupta: 'Fabrication of ZrB_2–Zr cermet using laser sintering technique', *Materials Letters*, 2009, 63, 2529–2531.

107. F Monteverde and A Bellosi: 'Oxidation of ZrB_2-Based Ceramics in Dry Air', *J. Electrochem. Soc.*, 2003, 150(11), B552-B559.

108. A Rezaie, , WG Fahrenholtz, GE Hilmas: 'Evolution of structure during the oxidation of zirconium diboride-silicon carbide in air up to 1500 °C', *Journal of the European Ceramic Society*, 2007, 27, (6), 2495-2501.

109. XH Zhang, P Hu, JC Han: 'Structure evolution of ZrB_2-SiC during the oxidation in air, *Journal of Materials Research* 2008, 23(7),1961-1972.

110. D Sciti, M Brach, A Bellosi: 'Oxidation behavior of a pressureless sintered ZrB_2-$MoSi_2$ ceramic composite', *Journal of Materials Research* 2005, 20, (4), 922-930.

111. E Opila, S Levine, J Lorincz: 'Oxidation of ZrB_2- And HfB_2-based ultra-high temperature ceramics: Effect of Ta additions", *Journal of Materials Science,* 2004, 39, (19), 5969-5977.

112. J Zhao , HT Liu, JX Liu, GJ Zhang: 'ZrB_2 ceramics doped with AlB_2' , *Ceramics International,* 2014, 40, (6), 8915-8920.

113. BF Voitovich, EA Pugach: 'High-temperature oxidation of borides of the group IV metals - II. Oxidationof zirconium and hafnium diborides', *Soviet Powder Metallurgy and Metal Ceramics*, 1975, 14 (3), 231-235.

114. MM Opeka, IG Talmy, , EJ Wuchina, JA Zaykoski, SJ Causey, Mechanical, Thermal, and Oxidation Properties of Refractory Hafnium and zirconium Compounds, *Journal of the European Ceramic Society*, 1999, 19, (13-14), 2405-2414.
115. J Han, P Hu, X Zhang and S Meng: 'Oxidation behavior of zirconium diboride–silicon carbide at 1800 ^{o}C', *Scripta Materialia*, 2007, 57, 825–828.
116. J Han, P Hu, X Zhang and S Meng: 'Oxidation-resistant ZrB_2-SiC composites at 2200 °C' ,*Composites Science and Technology*, 2008, 68,(3-4), 799-806.
117. SS Hwang, , AL Vasiliev, NP Padture, Improved processing and oxidation-resistance of ZrB_2 ultra-high temperature ceramics containing SiC nanodispersoids. *Materials Science and Engineering A*, 2007, 464, 1-2, 216-224.
118. F. Peng, R.F. Speyer: 'Oxidation resistance of fully dense ZrB_2 with SiC, TaB_2, and $TaSi_2$ additives', *Journal of the American Ceramic Society*, 2008, 91, (5), 1489.
119. MK Dehdashti, WG Fahrenholtz, GE Hilmas: 'Effects of temperature and the incorporation of W on the oxidation of ZrB_2 ceramics', Corrosion Science, 2014, 80, 221-228
120. GR Anstis, P Chantikul, BR Lawn, and DB Marshall: 'A critical evaluation of indentation techniques for measuring fracture toughness: I, direct crack measurements', *J. Am. Ceram. Soc.*, 1981, 64, 533–538.
121. C Subramanian , T.S.R.Ch.Murthy, A.K Suri. Synthesis and consolidation of Titanium diboride International Journal of Refractory Metals and Hard Materials,25, [4], (2007), 345-350.
122. J.S. Haggerty, J.L. O'brien & J. F. Wenckus. Growth And Characterization Of Single Crystal Zrb2 Journal Of Crystal Growth ,1968 , 3, [4] 291—294.
123. Y Champion, S Hagege: 'A study of composite interfaces in the Zr-ZrB_2 system' *J. Mater. Sci. Lett.*, 1992, 11, 290–293.
124. Y Liu, WJ Lu, JN Qin, D Zhang: 'A new route for the synthesis of NdB_6 powder from Nd_2O_3–B_4C system', *J Alloys and Compd.* 2007, 431, 337–341.
125. XH Xu , HN Xiao, WM Guo, PZ Gao , SH Peng: 'Preparation and Reaction Mechanism of LaB_6 Powder by Solid-state Reaction at Atmospheric Pressure', *J. Inorg. Mater.*, 2011, 26, 417-421.
126. B Post, FW Glaser and D Maskowitz: 'Trasition metal diborides', *Acta Metall.*, 1954, 2, 20-25

127. M. N. Rahaman. Ceramic processing and Sintering, second Edition, CRC,Taylor and francis , New York, (2003).

128. M Mallik, KK Ray and R Mitra: 'Oxidation behavior of hot pressed ZrB_2–SiC and HfB_2–SiC composites', *J. Euro. Ceram. Soc.*, 2011, 31, 199–215.

129. TA Parthasarathy, RA Rapp, M Opeka, RJ Kerans: 'Effects of phase change and oxygen permeability in oxide scales on oxidation kinetics of ZrB_2 and HfB_2', *J. Am. Ceram. Soc.* 2009, **92**(5),1079–1086.

130. S Kumar, N Krishnamurthy: 'Synthesis and characterization of EuB_6 by borothermic reduction of Eu_2O_3', *Processing and Application of Ceramics*, 2011, 5 (3), 149–154.

131. WM Guo, JZ Guo, YM Kan and PL Wang: 'Oxidation of ZrB_2 powder in the temperature range of 650–800 ◦C', *Journal of Alloys and Compounds*, 2009, 471, 502-506.

132. SN Karlsdottir and J W Halloran: 'Formation of Oxide Scales on Zirconium Diboride–Silicon Carbide Composites During Oxidation: Relation of Subscale Recession to Liquid Oxide Flow', *J. Am. Ceram. Soc.*, 2008, 91(11), 3652–3658.

133. Z Wang, Z Wu and G Shi: 'The oxidation behaviors of a ZrB_2-SiC-ZrC ceramic', *Solid State Sci.*, 2011, 13 (3), 534-538.

134. WM Guo, XJ Zhou, GJ Zhang, YM Kan, YG Li and PL Wang: 'Effect of Si and Zr additions on oxidation resistance of hot-pressed ZrB_2–SiC composites with polycarbosilane as a precursor at 1500 °C', *Journal of Alloys and Compounds*, 2009, 471(1-2), 153-156.

135. T.S.R.Ch. Murthy, J.K. Sonber, C. Subramanian, R.C. Hubli, A.K. Suri.Densification, characterization and oxidation studies of TiB2 –WSi2 composite. Int. Journal of Refractory Metals and Hard Materials 2012,33, 10–21

136. T.S.R.Ch.Murthy, J.K.Sonber, C.Subramanian, R.K.Fotedar, M.R.Gonal and A.K.Suri, "Effect of CrB_2 addition on densification, properties and oxidation resistance of TiB_2" International Journal of Refractory Metals and Hard Materials, 2009, 27, 976-984.

137. T.S.R.Ch.Murthy, J.K.Sonber, C.Subramanian, R.K.Fotedar, M.R.Gonal and A.K.Suri "A new $TiB_2 + CrSi_2$ composite – Densification, characterization and oxidation studies" International Journal of Refractory Metals and Hard Materials, 2010;,28, 529-540

138. T.S.R.Ch.Murthy, C.Subramanian, R.K.Fotedar, M.R.Gonal, P. Sengupta, Sunil Kumar, A. K. Suri "Preparation and property evaluation of TiB_2+$TiSi_2$ composite" Int. J. Refract. Met. Hard Mater. 2009, 27, 629–636
139. T.S.R.Ch.Murthy, R. Balasubramaniam, B. Basu, A. K. Suri, and M. N. Mungole; "Oxidation of Monolithic TiB_2 and TiB_2-20 wt% $MoSi_2$ Composite at 850° C", J. Eur. Ceram. Soc., 2006, 26, 187-192.
140. G.B. Raju, K. Biswas and B. Basu. Microstructural characterization and isothermal oxidation behaviour of hot-pressed TiB2–10 wt.% TiSi2 composite. Scripta Materialia 2009, 61,104–107.
141. G.B. Raju and B. Basu, A.K. Suri. Oxidation Kinetics and Mechanisms of Hot-Pressed TiB_2–$MoSi_2$ Composites. J. Am. Ceram. Soc., 2008, 91 [10], 3320–3327

Annexure -1

Carbon and Oxygen analysis Method

Oxygen analysis

Method : Inert gas fusion:

Instrument : LECO TC -300

Principle:

The sample is heated to a high temperature in a graphite crucible with or without nickel flux depending upon the specimen under inert atmosphere. Oxygen is detected as carbon di-oxide by IR detector .

Carbon analysis

Method: Combustion and IR detection method

Instrument: ELTRA CS 300

Principle:

The sample is heated to a high temperature in an induction furnace in ceramic crucible with tungsten flux under oxygen atmosphere. Carbon is converted to carbon dioxide and is detected by the IR detector.

Annexure -2

Thermodynamic properties of Boron oxides

Boron monoxide, BO (gas)

Temperature (K)	C_p^o (cal/mol)	ΔH_f^o (Kcal /mol)	ΔG_f^o (Kcal /mol)
298	6.978	6.000	-0.765
400	7.068	6.032	-3.085
600	7.427	5.853	-7.614
800	7.810	5.527	-12.053
1000	8.108	5.142	-16.404
1200	8.324	4.719	-20.680
1400	8.480	4.259	-24.872
1600	8.595	3.753	-29.008
1800	8.682	3.198	-33.058
2000	8.749	2.590	-37.065

Boron dioxide, BO_2 (gas)

Temperature (K)	C_p^o (cal/mol)	ΔH_f^o (Kcal /mol)	ΔG_f^o (Kcal /mol)
298	10.343	-71.800	-73.137
400	11.351	-71.739	-73.605
600	12.730	-71.686	-74.552
800	13.501	-71.695	-75.505
1000	13.942	-71.745	-76.452
1200	14.209	-71.838	-77.389
1400	14.381	-71.980	-78.301
1600	14.497	-72.179	-79.200
1800	14.579	-72.439	-80.048
2000	14.639	-72.764	-80.888

Reference:

L.B. Pankratz, J.M. Stuve, N. A. Gokcen. Thermodynamic data for Mineral technology. Bulletin/ United States Department of Interior Bureau of mines. (1984)

Annexure-3

Microhardness measurement Data (load: 100 gm)

ZrB_2	ZrB_2 +10%$TiSi_2$	ZrB_2+ 10%$TiSi_2$ + 10%HfB_2
25.1	17.5	24.5
24.6	21.3	23.6
22.2	20.6	21.9
23.1	19.1	22.6
24.5	18.3	22.9